THE ANNUAL VARIATION OF ATMOSPHERIC MERIDIONAL HEAT TRANSPORTS

by

Philip Nalpanis

Atmospheric Physics Group

Imperial College of Science and Technology

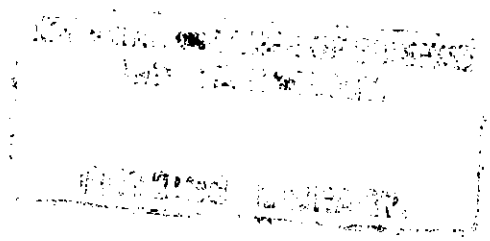

A thesis submitted for the degree of

Doctor of Philosophy

in the University of London

February 1983

ABSTRACT.

The relationship between global-scale meridional temperature gradient and eddy meridional sensible heat transport over an annual cycle is examined and found to display distinct two-valued behaviour. This occurs in a zone from 45° to 65°N throughout the depth of the troposphere; a similar annual cycle in heat transport occurs in the lower stratosphere also. Inclusion of eddy latent heat transport enhances the effect.

The two-valued behaviour is caused primarily by the variation of the stationary eddy component; this is verified in three different data-sets. The transient eddy heat transport is almost independent of temperature gradient; the sum of the two eddy components is found to be closer to the theoretical relationship with temperature gradient than is either of them separately. Since such a parameterization is held generally to apply to the transient eddy component only, the correctness of separating transient and stationary eddy components in the conventional way is called into question.

The effect of the stratospheric zonal wind in controlling upward propagation of stationary waves and hence poleward heat transport is irrelevant to this problem.

Spectral analysis shows that low zonal wavenumbers (1-4) describe well the stationary eddy heat transport in winter and spring; however, this misses completely the dominating influence of the deep wintertime trough over the northwest Pacific and eastern Asia.

Annual variations in stationary eddy heat transport are accounted for by changes in the land-ocean contrast in diabatic heating (thermal forcing of stationary waves). Variations in meridional temperature gradient are not directly related to this, but rather to changes in the latitudinal contrast in zonal-mean heating. Thus the stationary eddy heat transport and global temperature gradient are individual responses to separate forcing mechanisms, though the latter is probably modified by eddy heat transports.

CONTENTS

LIST OF SYMBOLS AND ABBREVIATIONS.

Only symbols used frequently appear below; others are defined in the text as they appear.

A	Any arbitrary quantity
$[A]$	Zonal-mean of A
$\bar{A}$	Time-mean of A
A^*	$A - [A]$
A'	$A - \bar{A}$
B	Static stability
c_p	Specific heat of dry air at constant pressure
E	Total eddy sensible heat transport
E_{ST}	Sensible heat transport by stationary eddies
E_{TR}	Sensible heat transport by transient eddies
f	Coriolis parameter
g	Acceleration due to gravity
L	Total eddy latent heat transport
L_c	Latent heat of condensation at $0^\circ C$
L_{ST}	Latent heat transport by stationary eddies
L_{TR}	Latent heat transport by transient eddies
p	Pressure
q	Specific humidity
$r_2(v,T)$	$[\bar{v}^*\bar{T}^*]/([\bar{v}^{*2}][\bar{T}^{*2}])^{1/2}$
R_e	Radius of the Earth
T	Temperature
U	Zonal windspeed
v	Meridional windspeed
w	Vertical component of velocity
x	Distance East

y	Distance North
z	Geometric height
Z	Geopotential height
β	$\partial f/\partial y$
Δ	Square of meridional entropy gradient
ϕ	Dry entropy (log. potential temperature)
φ	Latitude
λ	Longitude
ψ	Streamfunction
DW	German Weather Service monthly-mean charts
LM	Lejenas and Madden (1982)
OR	Oort and Rasmusson (1971)
OVH	Oort and Vonder Haar (1976)
Ja	January
Fe	February
Mr	March
Ap	April
My	May
Jn	June
Jy	July
Au	August
Se	September
Oc	October
No	November
De	December

INTRODUCTION.

A major component of the atmosphere's energy balance is the large-scale poleward transport of heat, which results from the atmospheric motions caused by heating. This transport is accomplished partly by the mean meridional circulation, partly by eddies or waves; in midlatitudes it is the eddies which dominate the transport.

Eddies are conventionally divided into two kinds: 'stationary eddies', the wavelike features which can be seen on monthly- or seasonal-mean charts, and 'transient eddies', the travelling cyclone-scale waves seen on daily weather analyses. Both kinds are important in transporting heat, though their relative magnitudes vary considerably through the year.

It has been argued that this distinction is arbitrary, existing for numerical convenience rather than as a consequence of a true physical distinction between the two. The forcing mechanism for transient eddies is known to be baroclinic instability, which is also cited by some as being the principal cause of stationary eddies. The case is far from clear, however: others hold that stationary eddies result from thermal and/or orographic forcing, yet others that they are due to some combination of the two mechanisms.

Several theoretical and numerical studies have related the eddy heat transport (either the transient component or the total) to the meridional or zonal-mean temperature structure of the atmosphere. These are reviewed in Chapter 1, together with some other studies on eddy heat transport and stationary eddies. The theoretical studies suggest that the eddy sensible heat transport should be a single-valued function of temperature gradient; this chapter presents

observational evidence suggesting that it is a two-valued function, the problem which has engendered the present study. A discussion of the validity of the conventional partitioning into stationary and transient components is also presented in this chapter.

The spatial extent of this two-valued behaviour is examined in Chapter 2, together with the relative importance and effect of other energy transports.

In Chapter 3, further data relating to stationary eddies, their heat transport, and the tropospheric temperature structure are examined in order to define more precisely the nature of the problem. The Fourier spectrum of the wind and temperature fields constituting the stationary eddy sensible heat transport is presented.

The heart of this work is contained in the next two chapters. Some simple theories to account for the problem are considered in Chapter 4, leading to a discussion of the requirements for a solution to the problem and the formulation of a solution satisfying these.

A simple energy budget for the atmosphere, incorporating ocean-atmosphere heat transfer, is derived in Chapter 5 in order to investigate how longitudinally- and latitudinally-asymmetric diabatic heating varies through the year: it is this which gives rise (in part at least) to the observed variations in stationary eddy heat transport and meridional temperature gradient respectively.

In order to investigate what effect transient eddies might have on the stationary eddy heat transport, a simple analytic model is developed in Chapter 6, the effect of transient eddies being represented by a diffusion term.

CHAPTER 1

THEORIES AND OBSERVATIONS OF EDDY HEAT TRANSPORT

Introduction.

All atmospheric (and oceanic) motions are ultimately caused by heating, more precisely by the latitudinal, longitudinal and vertical variation of that heating. The existence of a meridional temperature gradient does not in itself imply that there will be poleward transport of heat; however if at some initial time there were no heat transport, then the establishment of radiative equilibrium at each latitude between equator and poles would lead to a meridional temperature gradient large enough to cause hydrodynamic instability which would create waves transporting heat. This would alter the heat balance of the atmosphere and hence the means of maintaining thermal equilibrium. The situation is further modified by the presence of oceans (which act as resevoirs of heat, as well as transporting it), such that there is heat transfer at the atmosphere-ocean interface; also by thermal and elevation contrasts between continents and oceans inducing waves in the atmospheric flow which are observed to transport heat polewards. Thus poleward eddy heat transport is a necessary consequence of atmospheric motions; an understanding of the mechanism or mechanisms of eddy heat transport is vital to a full picture of the general circulation of the atmosphere, and may also provide insight into other aspects of the eddies.

Since the atmosphere's temperature structure in some way induces heat transport, and heat transport will either maintain or modify the temperature structure, it has long been considered appropriate to seek some simple relation between the two, often in order to parameterize the fluxes in climate models where explicit representation of eddies would add an unnecessary computational burden; the proposed relations can be tested by examination of climate data, and the validity or

otherwise of the assumptions on which the relations are formulated thereby demonstrated. Commonly-used existing parameterizations are time-independent relations between zonally-averaged eddy sensible heat transport and zonally-averaged meridional temperature gradient: these are examined in Section 1.1 below.

The tilt of the Earth's rotation axis relative to its orbital plane gives rise to an annual cycle in the insolation, resulting in annual cycles in both temperature structure and eddy heat fluxes in the atmosphere. Relating these two in any time-dependent sense raises the question of whether and how one may affect the other, in that change in one may precede (and hence be said to 'force') change in the other. The problem of relating them in this way is the subject of the present study.

1.1 Theoretical Studies.

The starting-point for parameterization of eddy sensible heat transport has been to regard it as analogous to small-scale diffusion, with the transport proportional to the temperature gradient: this approach was first proposed by Defant (1921). Saltzmann (1968) argued that the constant of proportionality, or "Austausch coefficient", should itself be proportional to the temperature gradient, so that

$$E = k(\partial[\bar{T}]/\partial y)^2 \qquad (1.1)$$

where

E is eddy sensible heat transport

k is a constant, to be determined empirically

[ ] signifies a zonal average

Overbar signifies a time average

T and y have their usual meaning

The problem of whether E should be the total eddy sensible heat transport or only the transient component is discussed in Section 1.4 below; suffice it to say at this point that different authors have interpreted it in various ways, here it is the form of the functional dependence of eddy heat transport upon meridional temperature gradient that is of interest.

Green (1970) calculates the eddy kinetic energy released by adiabatic redistribution of mass to a state of minimum potential energy. Given a total variation with latitude in ϕ, log. potential temperature, of $\Delta\phi$, the vertically-integrated eddy sensible heat transport is given by

$$[\overline{v\phi}] = \alpha(g/B)^{1/2}[\Delta\phi]^2 \qquad (1.2)$$

where

B is static stability, $\partial\phi/\partial z$

α is a constant

This is essentially the same relation as Saltzmann proposed, but is arrived at by a different argument. Green's relation is obtained by considering conversion of available potential energy to kinetic energy, whereas Saltzmann's result is derived from linear models of amplifying baroclinic instability. Stone (1972) used Eady's (1949) linear model to calculate the sensible heat transport for small-amplitude baroclinic instabilities from stability theory; his

relationship is of the form

$$[\overline{v\theta}] = kB^{1/2}(\partial[\bar{\theta}]/\partial y)^2 \qquad (1.3)$$

where

θ is potential temperature

In addition to relying on linear theory, this derivation makes an assumption about the velocity scale (dependent on vertical shear and scale height) which Green's does not have; Green's is a more general derivation, resting on assumptions which are rather less arbitrary. However, both arrive at a square-law dependence of eddy sensible heat flux on meridional temperature gradient.

The different functional dependences on static stability, B, in Eqs. (1.2) and (1.3) arise from the different means of deriving the relations; Stone suggests that Green's empirical constant α should be proportional to B. However, the value of B used is a typical zonal-mean value, the annual variation of which is negligible compared with that of $\Delta\bar{\phi}$; hence the functional dependence is not important, and α may reasonably be taken as constant for large-scale zonal-mean heat transport.

Note that in all of Eqs. (1.1), (1.2), and (1.3) the eddy sensible heat transport is related to the square of the zonal-mean temperature gradient rather than the zonal-mean (temperature gradient)^2. Numerically, the difference is of little consequence: for the variation between January and July temperature gradients it is about 2%.

Note also that we do not necessarily expect a relation of the

form of Eq. (1.2) to hold locally, as the 'local' temperature gradient experienced by a parcel of air is difficult to define (unless we know accurately its trajectory). Clapp (1970) showed that, observationally, Eq. (1.2) does not hold locally.

Held (1978) discusses how the vertical extent of eddy motions affects the relationship between poleward eddy heat flux and meridional temperature gradient. Using a simple linear model (based on Charney's quasi-geostrophic β-plane model), he shows that a square-law dependence is appropriate when the vertical extent of the eddies is much greater than the scale-height of the atmosphere, which is the case when the β-effect is negligible; when the β-effect is strong, as in low latitudes, the relevant vertical scale is itself proportional to the horizontal temperature gradient, and a fifth-power relation becomes appropriate.

All these studies have two important features in common:-

(i) The poleward eddy sensible heat transport in midlatitudes is proportional to the square of meridional temperature gradient.

(ii) A given temperature gradient will have a unique value of eddy sensible heat transport associated with it (for the same static stability).

The rest of the chapter is mainly concerned with examining the validity of these two hypotheses.

1.2 Numerical Studies.

The most comprehensive numerical study to date of the general circulation of the atmosphere is that by Oort and Rasmusson (1971): this is described in Section 1.3.1 below. The principal features of the annual cycle of zonal-mean eddy sensible heat transport shown by this are:-

(i) Maximum transports occur around January.

(ii) Largest poleward transports occur around 55°N and 850mb.

(iii) In midlatitudes, a significant eddy heat transport extends at least up to 50mb for most of the year.

(iv) In winter, the heat transport due to stationary eddies is at least as large as the transient component; in summer it is small and negative whereas the transient component is similar to its winter value.

The vertical extent of the transport indicates that, by Held's (1978) argument, a square-law relation between eddy sensible heat transport and meridional temperature gradient should hold.

Green (1970) tested his square-law hypothesis using data then available, finding that theory and observation were in 'promising' agreement; however his data only covers one whole year and part of another, whereas Oort and Rasmusson (1971) employ a 5-year data-set which provides a better test of hypotheses (some subsequent studies have used statistics taken from periods of up to 30 years).

Van Loon (1979) investigated the relationship between eddy

sensible heat transports and meridional temperature gradients in winter. He took temperature gradients over 10° of latitude (the validity of this choice will be discussed in Chapter 2, Section 2.4), and used eddy transports derived from 29 years of daily data. For Northern Hemisphere midlatitudes there is a positive correlation between both total and stationary eddy transport, and the meridional temperature gradient immediately to the south; a significant negative correlation between these transports and the temperature gradient to the north; and only small areas of statistically significant correlation between the transient component and temperature gradient. The strongest positive correlations are between the total or stationary eddy transport and the local meridional temperature gradient centred about 15° to the south, whereas Stone's (1974) linear model of eddy heat transport incorporating meridional variation predicts the correlation to be strongest for heat transport at the same latitude as the strongest temperature gradient; thus the local temperature gradient is not a good choice for eddy heat transport parameterization. Two important features emerge from this study:-

(i) The importance of stationary eddy heat transport in winter, and its strong correlations with temperature gradient.

(ii) The weakness of the correlation between transient eddy heat transport and meridional temperature gradient.

While these give some indication of the relationship between eddy heat transports and meridional temperature gradients, they do so for the spatial domain only. Nothing is said about the annual variation of the various quantities and their relationship in the temporal

domain, therefore understanding of the physical processes relating them is limited in that it is impossible to see whether temperature gradients change because of changes in the eddy heat transport or vice versa.

The second point is remarkable: the transient eddies result from baroclinic instability, which in turn depends on the meridional temperature gradient, also Eqs. (1.1) and (1.3) are essentially derived from baroclinic instability theory, so we should expect the transient eddy heat transport to be well-correlated with the temperature gradient. This problem is discussed more fully in Sections 1.3 and 1.4 below.

Both points cast doubt on current assumptions regarding the parameterization of eddy heat fluxes. We have no theory comparable with that for transient eddies to relate stationary eddy heat flux and meridional temperature gradient; parameterizations of transient eddy heat flux incorporating meridional dependence are in poor agreement with observed values.

Lorenz (1979) approached the problem from a different angle. He sought to establish whether motions on different time-scales were 'forced' or 'free'. Forced variations are defined as those which are responses to changes in external conditions (eg incoming solar radiation), generally thought of as climatic variations. Free variations are those which take place independently of changes in external conditions, fluctuations resulting from instabilities internal to the atmosphere. In the present context, variations in eddy heat flux would be forced if changes in the external heating of the atmosphere forced changes in the temperature gradient which in

turn forced variations in the heat flux, and free if variations in the eddy heat flux forced changes in the temperature gradient. By calculating covariances of eddy heat flux convergence and temperature from time-series of geopotential height and temperature for different time-periods it is possible to see whether variations in the eddy heat flux on various time-scales are forced or free, and to test the validity of the diffusion approach to parameterization.

Lorenz found by such covariance analysis that for motions on the annual and seasonal scale (and of corresponding space-scale), variations were definitely forced; variations on smaller time-scales appear to be free; variations on the scale of a month seem to lie on the boundary between forced and free regimes. In general, it seems that diffusion theory will not lead to a realistic parameterization of eddy heat flux except on time-scales of a year down to two months (or possibly one month), and hence on large space-scales only.

Diffusive parameterizations must therefore be used with caution and will almost certainly not represent well heat fluxes by eddies of time-scales less than one month, ie the transient eddies; these are the ones which it is usually required to parameterize. The annual cycle of stationary eddy heat flux should however be predictable from the temperature gradients throughout the year and indeed be defined physically by these.

Stone and Miller (1980) determined empirically both linear and power-law fits between poleward heat transport and meridional temperature gradient. By using monthly-mean values and 1000mb temperature gradients taken over 30 of latitude, they isolated the forced variations as defined by Lorenz (1979). Several interesting

results concerning midlatitude eddy heat fluxes emerge from their study:-

(i) The square-law parameterization of eddy sensible heat transport is shown to be approximately valid for the total eddy transport.

(ii) Eddy sensible heat transport is well-correlated with temperature gradients either at 1000mb or vertically-averaged, but not so well-correlated for higher levels north of 50^{0} N.

(iii) The total eddy sensible heat transport is much better correlated with temperature gradient than is either the stationary or transient component.

Point (ii) is surprising, since the 1000mb temperature gradient is not typical of the troposphere as a whole; 500mb or 700mb are more typical of the baroclinic zone of the troposphere, so that temperature gradients at these levels should be well-correlated with the eddy heat transports, as it is these which ostensibly give rise to the large-scale baroclinic eddies which accomplish the heat transport.

The problem of eddy classification is again raised by (iii). The authors suggest that there exists a negative feedback mechanism between stationary and transient eddies, which would be consistent with the negative correlation between the two over much of the Northern Hemisphere noted by van Loon (1979). This hypothesis will be discussed further in Section 1.4 below.

In general, these numerical studies have shown that while correlations do exist between eddy sensible heat transport and meridional temperature gradient, the proposed parameterizations should be used with caution, since it is not clear which component of the eddy heat transport can reasonably be thus parameterized: the evidence is that it should be the sum of the two, whereas existing theory suggests it should be only the transient component. Furthermore, the physical link between them is not well-understood, and the eddy time- and space-scale is important. The chapter proceeds with a re-examination of the validity of proposed parameterizations and a discussion of the classification of eddies into stationary and transient types.

1.3 Eddy Heat Transport: A Problem.

1.3.1 The Data-Set.

The basic data-set used for this study is that of Oort and Rasmusson (1971), which contains a comprehensive set of atmospheric general circulation statistics. They analysed daily data principally from the MIT General Circulation Library for a five-year period May 1958 - April 1963 to calculate monthly, seasonal and annual averages of zonal-mean statistics of wind, temperature, geopotential height and specific humidity, as well as appropriate spatial and temporal variances and covariances (the latter including horizontal and vertical energy transports). A vertical average (1012.5 - 75 mb) and values at 13 pressure-levels from 1000mb to 50mb are given.

There are several potential sources of error in these statistics:-

(i) Random observational errors - in measurement or coding.

(ii) Systematic observational errors - all data are for 0000 GMT irrespective of location.

(iii) Gridding errors - to calculate zonal-means, station data are transferred to a latitude-longitude grid by a sophisticated interpolation scheme.

(iv) The uneven distribution of observing stations (in particular, the sparse coverage over the oceans and in high latitudes).

Note also that the statistics give no indication of interannual variations; these are treated by Oort (1977) using the same data-set, and will be discussed in Chapter 3, Section 3.7.

Removal of obvious coding errors and a hydrostatic check to ensure vertical consistency of temperature and geopotential height for each radiosonde report in the original data processing eliminated the largest random errors, leaving the accuracy of measurement as the only random observational error. For a single measurement this is of the order of 1K in temperature or $2ms^{-1}$ in wind; but around 150 (daily) values were being used, and up to 51 values around a particular latitude circle, so the error in the zonal- and time-mean becomes insignificant.

By using only 0000 GMT data throughout, values are selected at particular locations from particular parts of the diurnal cycle which may not be typical of those, for example, producing significant

poleward heat transport, in such a way that the zonal average contains a systematic error. For example, the radiation correction applied to radiosonde temperature measurements is possibly inadequate in winter daytime, so that at low latitudes over the Pacific the temperature at upper levels will be wrong by 2 or 3K; high levels are in winter darkness and hence not susceptible to the same error, so the meridional temperature gradient would be wrong by at least 10% in this region (the zonal-mean temperature difference between 20°N and 75°N being around 25K); however, when the zonal-mean is taken this is reduced to about 5%. Thus winter (October - March) temperature gradients calculated from this data-set should be used with this taken into account. This kind of error could also affect eddy sensible heat transports, but the magnitude of the effect cannot be determined without some knowledge of their spatial variation, which will be presented in Chapter 3.

The errors inherent in the gridding process are difficult to assess, but are probably of similar magnitude to random observational errors. Again, the effect of using a large quantity of data should render such errors insignificant (whereas for a forecast model they could well be important). This does not however apply to data-sparse regions, such as the Pacific Ocean (coverage over the Atlantic is rather better). Here, a longer time-series is of no help; we consider instead the effect on the zonal mean of errors on part of the latitude circle. A reasonable estimate of winter-time errors arising in the gridding process somewhere like the Pacific is 2K in temperature and $2ms^{-1}$ in wind, hence $4Kms^{-1}$ in the heat transport. If this size of error exists over 20% of a latitude circle, then the total error in the zonal mean will be $0.8Kms^{-1}$. Taking all the errors together, let

us say that the total error in the zonal mean is $1 Kms^{-1}$: this is no larger than the interannual variation (see error-bars on Fig. 1.1). The problem of errors is further discussed in Chapter 3, Section 3.4.

Provided the errors are no larger than suggested here, I believe this set of statistics can be taken to describe well the zonal-mean general circulation of the atmosphere.

1.3.2 Definitions of Key Variables.

In midlatitudes, the bulk of meridional heat transport is accomplished by eddies (see Fig. 1.2), which are conventionally divided into Stationary and Transient components. The zonal-mean eddy sensible heat transports for these are given by

$$E_{ST} = [\bar{v}^{*}\bar{T}^{*}] \qquad (1.4a)$$

$$E_{TR} = [\overline{v'T'}] \qquad (1.4b)$$

and $E = E_{ST} + E_{TR}$.

where

$v^{*} = v - [v]$ $\quad T^{*} = T - [T]$

$v' = v - \bar{v}$ $\quad T' = T - \bar{T}$

ST, TR refer to stationary and transient components respectively.

In accordance with Green (1970), eddy heat transports will be related to meridional entropy difference: this is here defined between two latitudes ϕ_1, ϕ_2 $(\phi_1 > \phi_2)$ as

$$\Delta = \left(\frac{[T(\phi_1)] - [T(\phi_2)]}{\frac{1}{2}([T(\phi_1)] + [T(\phi_2)])} \right) \times 10^3 \qquad (1.5)$$

In general, Δ will be taken between 20° and 75°N, a zone encompassing the main region of baroclinic instability, and also possessing good data coverage.

In the first part of this study, the heat transports in the troposphere as a whole are considered. It is therefore necessary to define a tropospheric pressure-average: this is taken over 1012.5 - 250mb, 250mb being roughly the annual-mean height of the tropopause in midlatitudes. For a quantity A defined at n discrete pressure-levels, this average is defined as

$$\bar{A}^{P} = \frac{\sum_{i=1}^{n} \delta p_i A_i}{\sum_{i=1}^{n} \delta p_i} \qquad (1.6)$$

δp_i is in general given by $\frac{1}{2}(p_{i+1} - p_{i-1})$, with p_0 effectively set at 1025mb, p_{n+1} = 200mb.

Tropospherically-averaged entropy gradients are found by taking the pressure-average of Δ's calculated at each level.

The true height of the tropopause in fact varies with both latitude and season; hence tropospheric averages defined as above may include part of the lower stratosphere, or else omit the upper troposphere. In particular, entropy gradients taken over 20° - 75°N may include a part above the tropopause near 75°N but below it near 20°N. The following table shows the effect of taking pressure-averages up to 150mb or 350mb (percentages are differences from 1012.5 - 250mb for preceding column).

Table 1.1

Zonal-mean meridional entropy gradients and eddy heat transports (Units: Kms^{-1}) pressure-averaged over different layers, for January and July.

	Range	Δ		E_{ST}	E_{TR}	E	
Jan	150 - 1012.5mb	14.0	-11%	10.5	8.4	18.9	+1%
	250 - 1012.5mb	15.7		10.1	8.7	18.8	
	350 - 1012.5mb	16.6	+6%	10.5	9.8	20.3	+8%
July	150 - 1012.5mb	3.4	-9%	-.9	5.7	4.8	+14%
	250 - 1012.5mb	3.7		-1.0	5.2	4.2	
	350 - 1012.5mb	3.8	+3%	-1.1	5.2	4.1	-2%

A height average up to 350mb (ie below tropopause for all latitudes and seasons) changes these quantities by no more than 8%, while inclusion of the stratosphere up to 150mb has a slightly greater effect. It appears that the upper height limit is not critical provided the average includes most of the troposphere and very little stratosphere.

It could be argued that as the temperature difference between 20° and 75°N is roughly constant from 2km up to 8km (Green (1970)), a pressure-average over this region should be typical of the troposphere as a whole (since it is outside the boundary layer and below the tropopause); but as the maximum eddy transport is at 850mb, such an average would exclude a major contribution to the tropospheric heat transport.

The effect of taking individual levels rather than the tropospheric average is discussed more fully in Chapter 2, Section 2.3.

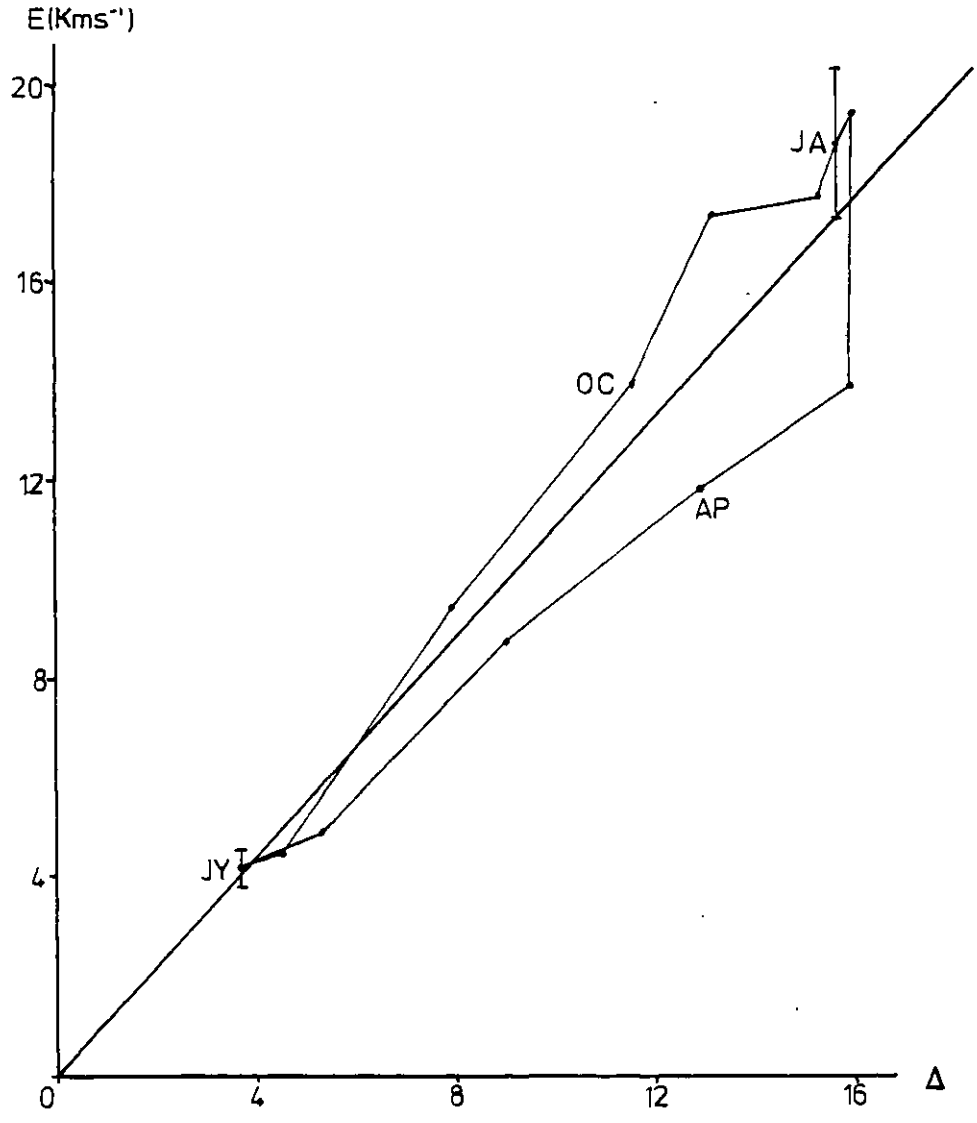

Fig. 1.1a: Monthly-mean tropospherically-averaged total eddy sensible heat transport, E, at 55° N against square of entropy gradient, Δ , taken between 20° and 75° N. Error-bars are interannual variation, 1 standard error.

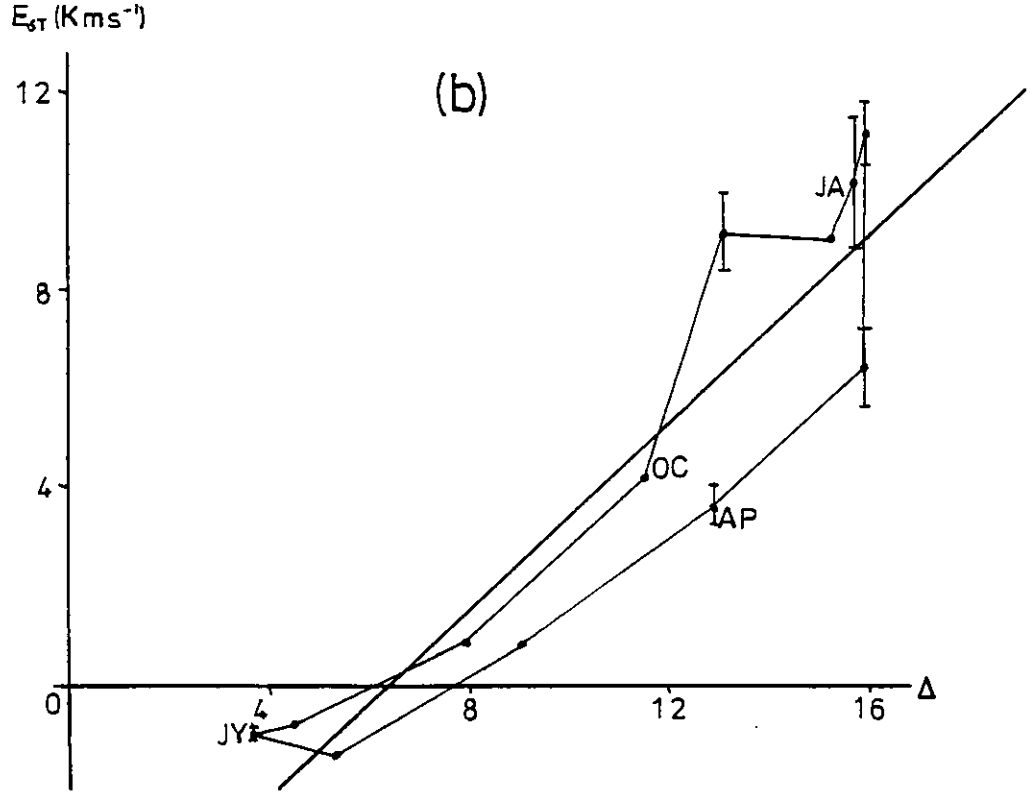

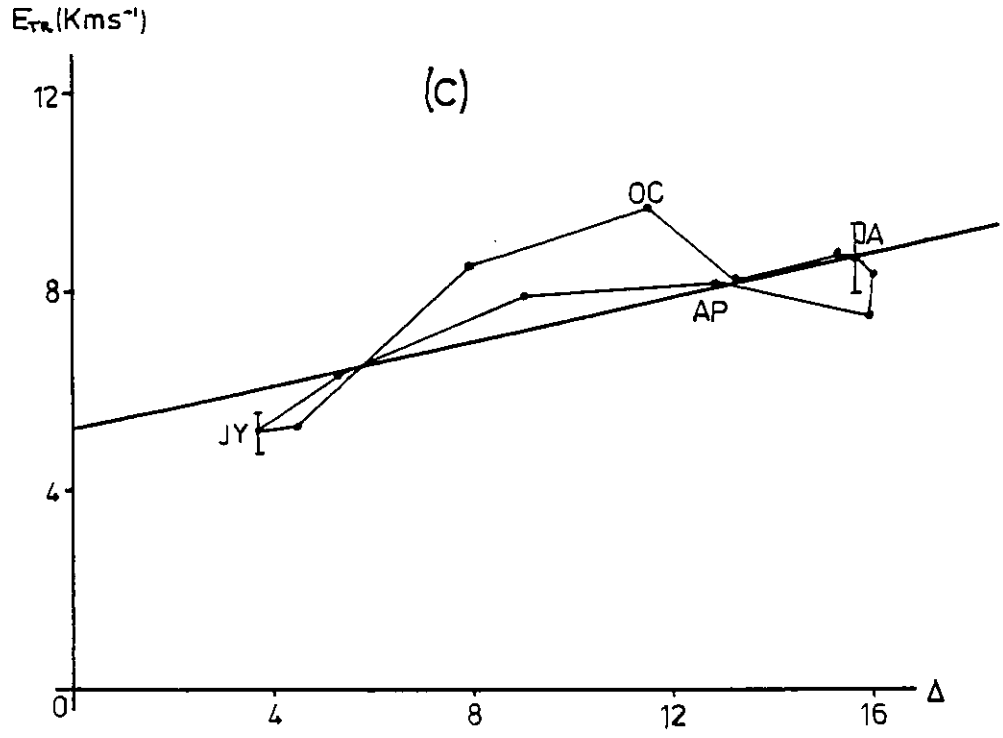

Figs. 1.1b and c: As Fig. 1.1a, but for (b) stationary and (c) transient eddy heat transport.

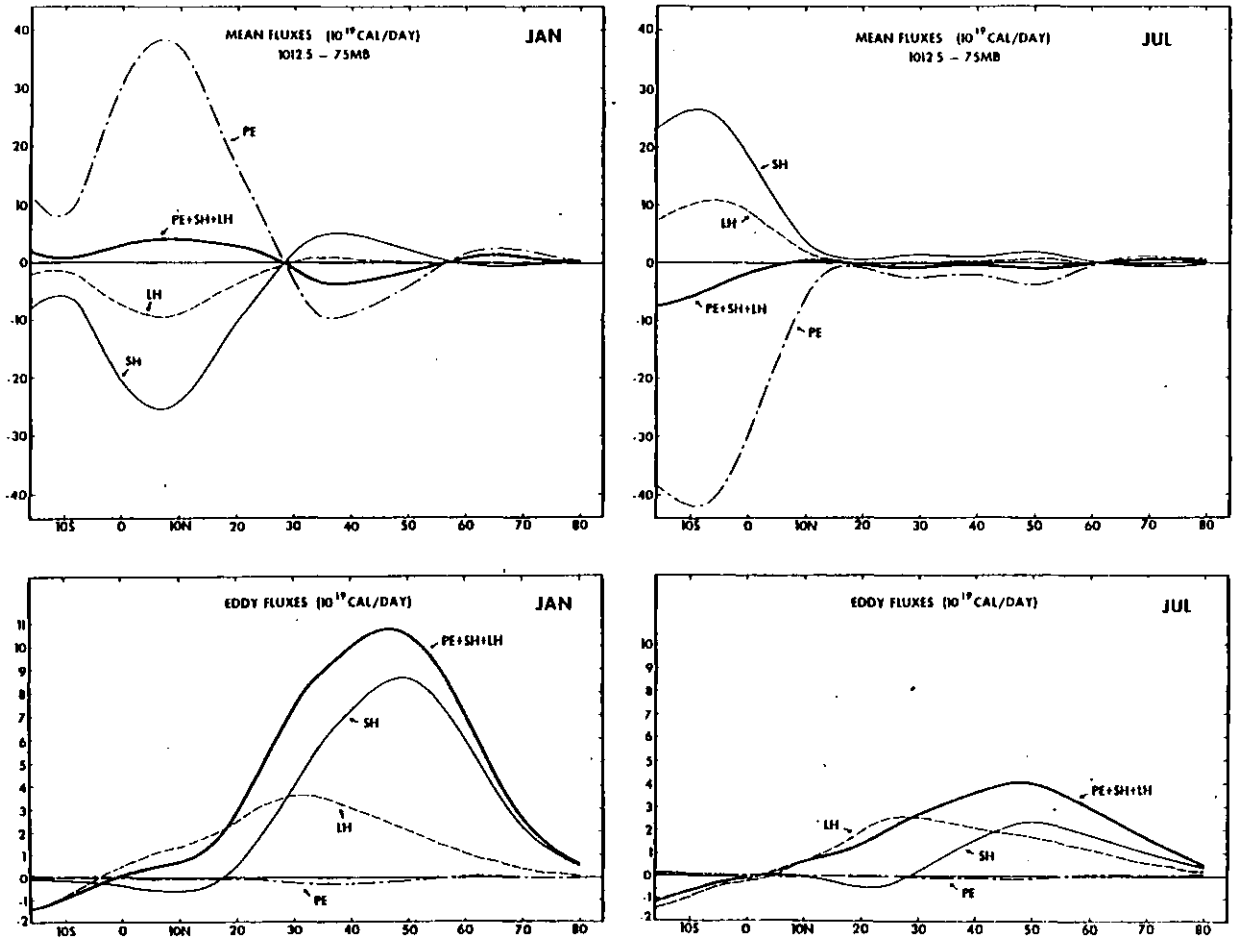

Fig. 1.2: Mean and eddy fluxes of potential energy, sensible heat, latent heat and total energy for January and and July. Fluxes are integrated over layer 1012.5-75mb. Units: 10^{19} cal day^{-1}. From Oort and Rasmusson (1971).

1.3.3 The Problem.

Fig. 1.1 shows the monthly-mean sensible heat transports for stationary and transient eddies, and the sum of the two, plotted against the square of entropy gradient as defined above. Several interesting features are apparent in this figure:-

(i) For the total eddy sensible heat transport, the points for each month lie on a 'loop' about the regression-line. The total transport is not a single-valued function of entropy gradient as Eqs. (1.1), (1.2) and (1.3) have suggested should be the case, but is rather a two-valued function depending on time of year, with transports larger in autumn than in spring. This behaviour is reproduced in the stationary component, but not so clearly in the transient.

(ii) The values for the total transport lie closer to a straight line with zero intercept than do either of the two components (see also Table 1.2 below). Again, this emphasizes that parameterizations of the form of Eq. (1.2) seem to apply best to the sum of transient and stationary eddy transports.

(iii) In winter (No - Fe), the stationary eddies transport more heat polewards than do the transient eddies; for large entropy gradients, they are more efficient at transporting heat. The transient eddy transport actually appears to decrease as the entropy gradient and stationary eddy transport approach their maximum values.

(iv) In summer (Jn - Au), the net stationary eddy sensible heat transport is equatorwards, hence counter-gradient. This shows that at this time of year the eddies are probably not baroclinic in origin.

If it can be shown that these are genuine properties of the atmospheric circulation rather than computational anomalies (as will be done in Chapters 2 and 3), then they show that theories of eddy heat transport such as that of Green (1970) need to be revised to include some other predictor of eddy sensible heat transport besides meridional temperature gradient, some seasonally-varying quantity which is not the same in spring and autumn, such that the transport can be a two-valued function of temperature gradient. An alternative possibility is a time-lag between variations in temperature gradient and heat transport. This is discussed in Chapter 4, Section 4.1.1.

The following table shows correlations between entropy gradient and transport, together with the root-mean-square deviations from the regression-lines of Fig. 1.1 for the total transport and its two components.

Table 1.2

	E	E_{ST}	E_{TR}
Correlation	.95	.93	.74
RMS Deviation (Kms^{-1})	1.9	1.8	1.0

Note that in Fig. 1.1a the intercept for the total transport was forced to be zero, since this is what we expect from Eq. (1.2). If this condition is not enforced, then the intercept is -0.5; the rms deviation is hardly smaller than the value in Table 1.2, so a

zero-intercept fit is equally acceptable.

Since the rms deviation for the transient component is smaller than for the stationary component or total transport, one might expect a higher correlation. However, the transient eddy heat transport is relatively independent of entropy gradient (as Fig. 1.1c shows), so the correlation will be low; it is nevertheless still possible for the rms deviation to be small also (the correlation is in general essentially a measure of how strong the dependence is of one quantity on another).

The total transport is well-correlated with entropy gradient, and much better correlated than the transient eddy component. When the regression-line for the stationary eddy component is forced through the origin (it being reasonable to assume zero heat transport in the absence of a temperature gradient), the rms deviation is $3.0 Kms^{-1}$.

The behaviour of the transient eddy transport with respect to temperature gradient is far from that suggested by Eq. (1.2): for half the year (October - April) the transport appears to be almost independent of temperature gradient, so that setting it as a constant would be a better parameterization (with an rms deviation of $1.5 Kms^{-1}$, compared with $2.4 Kms^{-1}$ for the zero-intercept case). It is only in summer (June - August) that the transient component is closely related to temperature gradient, when the stationary component is small. Clearly, either the division of eddies into 'transient' and 'stationary' types is not a division between physical processes (in that baroclinic instability is not responsible for the transient eddies alone, except (probably) in summer when the stationary eddy transport is equatorwards), or something else apart from meridional

temperature gradient determines the transient eddy transport, or both.

The existence of a 'negative feedback mechanism' postulated by Stone and Miller (1980) is an attractive explanation of the downturn in transient eddy transport for near-maximum stationary transports, but the physical justification for this is at present lacking.

A relation of the form of Eq. (1.2) is clearly best applied to the total eddy sensible heat transport; however, this still leaves the problem of why this transport is a two-valued function of temperature gradient. Thus the principal difficulty with the theory from which Eq. (1.2) is derived is that it suggests that meridional temperature gradient is the only predictor required to define the heat transport, which it clearly isn't.

Looking more closely at Fig. 1.1, there is a decrease of 40% in the total eddy transport from February to March, although the meridional entropy gradients for the two months are almost identical. 85% of the decrease is accounted for by the change in the stationary component, which is perhaps surprising in view of the high correlation between this and entropy gradient. March and October have identical values of total eddy transport, due to a larger transient component in October, although Δ is 30% smaller then. April and November have widely differing values of total eddy transport, for similar values of entropy gradient, this being entirely accounted for by the difference in the stationary eddy transports for the two months - that for April is only 40% of November's. The February/March difference is interesting in that there is a large change in heat transport from one month to the next, although the spring/autumn difference as a whole gives rise to the 'loop'. Closer inspection reveals that the most

obvious causes of the 'loop' are the February/March and April/November differences in the stationary transports, however for September and October it is the transient component which causes the autumn fluxes to be larger than those in spring.

From all this, it seems that it is necessary to understand first how the stationary eddy heat transport is related to the atmospheric temperature structure and the physical basis for the stationary/transient division.

1.4 Classification of eddies

Figs. 1.1b and 1.1c show that the conventional division of eddies into stationary and transient components leads to the conclusion that, in the absence of any meridional temperature gradient, both classes will produce a net meridional transport of heat, an amount roughly half their winter values; furthermore, for the stationary eddies this is upgradient. The first result is especially surprising for the transient eddies, for which we expect Eq. (1.2) to hold, with zero intercept; it is not so surprising for the stationary eddies, whose heat transport is less certainly related to meridional temperature gradient.

It seems that the total eddy heat transport may be a more fundamental quantity than the two components. It is also suggested (Stone and Miller (1980)) that the conventional division between stationary and transient eddies represents a division which exists for numerical convenience rather than as a result of physical differences, such as different forcing mechanisms: longitudinal variations in diabatic heating and baroclinic instability, for example.

It has been suggested that there exists a 'negative feedback' between the two types of eddy (Stone and Miller (op. cit.)): this is supported by the negative correlation between the two components noted by van Loon (1979). There is also evidence for this in results from a General Circulation Model, described by Manabe and Terpstra (1974). They investigated, inter alia, the differences in the eddy transports arising from running the model with and without mountains: they found that while the total eddy heat transport was little different in the two cases, the balance between stationary and transient components was significantly different. This suggests that for a given radiation balance the heat transport is uniquely determined, but the relative magnitude of the components depends on the existence of longitudinal variations in stationary eddy forcing (in this case, orography). The atmosphere -- real and model -- will apparently develop a total eddy flux independent of the partitioning into stationary and transient components.

One plausible hypothesis is that the total eddy flux is of first importance; the stationary eddy flux is determined by whatever forcing mechanism(s) operates to produce it, and the transient eddy flux is then established as the residual, ie (total flux)-(stationary flux). Two problems are apparent in this: first, it gives no reason for the two-valued behaviour of eddy heat flux against temperature gradient; second, this does not explain why the atmosphere should require that a certain total flux, or meridional temperature gradient, be established.

A possible answer to the latter problem is provided by Stone's (1978) theory of 'baroclinic adjustment'. This states that the atmosphere adjusts the meridional heat fluxes to maintain local

temperature gradients close to the threshold for baroclinic instability. If the gradient increases much beyond this, the eddy fluxes due to the longest waves react so as to restore the gradient to its threshold value. This does however assume that these long waves result from baroclinic instability, which is not necessarily the case (see below).

Note also that if a feedback mechanism operated such that the transient fluxes acted to control the stationary, then in winter and in spring we should expect the transient flux to follow the temperature gradient closely, as it does the rest of the year, with stationary eddies perhaps adjusting themselves to make up the total flux required; hence, such a feedback mechanism must operate in the reverse direction (stationary fluxes controlling transient).

Another hypothesis is that the transient eddies transport heat down the local temperature gradient, which gives rise to a flux in the zonal as well as the meridional direction. This flux will act upon the stationary eddy fields, changing both amplitude and relative phase of wind and temperature waves so as to enhance the stationary eddy heat flux. However, the temperature gradients will partially be established in the first place by the stationary wave pattern, so that no simple picture of stationary eddy fluxes being controlled by the transient eddies can be formulated, as the interaction appears to work in both directions. Also, the meridional flux by transient eddies should still be related to the meridional temperature gradients in this case, whereas Fig. 1.1c shows that this is not what happens.

It is clear that the stationary and transient eddy heat fluxes are not independent of one another; what is not clear is the

relationship between them, and the origin and nature of the stationary eddies: it is to the latter problem that we turn now.

Various alternative (and not mutually exclusive) hypotheses exist. One is that the stationary planetary waves (zonal wavenumbers 1 - 4) are forced by zonal variations in orography and diabatic heating (the latter due to the different thermal properties of land and ocean), whereas the waves of zonal wavenumbers 5-8 (and higher) are essentially transient in nature, arising from baroclinic instability of the zonal flow. Observational studies have indicated that in winter a large part of the stationary eddy heat flux is in zonal wavenumers 1 - 4, with wavenumber 2 dominating (Wiin-Nielsen et al. (1963, 1964); see also Chapter 3 of the present work). Theoretical studies by Bates (1977) and Shutts (1978) show that thermally and/or orographically forced planetary waves will produce heat fluxes comparable with those observed for stationary waves in the real atmosphere.

Other authors have suggested that baroclinic instability is responsible for at least a part of the observed stationary wave pattern, based on both energy cycle studies and model results. Both Holopainen (1970) and Oort and Peixoto (1974) calculate conversion of available potential energy of the mean flow to that of the stationary eddies, and imply that the magnitude of this conversion in winter shows that the stationary eddies arise from baroclinic instability. However, the definition of the conversion term is such that a zonal-mean downgradient heat flux due to <u>any</u> eddy forcing will appear to give such a conversion, and does not automatically imply that baroclinic instability is the cause of this conversion (even if the eddy possesses characteristics of baroclinic eddies).

Yao (1980) describes a model in which the processes maintaining the stationary eddies can be studied, and concludes that for wavenumber 3 these waves are maintained by baroclinic processes. However, the model is limited in that it is forced by orography only, gets the surface winds wrong (easterly everywhere), and is very limited in the spectral domain; interpretation of results is again based on the premise that conversion of available potential energy of the mean flow to that of the eddies is proof of baroclinic instability as cause of the eddies. His results suggest that baroclinic processes are responsible for maintenance of the observed stationary waves only in the limited case of large meridional temperature gradient and zonal wavenumber 3 (whereas it is wavenumber 2 that is dominant in the stationary eddy flux). Furthermore, Shutts (1978) has suggested that in the lower troposphere thermally rather than orographically forced waves are predominantly responsible for stationary eddy heat transport. The nature of Yao's model is such that comparison with the real atmosphere is difficult, and certain assumptions may well be unrealistic.

However, there is a way in which baroclinic instability may well enhance the stationary eddy heat flux: it has been suggested that part of the stationary wave pattern is due to baroclinic eddies developing preferentially in regions of enhanced baroclinity whose locations are fixed by the stationary waves, so that eddies which are 'transient' in nature appear as stationary waves, and their heat fluxes contaminate the stationary eddy flux. A possible example of this would be the 'Icelandic Low'. Even Fourier analysis of long-wave patterns will not necessarily eliminate this kind of eddy. However, if it constituted a major component of the stationary eddy flux, then the large decrease

in eddy heat flux from February to March would still present a problem: the temperature gradient hardly changes at this time, so the flux should hardly change if it is due to baroclinic eddies. The fact that the stationary eddy flux in summer is small and upgradient is also evidence that the observed stationary wave pattern cannot contain a large component of baroclinic eddies developing in preferred locations on the long-wave pattern. Further discussion of this hypothesis will be presented in Chapter 4, in the light of data on the longitudinal variation of eddy fluxes.

The evidence for and against the observed stationary wave pattern being due to baroclinic instability in some form is not conclusive either way; the balance seems in favour of thermal/orographic forcing being the major cause, but with the possibility of a contribution from baroclinic instability. It would be convenient if the stationary eddy flux could be partitioned into a baroclinic component which could be included with the transient eddy flux in a parameterization of the form of Eq. (1.2), with the remaining part being due to orographic and thermal forcing, which could be represented explicitly in a model. This would have some physical justification, but it is not clear how or if the two parts can be separated numerically.

Such a partitioning might be achieved from a knowledge of the total eddy flux and a law relating heat transport by stationary eddies forced thermally/orographically to other observed parameters; however no such universal law has apparently been formulated, as numerical models generally carry this transport explicitly and its form depends on the model formulation. Such a law could only be defined from a model reproducing well the observed transports (and annnual variation of these), and even then it might be difficult to extract the true

stationary eddy heat transport as this should be modified by baroclinic instability in the model!

If realistic models of thermal and orographic forcing predict stationary eddy heat fluxes of the correct magnitude, and if variation of these fluxes is consistent with observed changes in thermal forcing, then the evidence for thermal/orographic forcing rather than baroclininc instability being the cause of the observed stationary waves is strong. Evidence from observational data is presented in Chapter 5 which suggests that variations in thermal forcing can explain the observed variations in stationary eddy heat transport.

CHAPTER 2

MERIDIONAL AND VERTICAL VARIATIONS IN EDDY HEAT TRANSPORT

Introduction.

In this chapter, the behaviour of eddy heat transport with respect to meridional entropy gradient is considered with the inclusion of other forms of energy transport, and over a range of latitudes and heights. It is shown that the observed two-valued behaviour is a genuine property of atmospheric heat transports, at least for this data-set.

2.1 Other Energy Transports.

Besides transporting sensible heat, eddies also transport latent heat, potential energy and kinetic energy; there is also transport of all these forms of energy by the mean meridional circulation. The relative magnitudes of all but kinetic energy transports (which are negligible by comparison with the other transports) are illustrated in Fig. 1.2. It can be seen from this that in midlatitudes the only fluxes which are significant are the eddy fluxes of sensible and latent heat, in both winter and summer.

The eddy latent heat transports are defined (cp. Eqs. (1.4a) and (1.4b)) as:-

$$L_{ST} = [\bar{v}^{*}\bar{q}^{*}] \qquad (2.1a)$$

$$L_{TR} = [\overline{v'q'}] \qquad (2.1b)$$

where

q is specific humidity

The low-latitude energy input to the eddies is in the form of both sensible and latent heat, with latent heat dominating but being

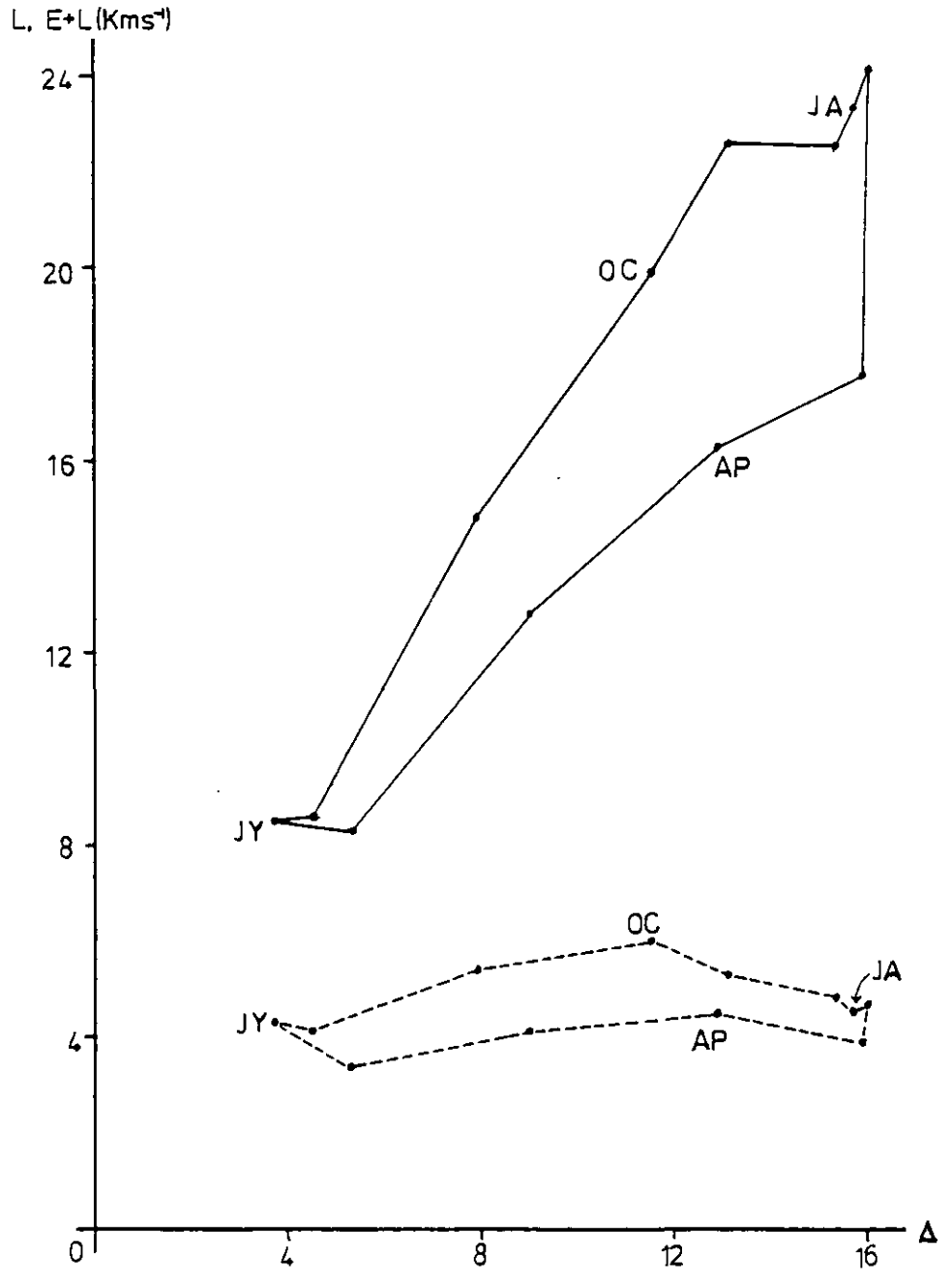

Fig. 2.1: Latent (•------•) and Sensible + Latent (•————•) meridional heat transport by eddies at 55°N against Δ as Fig. 1.1; all quantities tropospherically- averaged. Units: Kms^{-1}.

converted to sensible heat by condensation and rainfall as tropical air moves polewards. Since the two forms of heat transport are so closely linked, it could be postulated that the sum of latent and sensible heat fluxes might be a single-valued function of meridional temperature gradient.

Fig. 2.1 shows that this is not the case. The latent heat transport is about 25% higher in autumn than in spring, so that it enhances rather than reduces the two-valued nature of eddy heat transport with respect to meridional entropy gradient.

The difference in latent heat transport between spring and autumn is accounted for by the higher temperatures in autumn of the extratropical ocean and atmosphere near their interface, as shown by Monthly Meteorological Charts of the Oceans (Meteorological Office: 1947, 1949, 1950). Although the temperature differences between ocean and atmosphere are similar in both seasons, the nonlinear variation of saturated vapour pressure with temperature results in the specific humidity of the atmosphere being higher in autumn (relative humidity remaining roughly constant). This in turn increases q^* and q', and hence the latent heat transport.

Curiously, the observed annual variation in eddy latent heat transport is small compared with that of the wind and specific humidity fields. The (sensible + latent) heat lost by unit mass of air in moving from low to high latitudes, with temperature difference ΔT and specific humidity difference Δq between them is given by

$$c_p \Delta T + L_c \Delta q$$

This may be rewritten as

$$c_p \Delta T \left(1 + \frac{L_c}{c_p} \frac{\Delta q}{\Delta T} \right)$$

Substituting typical January and July values of Δq and ΔT (from Oort and Rasmusson (1971)) shows, firstly, that the term $(L_c \Delta q / c_p \Delta T)$ is between 0.25 and 0.5 in January, and around 1 in July, so that latent heat transport should be of similar magnitude to the sensible heat transport in summer, but smaller in winter, as is indeed observed (see Fig. 2.1). The latent heat content of unit air mass in July is about double its January value, but its poleward velocity perhaps half that in January, so that the latent heat will be roughly equal in both months, as observed. Finally, the total eddy heat transport in July should be around 30% to 40% of January's: Fig. 1.3 shows the actual fraction is 35%.

2.2 Latitudinal Variation.

The latitudinal extent of the region in which eddy sensible heat transport displays two-valued behaviour with respect to global-scale meridional entropy difference is shown in Fig. 2.2. This behaviour starts to appear at 45°N and is strongest at around 50° to 55°N (see also Fig. 1.1a), near the latitude of maximum eddy heat transport. At 65°N the effect shows up as an abnormally large eddy heat transport in November alone, which may, I suspect, be due in part to numerical errors in preparation of the original data (this will be discussed in Chapters 3 and 5). Thus the heat transport is two-valued in a zonal belt stretching from 45°N to 65°N, north of which the stationary eddy sensible heat transport is small compared with the transient

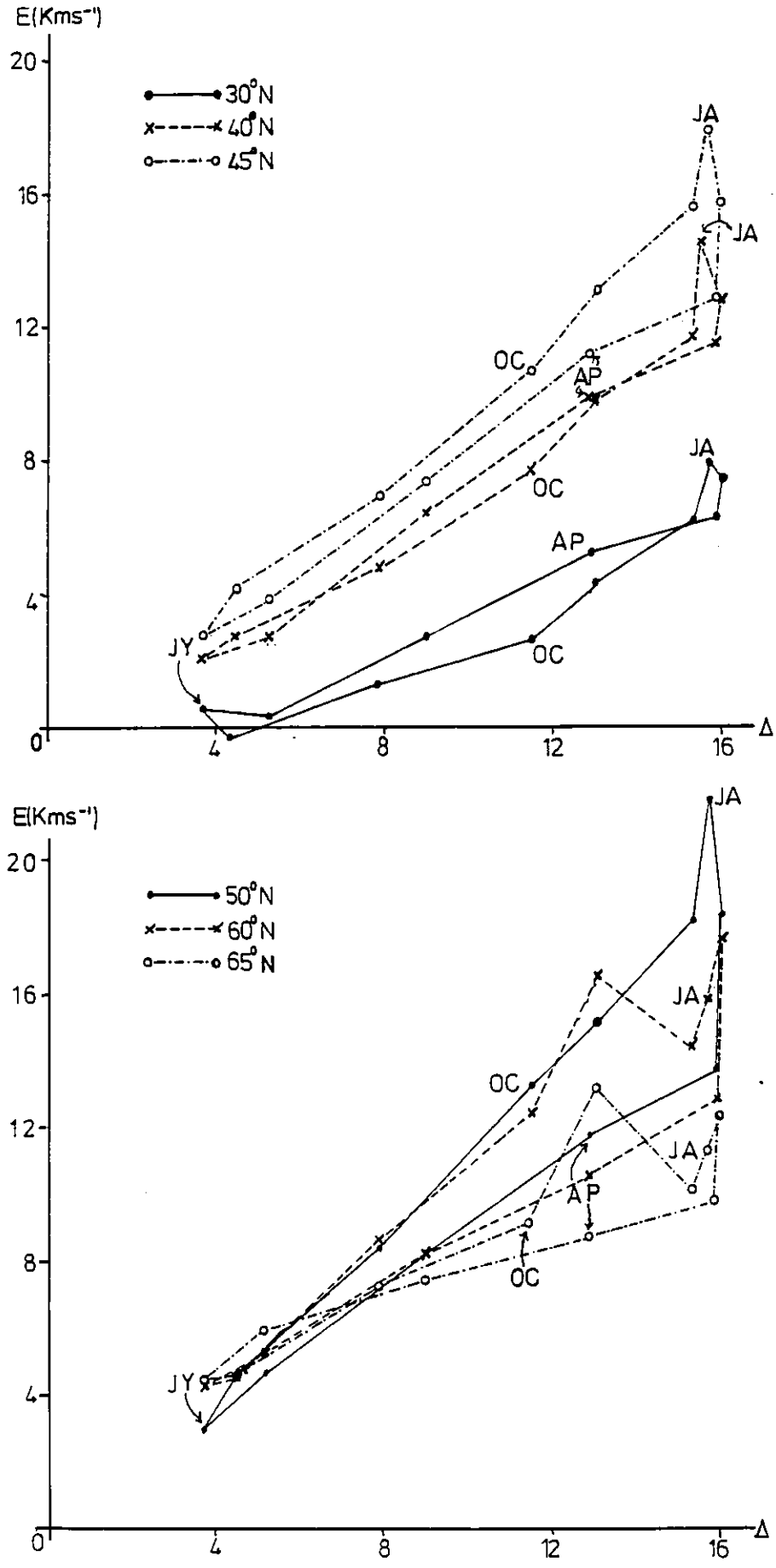

Fig. 2.2: Eddy meridional sensible heat transport at various latitudes against Δ as Fig. 1.1; all quantities tropospherically-averaged. Units: Kms^{-1}.

component, which itself undergoes an annual cycle of variation similar to that at 55°N.

Whereas Figs. 1.1 and 2.1 showed at 55°N a sharp fall in eddy heat transport from February to March, at 45°N the equivalent fall is spread over January to March (and is almost as large as that at 55°N); this was also noted, at 55°N, in a different data-set (see Chapter 3).

2.3 Vertical Variations.

2.3.1 Variations in the Troposphere.

In this section, the relation between eddy sensible heat transport and meridional entropy gradient at various pressure-levels in the troposphere and lower stratosphere is considered. There is some difficulty in interpreting heat transports at a particular level, especially in mid-troposphere, as the heat transport is slantwise rather than horizontal; however this will give us an idea of the vertical variation of the transports, and of their observed two-valued behaviour with respect to temperature gradient; it will also demonstrate the validity of using data at one level (500mb) for a deeper investigation of the problem, to be presented in Chapter 3.

Fig. 2.3 shows that at 850mb, 700mb and 500mb the autumn eddy sensible heat transports (both total and stationary) are significantly larger than those in the spring, as for the tropospheric averages (Fig. 1.1). At 400mb the two-valued behaviour is still apparent, although September's transport is now similar to that in May, and November has a marked peak in both stationary and total eddy transports. The 300mb picture is partially different, for although

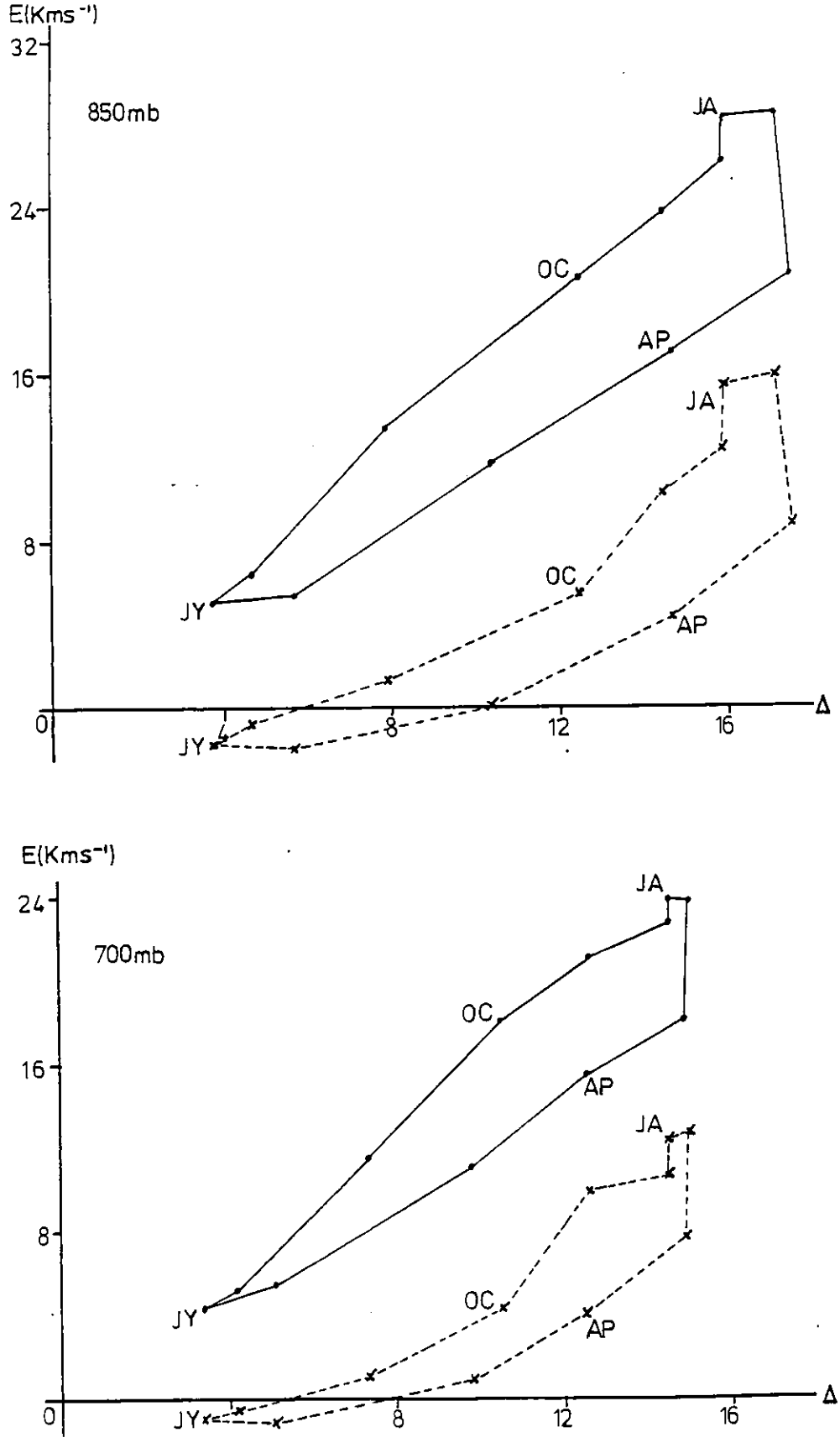

Fig. 2.3: Eddy meridional sensible heat transport at 55°N against Δ, at various pressure-levels. Units: Kms^{-1}.

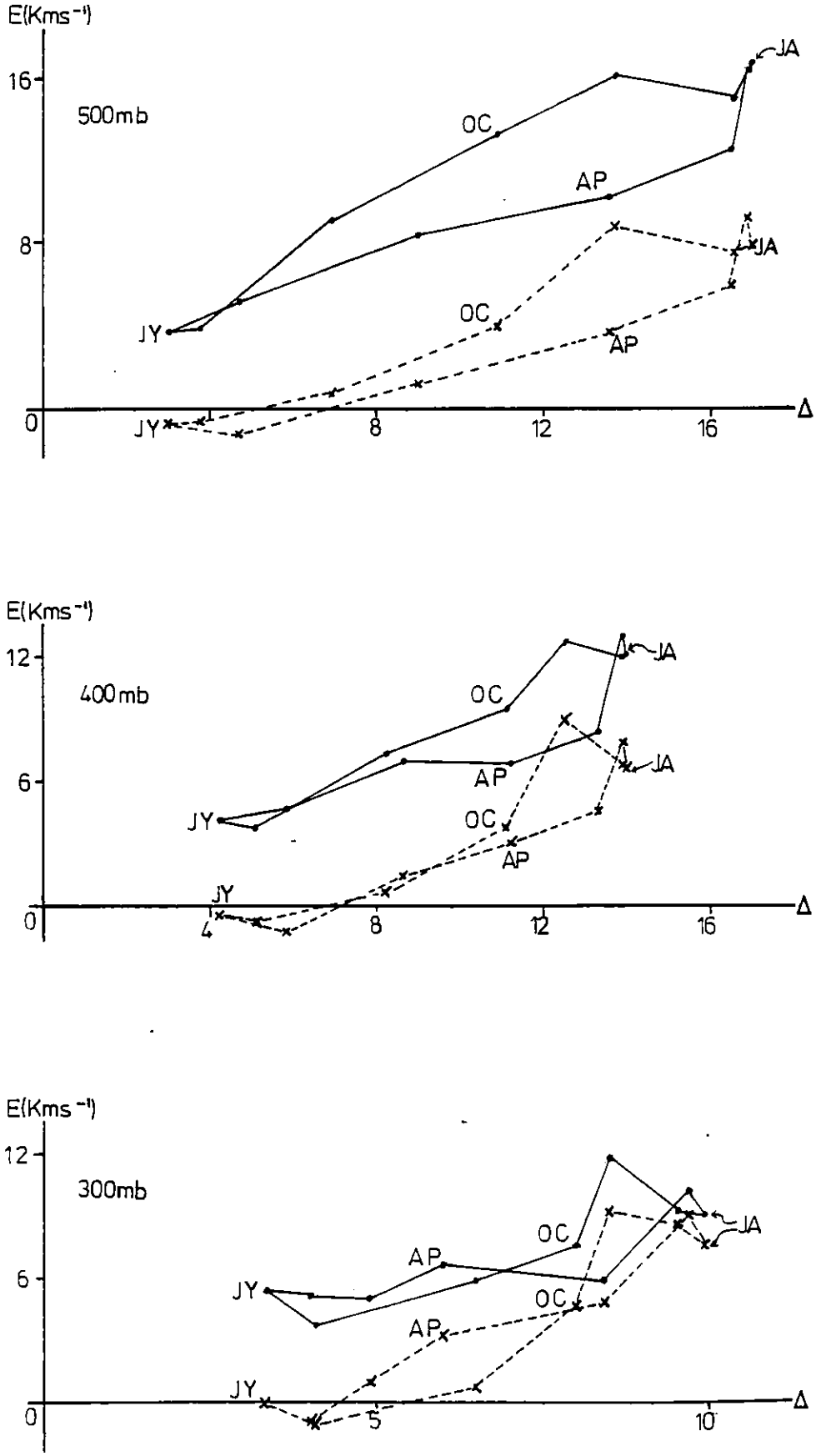

Fig. 2.3 continued.

the heat transport has a sharp peak in November and is much lower in March than in February (both features being due again to changes in the stationary eddy transport), in April and in May the total transport is apparently larger than in the equivalent autumn period. This is due to the variations in temperature rather than those in eddy heat transport, as the latter are similar to those at lower levels for both stationary and total eddy transports.

The annual cycles of total and stationary eddy sensible heat transport and of meridional entropy gradient at 700mb closely resemble those averaged over the troposphere as a whole; those at 500mb also show the principal features described in Section 1.3, although the transports are smaller.

The relationship between tropospherically-averaged total eddy sensible heat transports and the entropy gradients at 1000mb and 500mb is shown in Fig. 2.4. Several simple climate models (eg Budyko (1969), Sellers (1969), North (1975)) use the surface temperature gradient, which is similar to that at 1000mb, to parameterize eddy heat transports; 500mb is a mid-troposperic height where the entropy gradient is typical of the troposphere as a whole, and is used by Green (1970). At both levels, the characteristic two-valued behaviour is displayed, showing that choice of an entropy gradient other than the tropospherically-averaged one does not eliminate this behaviour. At 500mb the correlation between total eddy heat transport and entropy gradient is 0.95, as for the tropospheric-average gradient; the 500mb plot on Fig. 2.4 is very similar to Fig. 1.1a. One might expect the appropriate entropy gradient for tropospheric-average transports to be one typical of the whole troposphere; nevertheless, the correlation

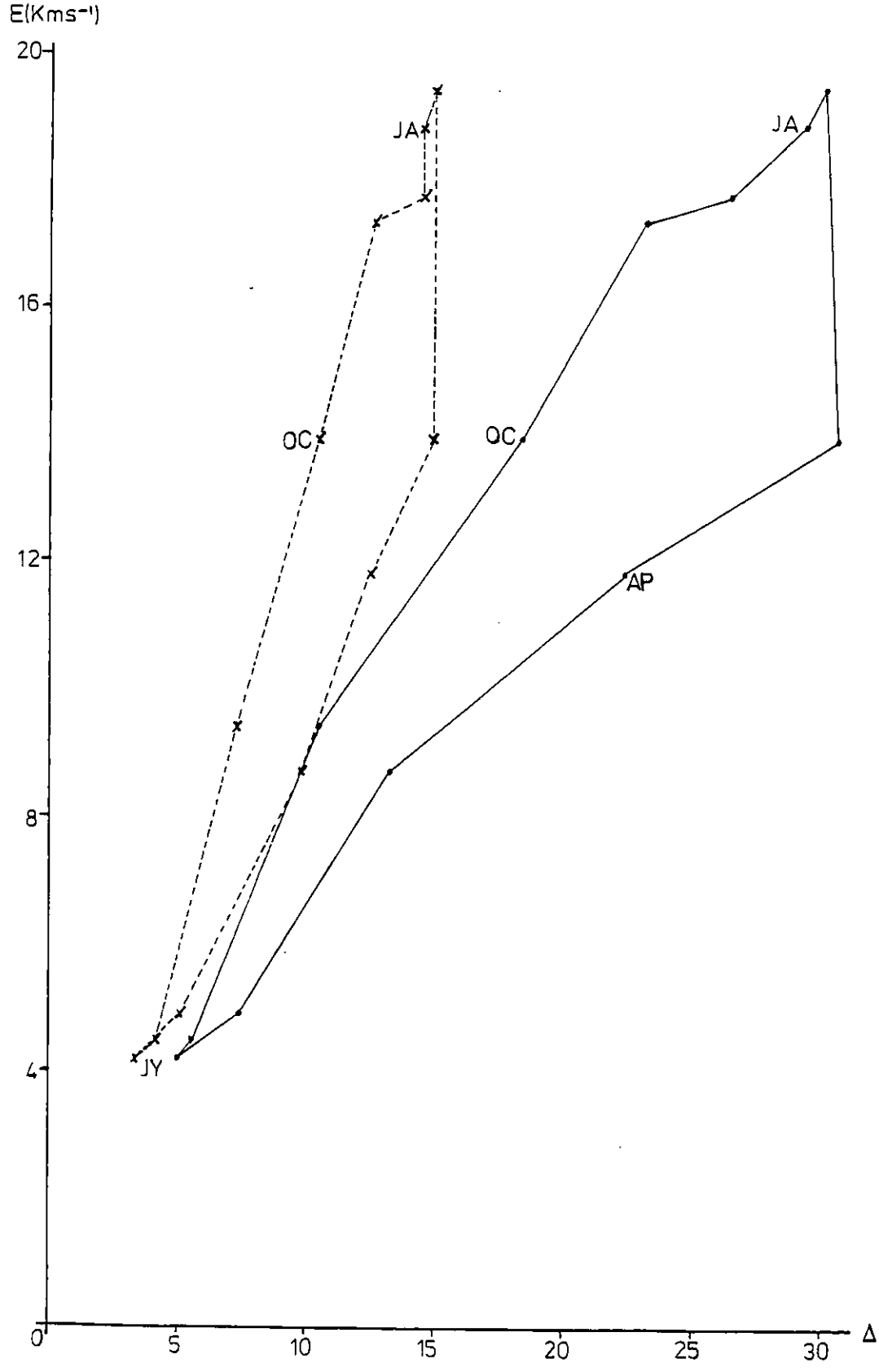

Fig. 2.4: Tropospherically-averaged sensible heat transport at 55°N against Δ at 1000mb (•——•) and 700mb (×- - - - -×). Units: Kms^{-1}.

with the 1000mb entropy gradient is also high, at 0.93. Thus the eddy sensible heat transport would be parameterized almost as well by the 1000mb entropy gradient as by the tropospherically-averaged one but the problem of the two-valued behaviour of the heat transport remains.

2.3.2 Variations in the Stratosphere.

The relationship to be expected between eddy heat transports and temperature gradients in the stratosphere is less clear. Stationary (planetary) waves in the stratosphere are believed to result from vertical propagation of tropospheric stationary waves (Charney and Drazin (1961)), and such vertical propagation is controlled by the sign and magnitude of the zonal wind. Thus the structure of the stratospheric stationary waves is closely related to those waves in the troposphere, whose heat transport is in turn supposedly related to the tropospheric meridional temperature gradient. The temperature structure in the stratosphere is very different from that of the troposphere, with the meridional temperature gradient above 200mb (and at that height for much of the year) being in the opposite sense. Oort and Rasmusson's (1971) statistics show that the stratospheric eddy heat transport is nevertheless polewards for nearly all the year, ie countergradient. It therefore seems more appropriate to relate stratospheric eddy heat transports to meridional temperature gradients in the troposphere rather than to those in the stratosphere.

Figs. 2.5 and 2.6 compare the results of plotting eddy heat transports at three levels in the stratosphere against entropy gradients at the same levels (Fig. 2.5) and tropospherically-averaged (Fig. 2.6). From Fig. 2.5 it is apparent that there is little

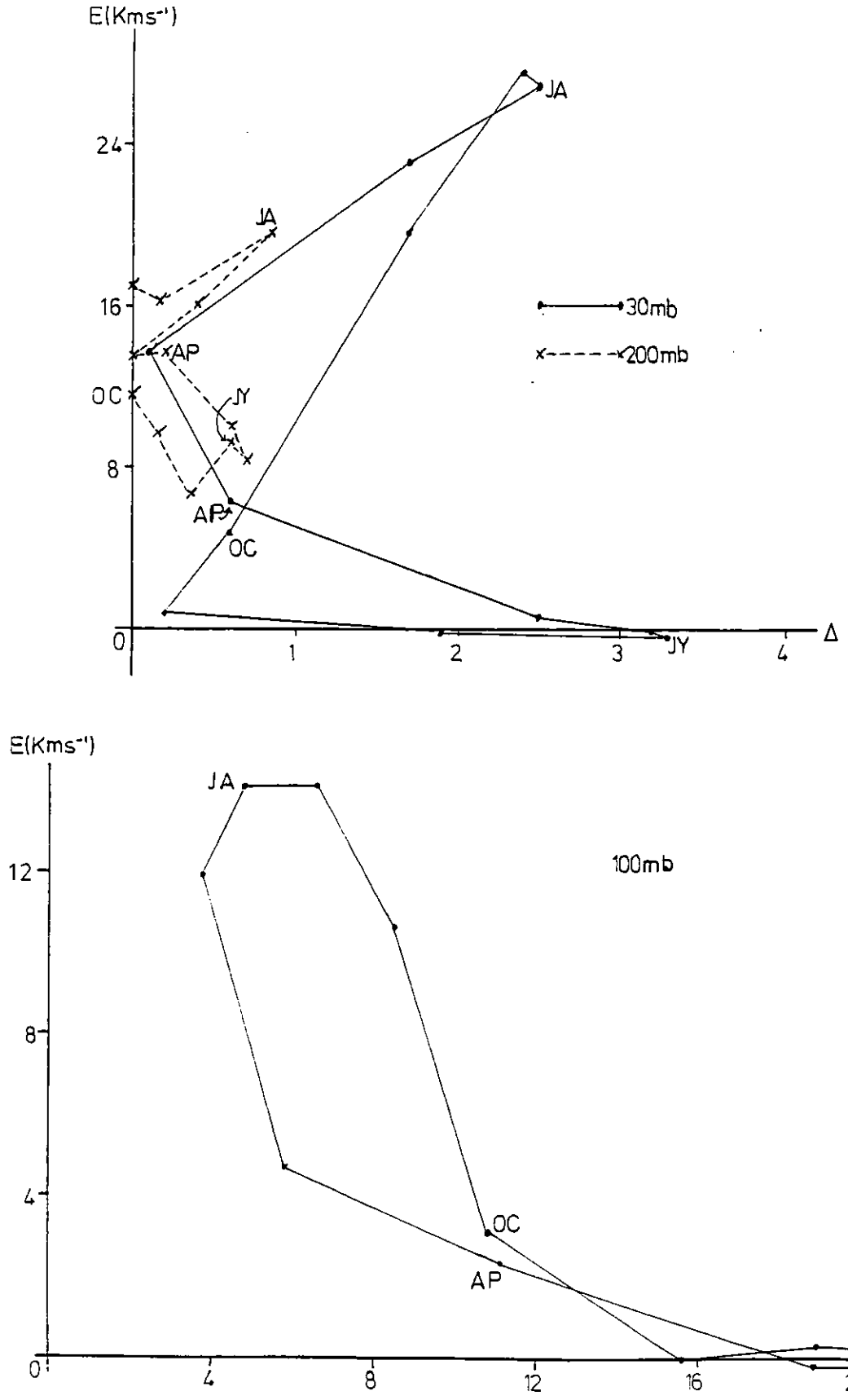

Fig. 2.5: Stratospheric stationary eddy meridional sensible heat transports at 55° N against Δ at same levels.
Units: Kms^{-1}.

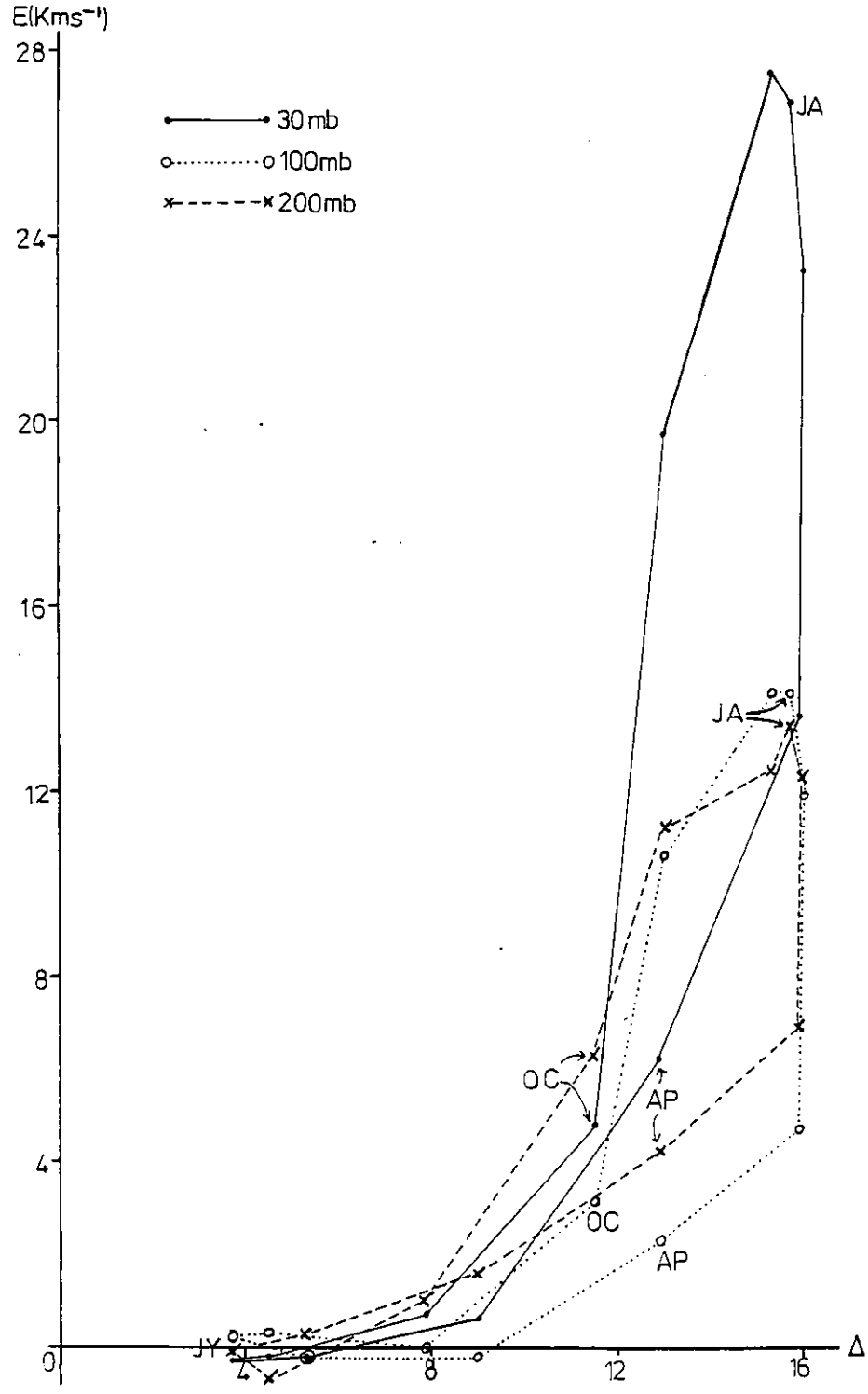

Fig. 2.6: Stratospheric stationary eddy meridional sensible heat transport at 55° N against tropospherically-averaged Δ. Units: Kms^{-1}.

relation between eddy heat transports at any level in the stratosphere and the entropy gradients at the same level; indeed at 100mb the relationship is inverse! However, at 30mb it appears that Eq. (1.2) or similar could relate eddy heat transport and entropy gradient if the months May-August are omitted. These are the months when the zonal wind at this level is easterly (Labitzke (1972)), leading to trapping of stationary waves (Charney and Drazin (op. cit.)) and hence poleward eddy heat transport close to zero irrespective of temperature gradient. Of the remaining months, March alone appears anomalous, with the heat transport being large when the entropy gradient is very small (and about to change sign). This is the opposite to the tropospheric case, but with the 200mb and 100mb eddy transport variations bearing little relation to those in entropy gradient at these levels, it is perhaps fortuitous that at 30mb the relationship between them appears stronger.

Fig. 2.6 shows that at 200mb and 100mb the variation of stationary eddy heat transport with entropy gradient displays the same features as at lower levels; at 30mb, although the transports are much larger for November - March than at lower levels, the same characteristic features pertain: a sudden decrease in transport from February to March and a large difference between April and November transports, with virtually identical entropy gradients for each pair of months. In general, the stratospheric stationary eddy sensible heat transport varies in a similar way to that transport in the troposphere.

It therefore appears that the characteristic features of the observed annual variation of stationary eddy sensible heat transport,

which lead to it being a two-valued function of meridional temperature gradient, occur throughout the depth of the troposphere and at least in the lower stratosphere.

We note also that these stratospheric transports are more closely related to tropospheric temperature gradients than to those in the stratosphere, which supports Charney and Drazin's (op. cit.) theory that stratospheric stationary waves result from vertical propagation of wave energy from the troposphere, and that an easterly zonal wind inhibits this vertical propagation.

2.4 Entropy gradients: Latitudinal limits.

Hitherto, entropy differences between 20° and 75°N have been used; here, the effects of varying both latitudinal limits are examined.

The latitudinal width of the zone over which the entropy gradient is taken is of prime importance. Van Loon (1979) used a 10° - wide zone; Stone and Miller (1980), following Lorenz (1979), chose one 20° wide, centred on the latitude being considered. However, instability theory (eg Eady (1949)) shows that the wave with the longest meridional wavelength will be the fastest-growing; trajectory analysis (Green, Ludlam and McIlveen (1966)) shows individual parcels of air moving over 30° or more of latitude. Srivatsangam (1978) showed in an observational study that a diffusion model of sensible heat transport is best applied only when nearly an entire hemisphere is treated as a zone of mixing. It is therefore sensible to choose a zone sufficiently wide to include the whole entropy difference experienced by warm air moving polewards (or cold air moving equatorwards), or

which is baroclinically unstable, or in which significant eddy heat transport occurs. Thus the appropriate temperature gradient to use should be taken over a wider zone than any of those used in the studies cited above. Green (1970) chooses 20° - 70°N, which fulfils these criteria.

The limits used in the present study encompass the zonal belt including the major part of the pole-equator temperature difference. Fig. 2.7 shows that in winter and spring this extends at least as far south as 20°N, with the local gradient being strongest south of around 45°N. Thus for fluxes at 55°N the southern latitudinal limit for the temperature gradient should be much further south than the 40°N which Stone and Miller's analysis would suggest; a northern limit of 75°N is however realistic as the gradient is relatively slack north of this.

Fig. 2.8 shows the effect of changing both the northern and southern latitudes (φ_1, φ_2) between which the entropy difference is calculated. Figs. 2.8a and 2.8b show that, keeping $\varphi_1 = 70°N$, the total eddy sensible heat transport is only two-valued with respect to entropy difference when $\varphi_2 \leq 30°N$, with the effect becoming more marked as φ_2 is moved further south. When $\varphi_2 = 35°N$, the eddy heat transport no longer behaves as a linear function of entropy difference, and the two-valued behaviour is lost. This can be attributed to the fact that when the transport approaches its maximum values in January and February, the temperature gradient <u>decreases</u> from its December value; as the transport drops sharply in March, so the gradient <u>increases</u> again before dropping with the transport in April. This is evidence that variations in heat transport influence the meridional temperature gradient rather than the other way round: in this case, the increasing transport reduces the meridional

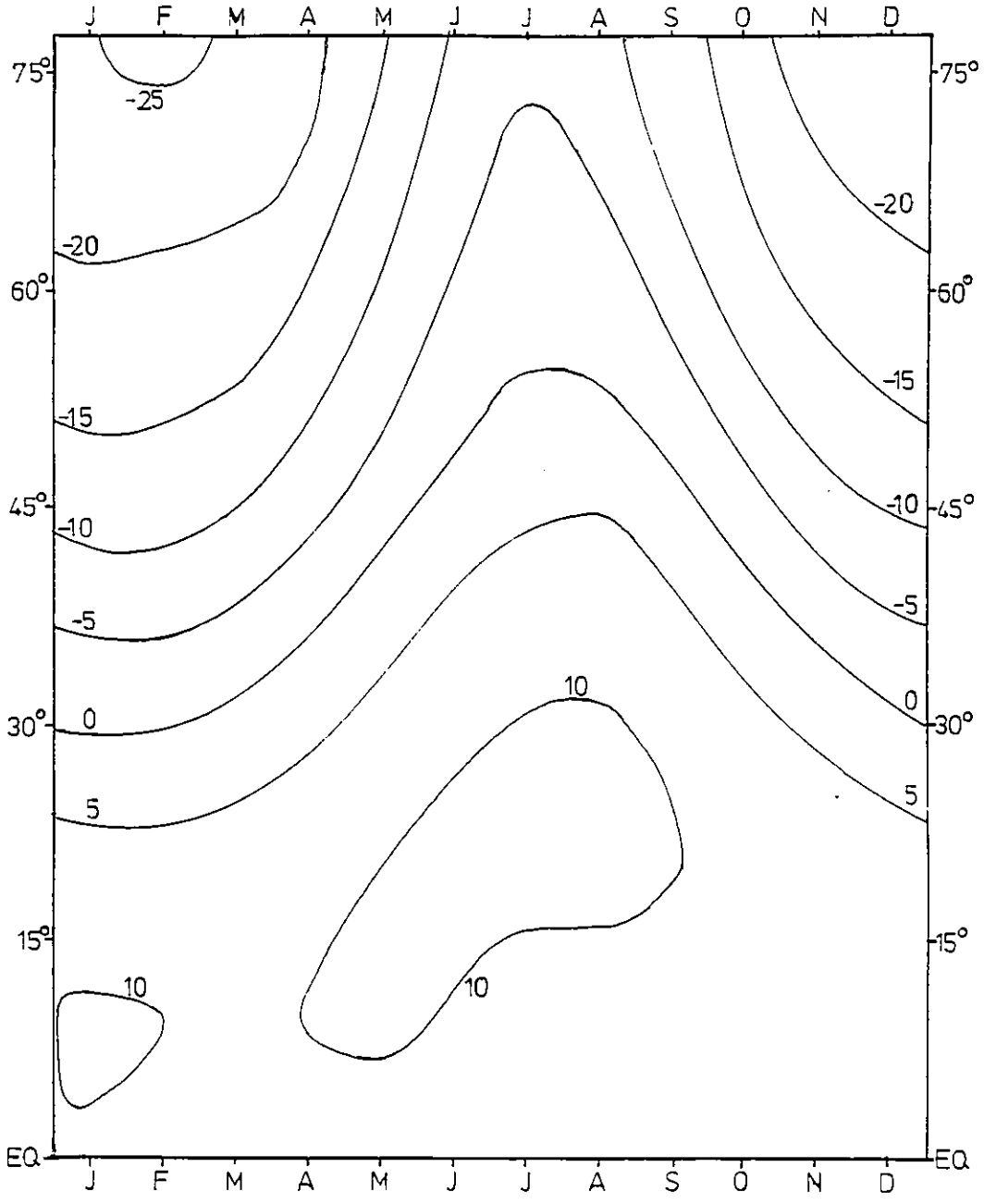

Fig. 2.7: Monthly-mean Northern Hemisphere temperatures at 700mb. Units: °C.

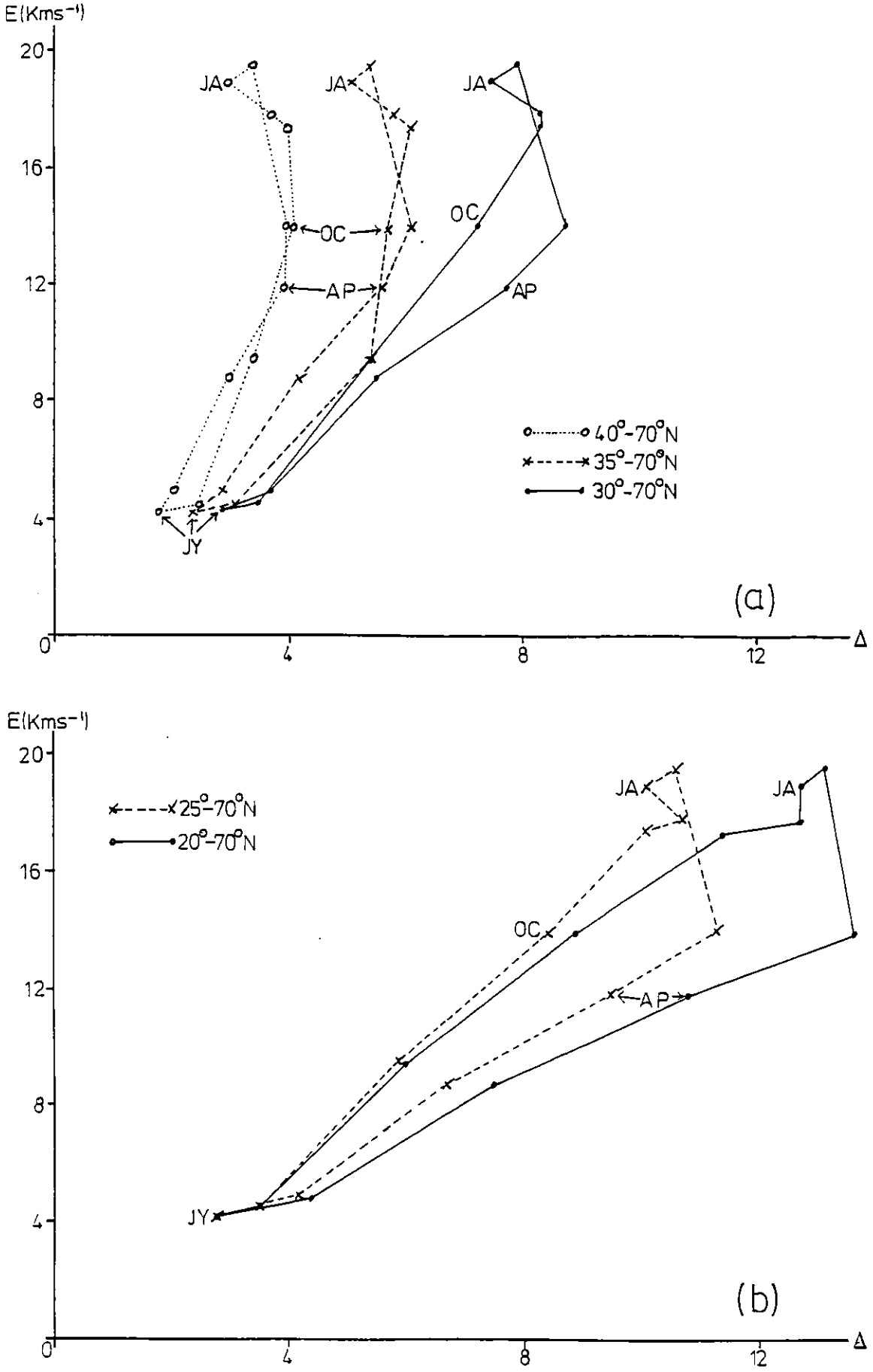

Fig. 2.8: Eddy meridional sensible heat transport at 55°N against Δ taken over various latitudinal limits; both quantities tropospherically-averaged. Units: Kms^{-1}.

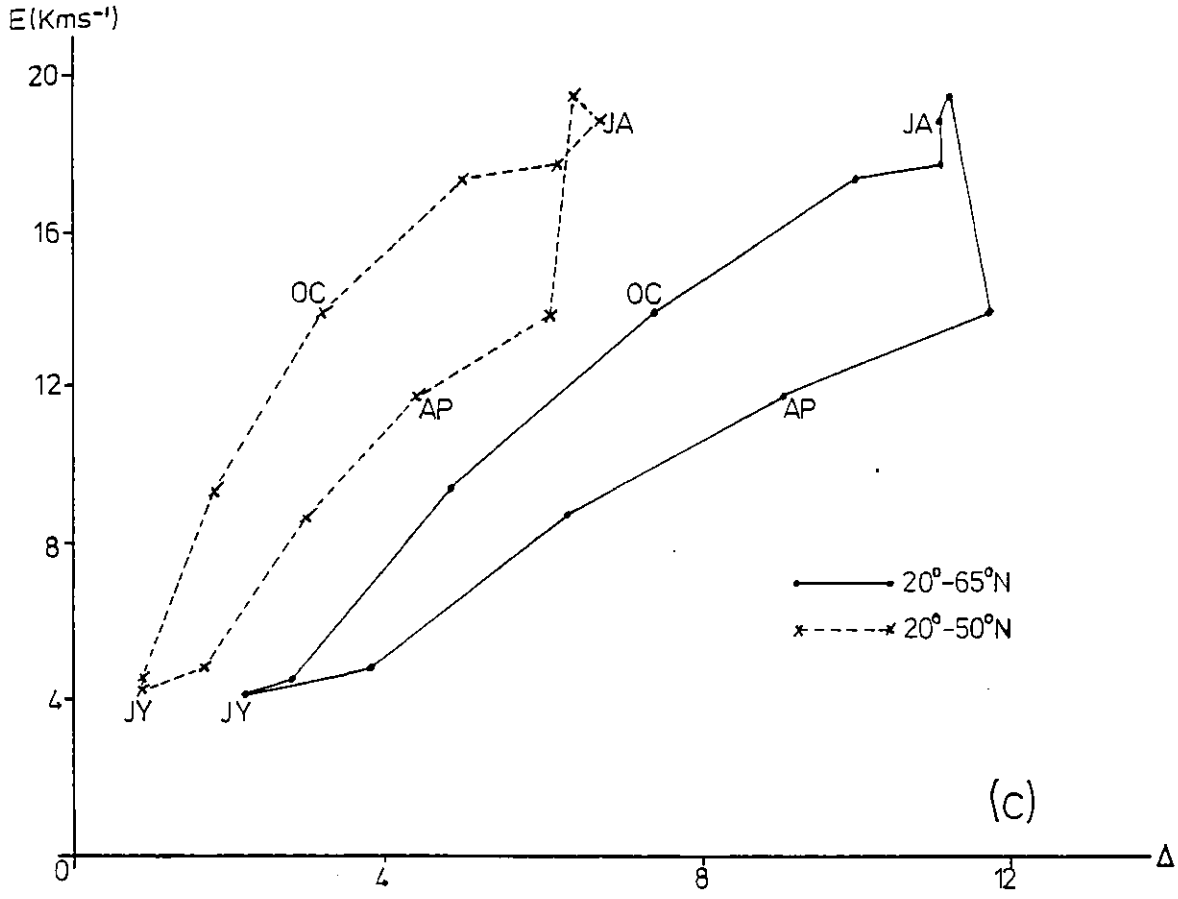

Fig. 2.8 continued.

temperature contrast at a time when the zonal-mean atmosphere-earth radiation balance changes only slowly; when the transport decreases, the temperature contrast increases as the change in the radiation balance does not counter this sufficiently rapidly (Energy balance in the atmosphere is discussed in more detail in Chapter 5). However, this only pertains to the zone north of 35°N; the action of the eddies south of this is to maintain the temperature contrast over the wider zone being considered (ie north of 20°N), indicating that the equatorward extent of the wintertime eddies is important.

Figs. 2.8b and 2.8c show that if ϕ_1 is moved to 70° or 65°N (keeping ϕ_2 at 20°N), the two-valued nature of the plot is just as pronounced, showing that any direct influence of polar ice, whose southern limit of extent is around 65°N, on the meridional temperature gradient as a cause of the observed two-valued behaviour is ruled out.

Finally, Fig. 2.8c also shows eddy heat transport against the entropy difference taken over 20° - 50°N, the region in which eddy heat transport increases with latitude (see Fig. 1.2), where local meridional temperature gradients are strongest (Fig. 2.7), and which may be regarded as a source of eddy heat transport. The eddy heat transport is clearly two-valued throughout most of the year in this case also, whence (together with the foregoing) we conclude that it is in the maintenance of the strong wintertime temperature gradient across this region into March when the eddy transport at the same time decreases sharply that the current problem may well lie.

Further evidence for the importance of this zone comes from van Loon's (1979) study. He found that eddy sensible heat transports (total or stationary) were most strongly correlated with local

temperature gradients to the south (as stated in Section 1.2); in particular, the transport at 55°N is most strongly correlated with the gradient in the region 25° - 45°N: again, the region where the gradients are strongest. Thus eddy transports will not be as well-correlated with an entropy gradient taken over a zone excluding this region; furthermore, the relationship between midlatitude eddy heat transports and temperature gradients in this region is probably not just a statistical correlation but a physical interaction also.

From all these results it is seen that the quasi-linear and two-valued behaviour of eddy sensible heat transport with respect to meridional entropy gradient seen in Fig. 1.1 occurs only when that gradient is taken over a region including most of the eddy heat transport source zone, 20° - 50°N, as we should expect from Fig. 2.7; in particular, the region 20° - 50°N is important to the midlatitude eddy heat fluxes in terms of its effect upon entropy gradients. The region 50° - 75°N plays a minor role in determining the form of eddy heat flux against entropy gradient.

2.5 Summary of Important Results.

(a) When the monthly-mean midlatitude eddy heat transport -- sensible or sensible plus latent -- is plotted against some large-scale extra-tropical meridional temperature gradient (both quantities being either tropospheric averages or values at individual pressure levels in the troposphere), it exhibits marked two-valued behaviour.

(b) This two-valued behaviour is principally a consequence of the variation of the stationary eddy heat transport.

(c) This behaviour is exhibited throughout the troposphere in the midlatitude zone 45° - 65°N; the stationary eddy sensible heat transport exhibits such behaviour in the lower stratosphere also.

(d) The existence of this behaviour is dependent on the temperature gradients in the zone 20° - 50°N, which is the source zone of eddy heat transport.

The problem of the observed two-valued behaviour seems now to be two problems, viz:-

(i) Why does the stationary eddy heat transport vary as it does (it cannot be because of temperature gradient variations)?

(ii) What controls the variation of temperature gradients?

CHAPTER 3

FURTHER INVESTIGATION OF EDDY HEAT TRANSPORT DATA

Introduction.

In this chapter, the longitudinal and latitudinal variations of the 500mb stationary eddy sensible heat transport and of its constituent wind and temperature fields are investigated in order to establish the nature of the changes in the atmospheric circulation which give rise to the observed variations of this heat transport. The changes in the zonal-mean variance fields and their correlation are first considered; these fields are then Fourier-analysed to determine the dominant space-scale of the observed variations in heat transport.

3.1 Zonal-Mean Variance Fields and Correlation.

The zonal-mean stationary eddy sensible heat transport is given by

$$E_{sT} = [\bar{v}^{*2}]\,[\bar{T}^{*2}]\,r_2(v,T) \qquad (3.1)$$

where

$r_2(v,T)$ is the spatial correlation between temperature and meridional wind fields.

Note that $[\bar{A}^{*2}]$, the spatial variance of some quantity A, is essentially a measure of the zonal asymmetry in A. The correlation $r_2(v,T)$ is a measure of some kind of phase difference between the two fields.

Tropospheric averages of $[\bar{v}^{*2}]$ and $[\bar{T}^{*2}]$ for each month and six latitudes are given in Table 3.1: they were calculated from the variances at different levels given in Oort and Rasmusson (1971). From these, values of $r_2(v,T)$ for the troposphere were calculated;

Table 3.1

Northern Hemisphere tropospheric averages of $[\bar{v}^{*2}]^{1/2}$, $[\bar{T}^{*2}]^{1/2}$ and $r_2(v,T)$ for each month, from Oort and Rasmusson (1971).

	$[\bar{v}^{*2}]^{1/2}$						$[\bar{T}^{*2}]^{1/2}$						$r_2(v,T)$					
	40	45	50	55	60	65	40	45	50	55	60	60	40	45	50	55	60	65
Jan	3.7	4.5	4.8	4.7	4.5	4.5	4.3	5.1	5.6	5.6	5.5	5.1	.43	.46	.45	.38	.27	.14
Feb	3.1	4.0	4.6	4.7	4.5	4.2	3.4	4.2	4.9	5.2	5.2	4.8	.41	.43	.45	.45	.39	.20
Mar	3.0	3.5	3.7	3.6	3.5	3.4	2.5	3.1	3.5	3.9	4.3	4.3	.29	.42	.46	.46	.38	.18
Apr	2.4	2.7	2.9	2.9	2.7	2.3	1.8	2.0	2.4	2.8	3.0	2.9	.11	.26	.39	.44	.38	.21
May	1.8	1.9	1.9	1.9	2.0	2.2	2.0	2.1	2.1	2.0	1.9	1.9	-.11	.07	.05	.21	.32	.24
Jun	2.0	1.9	1.8	1.9	2.0	1.8	2.3	2.3	2.3	2.1	1.9	1.8	-.15	-.29	-.43	-.35	-.11	.09
Jul	2.3	2.0	1.9	1.7	1.8	1.6	2.6	2.5	2.5	2.3	2.2	2.0	-.08	-.18	-.36	-.26	-.15	-.06
Aug	1.9	1.5	1.4	1.7	2.0	1.9	2.2	2.0	2.0	1.9	1.9	1.7	-.10	-.17	-.29	-.25	-.08	-.03
Sep	1.8	1.6	1.8	2.1	2.6	2.7	1.7	1.5	1.4	1.5	1.7	1.9	.20	.29	.28	2.9	.23	.16
Oct	2.0	2.4	2.6	2.9	3.2	3.0	1.8	2.3	2.8	3.2	3.5	3.6	.22	.34	.45	.45	.36	.20
Nov	2.7	3.2	3.2	3.2	3.4	3.6	2.7	3.6	4.4	4.8	4.9	4.8	.15	.28	.47	.59	.55	.34
Dec	3.2	3.9	4.0	3.8	3.3	2.9	3.5	4.5	5.1	5.2	4.9	4.4	.29	.36	.43	.46	.39	.15

these also are presented in Table 3.1.

This table shows that from 50°N northwards, between October and April $r_2(v,T)$ is roughly constant, save in November when it appears to be rather high at 55°, 60° and 65°N compared with the values round about. Closer inspection of Oort and Rasmusson (op. cit.) reveals that from 55°N northwards both $[\bar{v}^{*2}]$ and $[\bar{T}^{*2}]$ display values high compared with those round about in the upper half of the troposphere (though at 55°N the November peak in the tropospherically-averaged stationary eddy heat transport appears to be caused mainly by the large correlation). Without recourse to their original data-set it is impossible to say whether the problem is purely numerical or a genuine result caused by the behaviour of the atmosphere at least in the period used. However, the other data-sets to be discussed in this chapter do not show a similar peak in either the heat transport or the variances, whereas they do show the other key features of Fig. 1.1b (this is discussed more fully in Section 3.3). We believe therefore that this anomaly does not cast doubt on the general validity of Oort and Rasmusson's statistics; those for November at latitudes 55°N and northwards may contain some error.

We now look at each of the four quantities in Eq. (3.1) for the pairs of months when the difference in heat transport is greatest, namely February - March and April - November (the latter notwithstanding the foregoing: some useful information can be obtained, though the results must be interpreted with caution). 500mb values are presented in Tables 3.2a and b, using this level rather than a tropospheric average to permit comparison (below) with other data-sets.

Table 3.2a

$[\bar{v}^{*2}]$, $[\bar{T}^{*2}]$, $[\bar{v}^*\bar{T}^*]$ and $r_2(v,T)$ at 45° and 55°N, 500mb for February and March; from OR.

	45°N				55°N			
	$[\bar{v}^{*2}]$	$[\bar{T}^{*2}]$	$[\bar{v}^*\bar{T}^*]$	$r_2(v,T)$	$[\bar{v}^{*2}]$	$[\bar{T}^{*2}]$	$[\bar{v}^*\bar{T}^*]$	$r_2(v,T)$
February	21	11.2	5.9	.38	30	14.5	9.1	.43
March	16	6.2	4.3	.43	16	8.9	5.9	.49
March/February	.76	.55	.73	1.13	.53	.61	.65	1.14

Table 3.2b

As Table 3.2a, but April and November.

	45°N				55°N			
	$[\bar{v}^{*2}]$	$[\bar{T}^{*2}]$	$[\bar{v}^*\bar{T}^*]$	$r_2(v,T)$	$[\bar{v}^{*2}]$	$[\bar{T}^{*2}]$	$[\bar{v}^*\bar{T}^*]$	$r_2(v,T)$
April	9	2.0	2.0	.47	11	4.4	3.7	.53
November	12	10.6	2.9	.26	12	18.3	9.6	.65
April/November	.75	.19	.69	1.81	.92	.24	.39	.82

For February - March, the change in heat transport is entirely due to changes in the amplitudes of the temperature and wind fields at both latitudes, since their correlations are slightly larger in March. At 55°N the change is almost equally distributed between the two variances; at 45°N there is more change in the temperature variance. For April - November, at 55°N some of the difference lies in the correlation, very little in the wind variance, and most of it in the temperature variance; at 45°N the correlation is very much higher in April but the heat transport smaller then, due mainly to a very much smaller temperature variance. The behaviour of the tropospheric averages is similar (see Table 3.1), though the April - November difference in $[\overline{T}^{*2}]$ is not as great as at 500mb.

Thus these variations in stationary eddy sensible heat transport appear to be due to changes in the magnitude of the variances rather than in their correlation (or phase difference). In March the meridional wind and temperature fields are more zonally symmetric than in February, similarly for April compared with November.

3.2 Calculation of Local Values of E_{ST}.

3.2.1 Data-Sets.

In the following study, two other data-sets besides that of Oort and Rasmusson (1971 - hereafter designated OR) were used: monthly - mean charts published by the German Weather Service (hereafter designated DW), and Fourier components of the 500mb geopotential height and temperature fields contained in a report by Lejenäs and Madden (1982 - to be referred to as LM). This is done for the folllowing reasons:-

(i) To test the statistical significance of the observed heat transport variations.

(ii) To test whether the observed behaviour is reproduced year - by - year rather than being due to one highly anomalous year.

(iii) To test whether the behaviour is reproduced for a period different from that used in OR.

(iv) To investigate directly the longitudinal variation of the stationary eddy sensible heat transport and its component fields.

(v) To carry out a zonal harmonic analysis of wind and temperature fields.

3.2.1a German Weather Service Data.

Monthly-mean charts of the Northern Hemisphere up to October 1979 show values at regular latitude-longitude intervals as well as contours of most fields. The fields used are the 500mb and 300mb geopotential height and the 500/1000mb thickness: from these, local values of the 500mb temperature and meridional wind are calculated, the method of which is described in Section 3.2.2 below, and from these gridpoint values of eddy sensible heat transport can be determined.

This enables an average over several years' data to be taken, to

determine the latitudinal and longitudinal variations of the heat transport for each month; this can also be done for any individual month, enabling interannual variations to be investigated and the significance of month - to - month variations to be determined from the spread for each month. Zonal-mean statistics can be evaluated and compared with those in OR.

The disadvantage of the DW data is that it is only presented for full latitude circles down to 35° N. This means that it is not possible to obtain a plot of heat transport against entropy gradient, in the manner of Fig. 1.1b, since such a comparison requires that the entropy gradient be taken with a southern limit of 20° or 25° N - see Chapter 2, Section 2.4. However, the key features of the annual variation of heat transport will be compared.

The data is taken from the years 1967-72 and 1975-7, nine years in all.

3.2.1b Data from Lejenäs and Madden (1982).

This report presents the coefficients obtained from the double Fourier decomposition of daily 500mb geopotential heights and temperatures, and surface pressures, taken over 30, 17 and 30 years respectively. The decomposition is in longitude and time: for each 5° of latitude from 20° N to 85° N, the first six zonal wavenumbers are given, decomposed into the first four harmonics of the annual cycle. This enables any of the above fields to be recreated for most of the Northern Hemisphere for any day of the year, although as the fields are smoothed (by the choice of only four harmonics in time) the values for any particular day may be taken as similar to averages for some

arbitrary period around that day of about one month.

It seems surprising that just four annual harmonics should resolve individual months. Lejenäs and Madden state in their report that this is sufficient to represent the annual cycle where that cycle is large, citing earlier studies showing this to be valid. Provided the changes are smooth from one month to the next, the harmonics given will suffice (provided a significant change from one month to the next is large enough to be resolved: whether this is true in the present context will be discussed in Section 3.3 below).

Having reconstructed the 500mb fields, the stationary eddy heat transport at that level can be evaluated. This enables the long-term average heat transport distribution and entropy gradient to be calculated for each month; the temperature field is derived from the 17 years of data commencing in January 1963, so that it covers a period almost entirely different from that of OR (see Section 1.3.1 of Chapter 1) as well as longer, so comparison with OR can be made. This also has the advantage over DW in that 500mb temperatures are found directly rather than from thicknesses and by interpolation.

For both data-sets, winds are computed from geopotential heights, ie they are assumed to be geostrophic. At 500mb, this should be a good approximation both locally and for the zonal-mean (as $[\bar{v}^{*2}] \gg [\bar{v}]$).

3.2.2 Calculation of Sensible Heat Transport.

The geostrophic meridional wind is given by

$$\bar{v} = \frac{\partial \psi}{\partial x} = \frac{g}{f}\frac{\partial Z}{\partial x} \qquad (3.2)$$

where

ψ is streamfunction

Z is geopotential height.

Values of Z are given at 10° longitude intervals in DW; let this be a distance Δx. The meridional wind at the j^{th} point is then given by

$$\bar{v}_j = \frac{g(Z_{j+1} - Z_{j-1})}{2f\Delta x}$$

As $[\bar{v}] = 0$, we can write

$$\bar{v}_j^* = \frac{g(Z_{j+1} - Z_{j-1})}{2f\Delta x} \qquad (3.3)$$

For DW data, the temperature is obtained from the Hydrostatic Equation, using given thickness values for the 500/1000mb layer or thicknesses calculated from the 500mb and 300mb heights. The mean temperature for a layer of thickness ΔZ between pressure surfaces p_1, p_2 $(p_1 > p_2)$ is given by

$$T = \frac{g\,\Delta Z}{R \ln(p_1/p_2)} \qquad (3.4)$$

A pressure-weighted mean of the 500/1000mb and 300/500mb mean temperatures is used as the 500mb value. Taking these temperatures as being 750mb and 400mb values respectively, the weighting used is $T_{500} = \frac{2}{7}T_{750} + \frac{5}{7}T_{400}$. For the zonal-mean, values of $[\bar{T}^{*2}]$ at 45° and 55° N calculated by similar means from OR values at 700mb and 400mb are generally close to the 500mb values except in Summer at 45° N. There is no means of telling whether they are similar locally, but looking at contours on the charts will give an idea of the temperature and

wind fields and resultant heat transport, which can be used as a rough check on the numerical values obtained.

The zonal-mean spatial variance of the temperature field in LM is given by

$$[\bar{T}^{*2}] = \sum_{m=1}^{6} m^2 (g_m^2 + h_m^2) \qquad (3.5)$$

where

g_m, h_m are the cosine and sine coefficients for zonal wavenumber m in the Fourier expansion of T.

Similarly, the zonal-mean spatial variance of the meridional wind field is given, using Eq. 3.2, by

$$[\bar{v}^{*2}] = \frac{g}{f R \cos\phi} \sum_{m=1}^{6} m^2 (a_m^2 + b_m^2) \qquad (3.6)$$

where a_m, b_m are the Fourier coefficients for Z.

3.3 Zonal-Mean Statistics for DW and LM Data.

As a test of accuracy for the DW results, and to compare both DW and LM with OR, the zonal-mean statistics obtained from both DW and LM are here presented. Since OR heat transports are calculated from actual 500mb temperatures and winds, OR is taken as giving definitive values for the heat transport.

The 500mb spatial variances, correlations and heat transports at 45° and 55° N obtained from these data-sets are given in Tables 3.3 and 3.4; the ratios of these values to those in OR are given in Table 3.5. The DW values are averages of the 9 separate years analysed.

Table 3.3

As Table 3.2a, but data from DW.

	45°N				55°N			
	$[\bar{v}^{*2}]$	$[\bar{T}^{*2}]$	$[\bar{v}^{*}\bar{T}^{*}]$	$r_z(v,T)$	$[\bar{v}^{*2}]$	$[\bar{T}^{*2}]$	$[\bar{v}^{*}\bar{T}^{*}]$	$r_z(v,T)$
February	32.9	15.8	9.5	.42	37.9	17.6	10.1	.39
March	23.7	8.6	5.8	.41	23.2	10.9	6.8	.43
March/February	.78	.57	.68	.98	.63	.62	.68	1.10

Table 3.4

As Table 3.2a, but data from LM.

	45°N				55°N			
	$[\bar{v}^{*2}]$	$[\bar{T}^{*2}]$	$[\bar{v}^{*}\bar{T}^{*}]$	$r_z(v,T)$	$[\bar{v}^{*2}]$	$[\bar{T}^{*2}]$	$[\bar{v}^{*}\bar{T}^{*}]$	$r_z(v,T)$
February	22.2	17.2	6.2	.32	18.7	15.7	7.1	.41
March	16.9	10.7	3.9	.29	13.1	11.7	5.0	.40
March/February	.76	.62	.63	.91	.70	.74	.70	.98

Table 3.5a

Ratios of DW/OR values of quantities in Eq. 3.1 at 500mb, 45° and 55°N.

	45°N				55°N			
	$[\bar{v}^{*2}]$	$[\bar{T}^{*2}]$	$[\bar{v}^*\bar{T}^*]$	$r_2(v,T)$	$[\bar{v}^{*2}]$	$[\bar{T}^{*2}]$	$[\bar{v}^*\bar{T}^*]$	$r_2(v,T)$
February	1.57	1.41	1.61	1.08	1.26	1.21	1.11	.93
March	1.48	1.39	1.35	.91	1.45	1.22	1.15	.90
March/February	1.03	1.04	.93	.89	1.19	1.02	1.05	1.00

Table 3.5b

As Table 3.5a, but ratios LM/OR.

	45°N				55°N			
	$[\bar{v}^{*2}]$	$[\bar{T}^{*2}]$	$[\bar{v}^*\bar{T}^*]$	$r_2(v,T)$	$[\bar{v}^{*2}]$	$[\bar{T}^{*2}]$	$[\bar{v}^*\bar{T}^*]$	$r_2(v,T)$
February	1.06	1.54	1.06	.84	.62	1.08	.78	.95
March	1.06	1.73	.91	.67	.82	1.31	.85	.82
March/February	1.00	1.13	.86	.81	1.32	1.21	1.08	.86

From these tables it can be seen that DW data produces variances and heat transports more than 10% greater than OR's, especially at 45°N; LM variances and heat transports vary considerably in relation to OR's, and the March/February ratios for DW are closer to OR's than are LM's. Both sets do however show the same features as OR, namely that the fall in heat transport from February to March is due to changes in the variances rather than in their correlation, roughly equally distributed between them at 55°N but larger in $[\bar{v}^{*2}]$ at 45°N.

It is noticeable that both DW and LM underestimate the changes in the variances compared with OR, especially at 45°N; they overestimate the fall in heat transport at 45°N and underestimate that at 55°N. This suggests that changes visible in maps or sections of these fields calculated from DW or LM will in most cases be smaller than those to be found in OR's original data-set.

The difference between April and November heat transports is marked in DW: 3.3 and 7.6 Kms^{-1} for the two months respectively; it is not so obvious in LM (see below).

There is of course no strong reason to suppose that OR defines the long-term climatic means more accurately than the other two data-sets (except that the analysis is more rigorous and complete), since all are for different periods, and of these OR spans the shortest time. In fact, the fields described by LM are probably closest to the long-term mean as they are for the longest period, despite the truncations in space and time.

It seems reasonable to use results from both DW and LM to obtain a qualitative description of the change in the circulation from

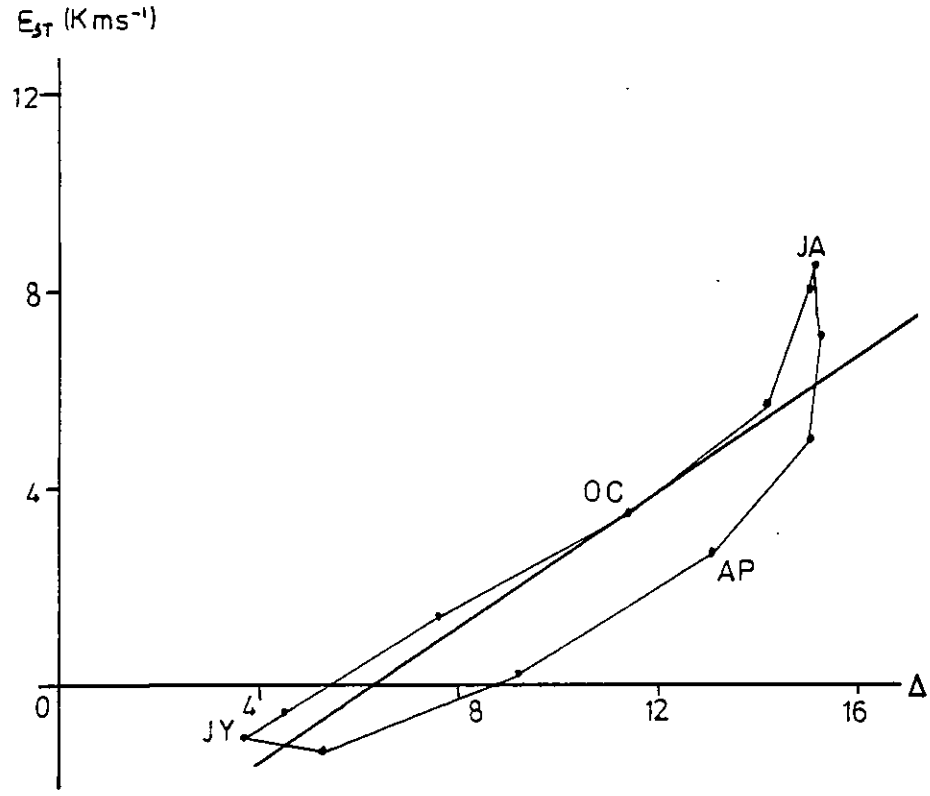

Fig. 3.1: 500mb zonal-mean stationary eddy sensible heat transport at 55°N against square of meridional entropy gradient, from LM data.

February to March, but not to regard them as quantitatively accurate, since both have deficiencies in the information presented.

The annual cycle of stationary eddy sensible heat transport at 55°N plotted against Δ, both taken from LM, is shown in Fig. 3.1. It is very similar to that in Fig. 1.1b, showing distinct two-valued behaviour, save that November no longer displays such an anomalously large transport. Also, the sharp fall in heat transport from February to March seen in Fig. 1.1b is here spread over January to March, the fall over this period being proportionally the same as that for February-March in OR. This may be due to the temporal truncation at four annual harmonics (see Section 3.2.1b), indicating that the temperature and/or geopotential height fields do not change that smoothly; however, the resolution is adequate for our purposes as it shows the desired two-valued behaviour.

I believe therefore that the two-valued behaviour of zonal-mean stationary eddy heat transport with respect to entropy gradient is a genuine property of the variation of atmospheric eddy heat transports, since it is reproduced in two data-sets covering different periods of time and independently derived; its most obvious manifestation, the sharp fall from February to March, is also seen in the third set (DW).

3.4 Statistical Tests.

In order to be certain that the observed behaviour of the stationary eddy sensible heat transport is significant, a knowledge of the interannual variation is required. Such a study was undertaken by Hsiao (1979) but only covers the months of January, April, July and October; Oort's earlier (1977) study is even more partial. We have

therefore used the results from DW to look at differences in the stationary eddy sensible heat transport at 55°N.

Error-bars shown in Fig. 1.1 are 1 standard error. For February - March and April - November, they show that it is improbable that the heat transports for each pair of months are in fact the same. The hypothesis that the values of heat transport for each of the nine Februaries and nine Marches are in fact part of the same population (and hence that the heat transport is really the same for the two months) can be tested using Student's t, similarly for the seven Aprils and Novembers (data being incomplete for these months in two of the years). The values of t are:-

February - March: $t = 3.30$ (16 degrees of freedom)

April - November: $t = 3.51$ (12 degrees of freedom)

These values mean that the two sets of values for each pair of months belong to <u>different</u> populations to better than 99% confidence, ie that the heat transports in February and March are <u>not</u> the same (similarly April and November).

The systematic nature of the deviation from the regression-line of both the total and stationary eddy heat transport also suggests that the two-valued nature of the plot is a physical rather than a statistical phenomenon.

Table 3.6 shows the stationary eddy heat transport for the four key months in the individual years (as calculated from DW), and the ratios for each pair of months. From this, and from the results of Section 3.3 above, it is clear that the two-valued behaviour of this transport is not limited to one or two highly anomalous years, or even

Table 3.6

Stationary eddy sensible heat transport at 500mb, 55°N for four key months.

	1967	1968	1969	1970	1971	1972	1975	1976	1977	MEAN
February	12.8	8.5	11.1	10.4	6.8	8.8	11.2	10.5	10.9	10.1
March	7.9	3.0	7.3	10.2	6.8	5.3	5.4	10.2	5.1	6.8
April	5.7	1.6	4.3	2.1	2.1	2.5	-	5.0	-	3.3
November	10.8	7.2	7.0	3.2	6.4	7.0	-	11.5	-	7.6
March/February	.62	.45	.66	.98	1.00	.60	.48	.97	.47	.68
April/November	.53	.22	.61	.66	.33	.36	-	.43	-	.43

to one period of a few years, but is a regular phenomenon (though it does not occur in every year - this will be discussed further in Section 3.7) characteristic of the annual variation of the atmospheric circulation.

We conclude that the two-valued behaviour of stationary eddy sensible heat transport with respect to meridional entropy gradient is a statistically significant phenomenon occuring in many years.

3.5 Spatial Variation of 500mb Stationary Eddy Heat Transport.

Fig. 3.2 shows the stationary eddy meridional sensible heat transport at 500mb over most of the Northern Hemisphere for January, February and March, calculated from LM. The component wind and temperature fields are shown in Figs. 3.3 and 3.4, the geopotential height field in Fig. 3.5.

Fig. 3.2 shows two main regions of strong poleward heat transport in January, the stronger centred over NE China, and to the southwest of the centre of a trough over the North Pacific; the second is centred at about 50°N 35°W, over the Atlantic. There is a smaller maximum over the eastern Pacific, and a region of southward heat transport NE of Japan (SE of the Pacific trough). The maximum associated with the Pacific trough is due to strong southward transfer of cold air; that over the Atlantic results from poleward transport of warm air. The latitude of maximum heat transport is 50°N for all these months. The February map is similar to that for January: the maxima are in the same place, but slightly reduced in amplitude.

The March map shows clearly that while the peaks in heat transport remain in the same place, that to the southwest of the

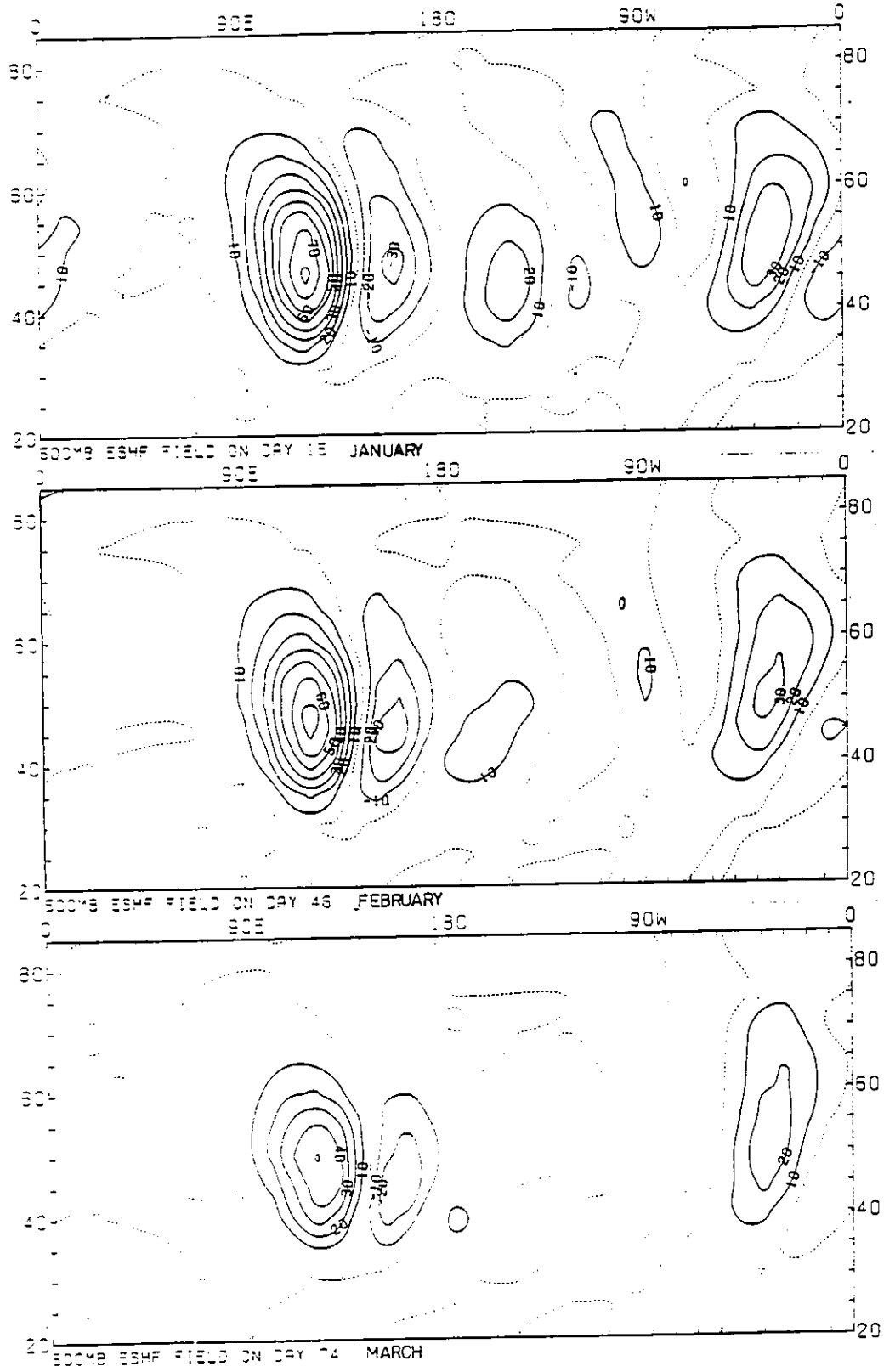

Fig. 3.2: 500mb stationary eddy sensible heat transport (meridional component) in January, February and March, from LM data. Units: Kms^{-1}.

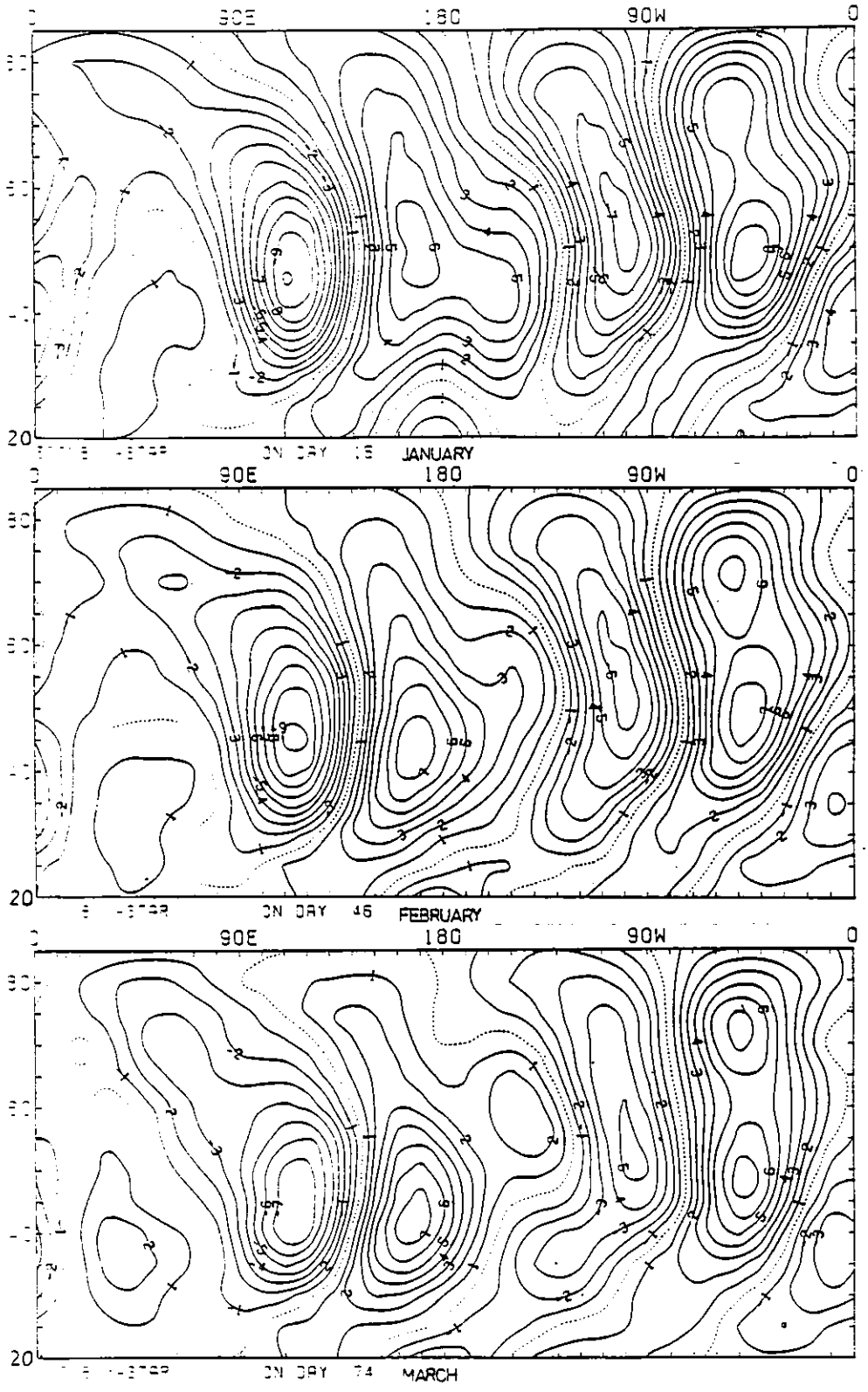

Fig. 3.3: 500mb meridional wind in January, February and March, from LM data Units: ms^{-1} .

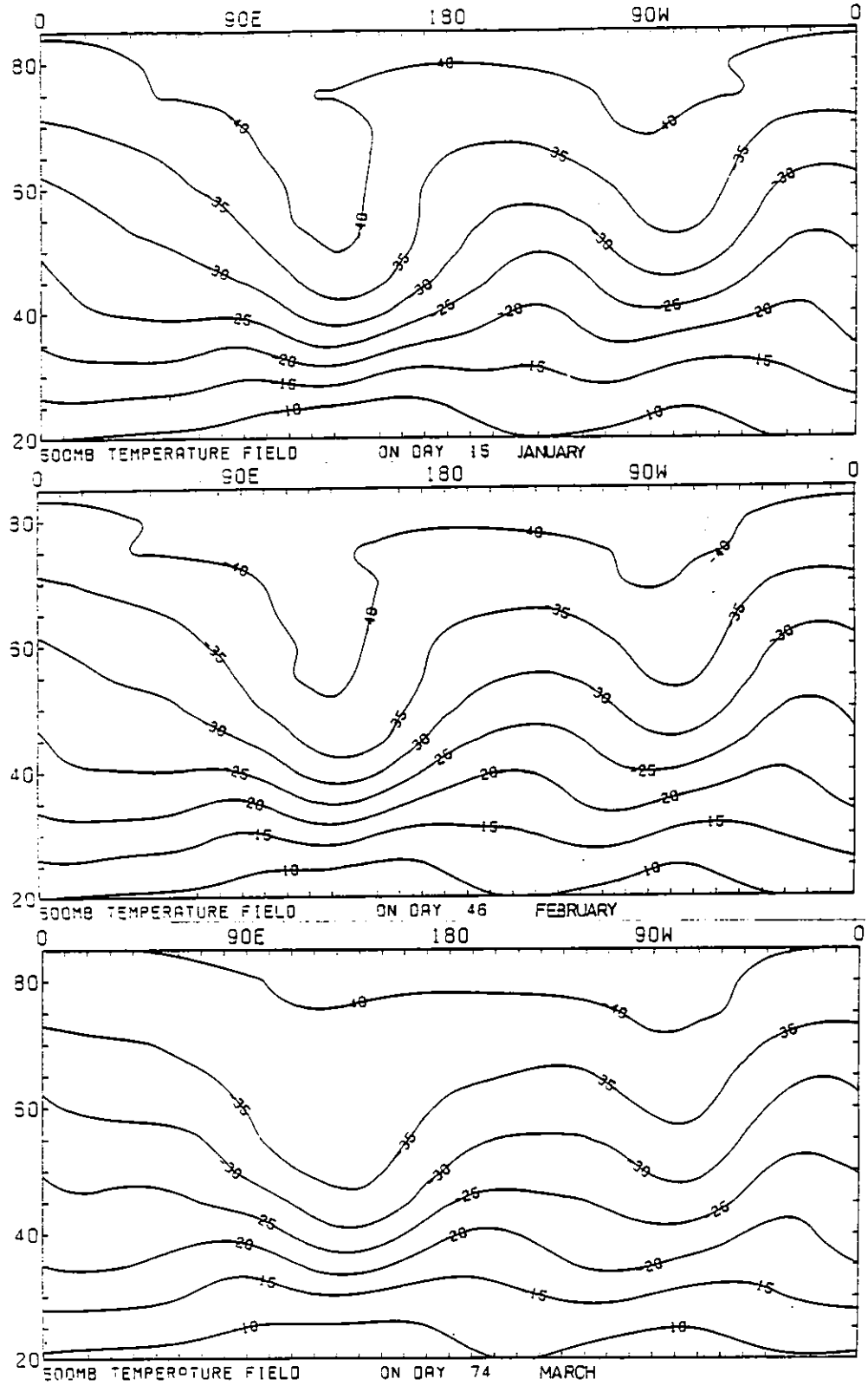

Fig. 3.4: 500mb temperature in January, February and March, from LM data. Units: °C.

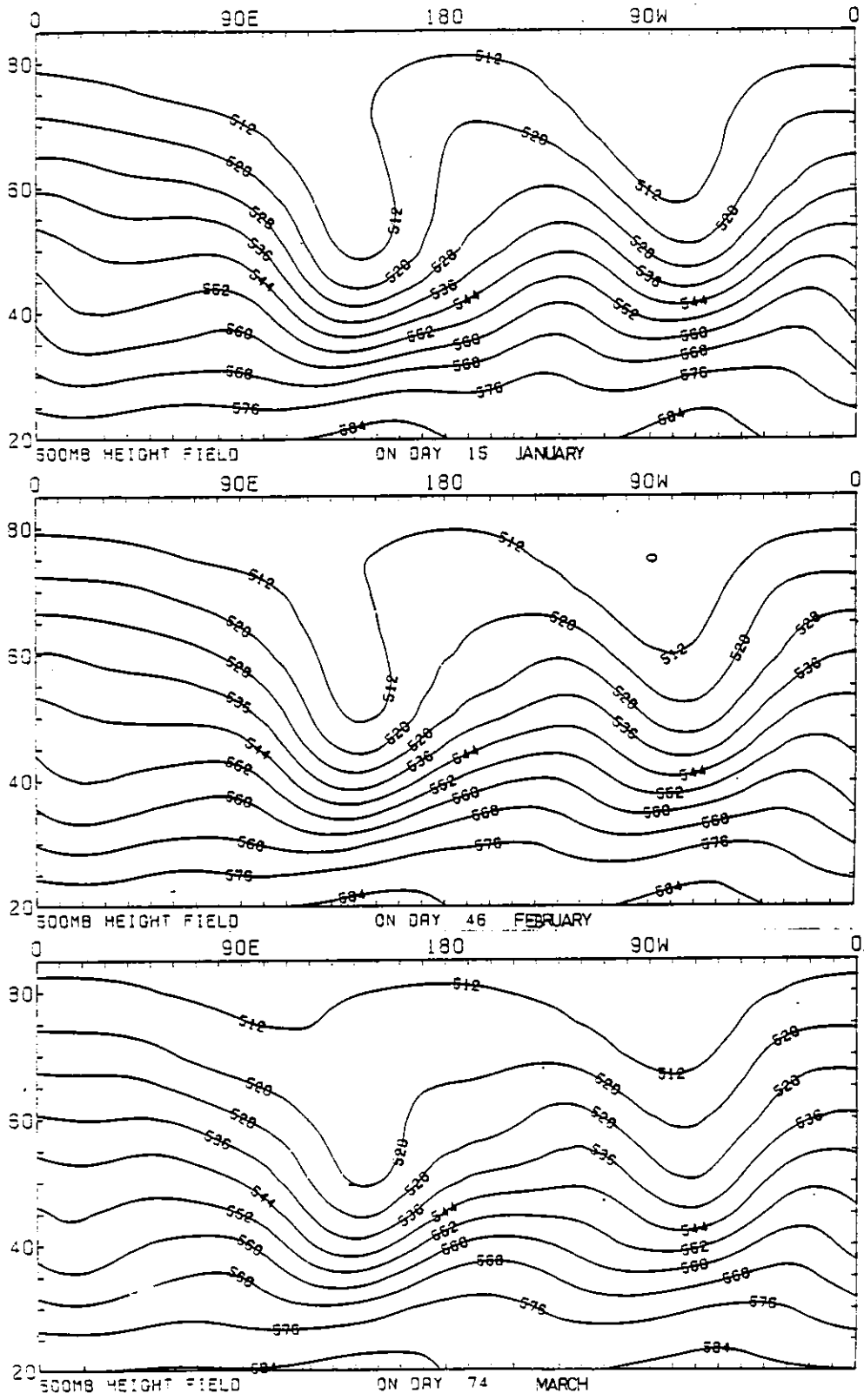

Fig. 3.5: 500mb geopotential height in January, February and March, from LM data. Units: 10gpm.

Pacific trough in particular is much reduced in amplitude; that over the Atlantic, and the region of southward transport over the Pacific, are also smaller in intensity.

Dividing the latitude circle 55°N into regions of peaks and troughs in the heat transport, the heat transports for each month, and the change to March, are given in Table 3.7 below. The boundaries between sectors are in general intended to be points where the flux changes sign; the boundary longitudes given are the outer grid-points used in calculating each sector contribution.

It is clear from this that two-thirds or more of the change from January to March is accounted for by the fall in heat transport to the southwest of the Pacific trough, the Atlantic peak also contributing an important fraction. Thus the large change in heat transport during these months is concentrated in two regions of large poleward heat transport which together cover only one-third of the latitude circle.

Table 3.7

Heat Transport Contributions at 55°N by Sectors for January, February and March (Units: Kms^{-1}).

				CHANGE	
Sector	January	February	March	Mar-Jan	Mar-Feb
0° - 60°E	-.9	-.6	-.2	+.7	+.4
70°E - 140°E	6.2	5.5	3.8	-2.4	-1.7
150°E - 180°	-1.5	-1.5	-1.2	-.7	+.3
170°W - 130°W	1.1	.8	.4	-.7	-.4
120°W - 60°W	.3	.1	.2	-.2	+.1
50°W - 10°W	3.2	2.8	1.9	-1.3	-.9
ZONAL MEAN	8.5	7.1	5.0	3.5	2.1

From Figs. 3.3 - 3.5 it is seen that the change in heat transport is due to both the wind and temperature fields becoming less zonally asymmetric (the flow is more zonal). In particular, the Pacific trough is much less deep in March; the associated temperature trough is also smaller in amplitude. Thus the fall in heat transport is due principally to the decay of the Pacific trough and also that over central North America, occurs in a relatively narrow region, and is associated with reduction in longitudinal contrasts as well as meridional ones.

The mean values of $\bar{v}^*$ and $\bar{T}^*$ in the two key sectors are given in Table 3.8.

Table 3.8

Mean $\bar{v}^*$ and $\bar{T}^*$ at 500mb, 55° N in key sectors for January - March, from Lejenäs and Madden (1982)

	$\bar{v}^*(ms^{-1})$		$\bar{T}^*(K)$	
	70° E-140° E	50° W-10° W	70° E-140° E	50° W-10° W
January	-4.6	5.5	-5.0	4.7
February	-4.5	5.0	-4.7	4.5
March	-4.0	3.9	-3.8	4.1

This shows that in the Pacific sector it is the temperature field which changes most, whereas over the Atlantic much of the change is in the wind field. Fig. 3.4 shows this clearly: over the North Pacific region, very cold air (around -40° C) is no longer being brought southwards in March (due to the change in intensity of the trough there), whereas the decrease in amplitude of the trough over Canada has little effect on the temperature field around that region, but

results in increased zonality of the flow and hence smaller meridional winds.

It was suggested earlier that $[\bar{v}^{*2}]$ and $[\bar{T}^{*2}]$ change by about the same amount from February to March: if the principal features of the stationary wave pattern are thermally-forced, then we should expect this to be true locally also. The Pacific trough is probably due to thermal forcing (strong heating in the region of the Kuroshio current: see next chapter, Sections 4.1.6 and 4.3.3): the results above appear at first sight inconsistent with this, but it must be borne in mind that the temperature and meridional wind fields are not in phase, and so the sectors chosen above do not cover equivalent parts of these two fields (eg 40° either side of the maxima in each).

The fall in heat transport from January to March is therefore due to the reduced intensity of the two troughs whcich dominate the mid- and high-latitude circulation in winter, in particular that over eastern Siberia; the change in this has a particularly marked effect on the associated temperature field. The differences between the April and November fields are similar to those for January - March, though the differences between the temperature fields in the Atlantic sector make a significant contribution to the difference in heat transport in that region between the two months. The problem of why the stationary eddy heat flux varies as it does through the year is thus reduced to explaining why these two troughs change as they do: this is discussed in Chapters 4 and 5.

3.6 Fourier Analysis.

Introduction.

An alternative approach to the study of the annual variation of eddy heat transports is to carry out a Fourier analysis of the component fields (whence the Fourier analysis of their product, ie the heat transport, can be derived). This is of particular value for spectral climate models, enabling comparison for individual modes between real and model atmospheres, and also yields information on both the zonal-mean and zonally-asymmetric components of the heat transport field, as well as on the space-scale of the variations. LM already has the Fourier analysis of the component fields; those in DW require Fourier analysis; the breakdown of the heat transport into interactions between pairs of wavenumbers (one in wind, the other in temperature) needs to be carried out for both sets.

Several other studies besides that of Lejenäs and Madden (op. cit.) have described the atmospheric circulation in terms of zonal or spherical harmonics. Eliasen (1958) looked at the 500mb and 1000mb geopotential height, kinetic energy and momentum transport for October-November 1950, finding that at 50°N and 60°N zonal wavenumbers 1, 2 and 3 dominated. Van Loon, Jenne and Labitzke (1973) studied the amplitude and phase of those three wavenumbers in January and July (which at 50°N account in January for 96% of the total variance of geopotential height), for geopotential height from the surface up to 10mb in the Northern Hemisphere, and also the tropospheric temperature waves at selected latitudes. Their data-set comes from the years 1964-1970. For the geopotential height at 50°N and 500mb, their results are very similar to those of LM, both in longitudinal cross-section and in the Fourier amplitudes. Wavenumber 1 is

strongest, with wavenumbers 2 and 3 equal in amplitude (wavenumber 3 is smaller in LM).

These and other studies have generally concentrated on the geopotential height field, either for seasons or for single non-consecutive months. In this section, Fourier analysis of temperature and wind fields at 500mb, principally for the months January, February and March, will be presented, together with the resultant heat transport due to interactions between wavenumbers.

3.6.1 Methods of Fourier Analysis of Fields.

The Fourier representation of some quantity A^* at longitude λ on a latitude circle, with A^* defined at 2M points on the circle, is given by

$$A^*(\lambda) = \sum_{m=1}^{M} a_m \cos m\lambda + \sum_{m=1}^{M} b_m \sin m\lambda \qquad (3.7)$$

A zonal harmonic analysis was applied to the $\bar{v}^*$ and $\bar{T}^*$ fields calculated from DW data for each month used, covering just zonal wavenumbers 1-6. This is sufficient to represent nearly all ($>99\%$) of the monthly-mean fields, and is also a practical limit since higher wavenumbers are not well represented by 36 points. Eq. (3.3) may therefore be written, in amplitude and phase form, as

$$A^*(\lambda) \approx \sum_{m=1}^{6} c_m \cos(m\lambda - \chi_m) \qquad (3.8$$

where

$$c_m^2 = a_m^2 + b_m^2$$

$$\chi_m = \tan^{-1}(b_m/a_m)$$

The contribution ξ_m by wavenumber m to the variance $\lceil \bar{A}^{*2} \rceil$ is given by

$$\xi_m = \frac{c_m^2}{\sum_{m=1}^{6} c_m^2} \tag{3.9}$$

This is the form used in the presentation of the analysis of PW.

Given the cosine and sine coefficients of meridional wind (a_m, b_m) and temperature (g_n, h_n) for the wavenumbers m and n respectively in these fields, the contribution of that particular combination of wavenumbers to the heat transport can be calculated. There is a contribution to two wavenumbers: (m + n) and |m - n|. Let the cosine and sine coefficients for one wavenumber of the heat transport be d and e respectively; then

$$\begin{aligned} d_{|m-n|} &= \tfrac{1}{2}\,(a_m g_n + b_m h_n) \\ e_{|m-n|} &= \tfrac{1}{2}\frac{(m-n)}{|m-n|}(b_m g_n - a_m h_n) \\ d_{(m+n)} &= \tfrac{1}{2}\,(a_m g_n - b_m h_n) \\ e_{(m+n)} &= \tfrac{1}{2}\,(a_m h_n + b_m g_n) \end{aligned} \tag{3.10}$$

The cosine and sine coefficients for each wavenumber l in the heat transport can be obtained by summing all the coefficients d and e for which |m - n| = l and (m + n) = l. The total heat transport at longitude λ is then given by

$$\begin{aligned} E_{ST}(\lambda) = \sum_{m=1}^{6}\sum_{n=1}^{6}\{ & d_{|m-n|}\cos(|m-n|\lambda) + e_{|m-n|}\sin(|m-n|\lambda) \\ & + d_{(m+n)}\cos((m+n)\lambda) + e_{(m+n)}\sin((m+n)\lambda)\} \end{aligned} \tag{3.11}$$

When m = n, the wind and temperature fields interact to produce wavenumbers 1 = 0 and 1 = 2m in the heat transport: the former is the zonal-mean, which is thus given by

$$\overline{E}^{\lambda}_{ST} = \frac{1}{2}\sum_{m=1}^{6}(a_m g_m + b_m h_m) \qquad (3.12)$$

Thus the zonal-mean stationary eddy sensible heat transport can be broken down by wavenumbers in the constituent fields; it is due only to interactions between the same wavenumbers in both fields. This component can be decoupled from the zonally-asymmetric part of the heat transport, which is composed of interactions between both identical and different wavenumbers in the constituent fields.

3.6.2 Fourier Analysis of Wind and Temperature Fields.

The amplitudes, phases and contributions to the variance of the 500mb, 55°N meridional wind and temperature fields for February and March from DW and for January and March from LM are given in Figs. 3.6a and 3.6b respectively. In general both sets show the same features in both fields, especially for wavenumbers 1-3; the contributions to the variances are particularly close. The phases from LM generally seem to lie 10° - 20° east of those from DW, and also to give a phase difference between wind and temperature field some 10° larger; it is difficult to say why this should be so.

In January (LM) and February (DW), the strongest wavenumber in the temperature field is wavenumber 2, with wavenumber 1 the next strongest; besides these only wavenumbers 3 and 4 contribute significantly. The most significant fall to March is in wavenumber 2; wavenumber 1 is hardly changed, wavenumber 3 changes by more but

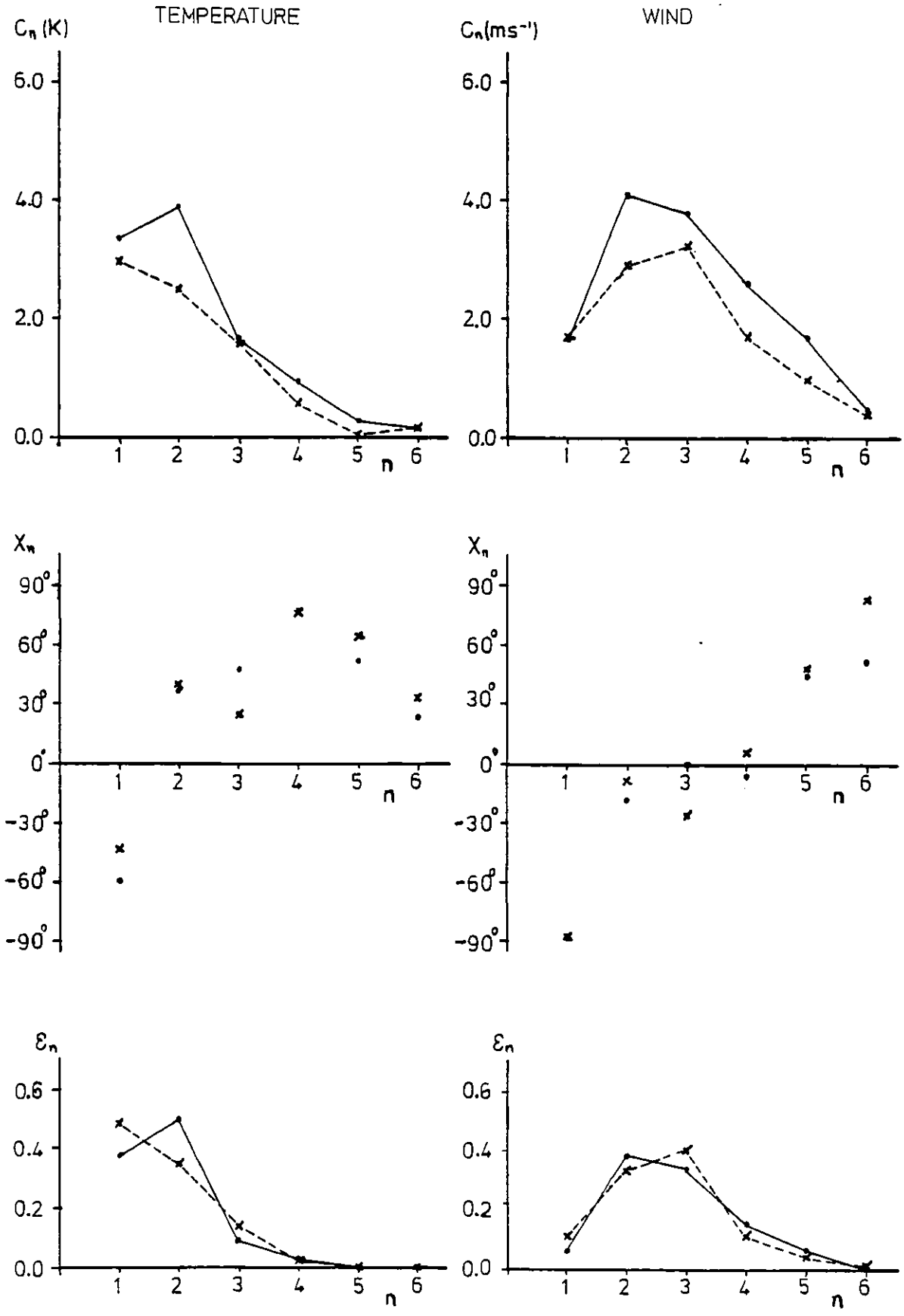

Fig. 3.6a: Amplitudes (C_n), phases (X_n) and variance contributions (ε_n) of February (•——•) and March (×- - - -×) temperature and meridional wind at 500mb, 55° N against wavenumber (n), from DW data.

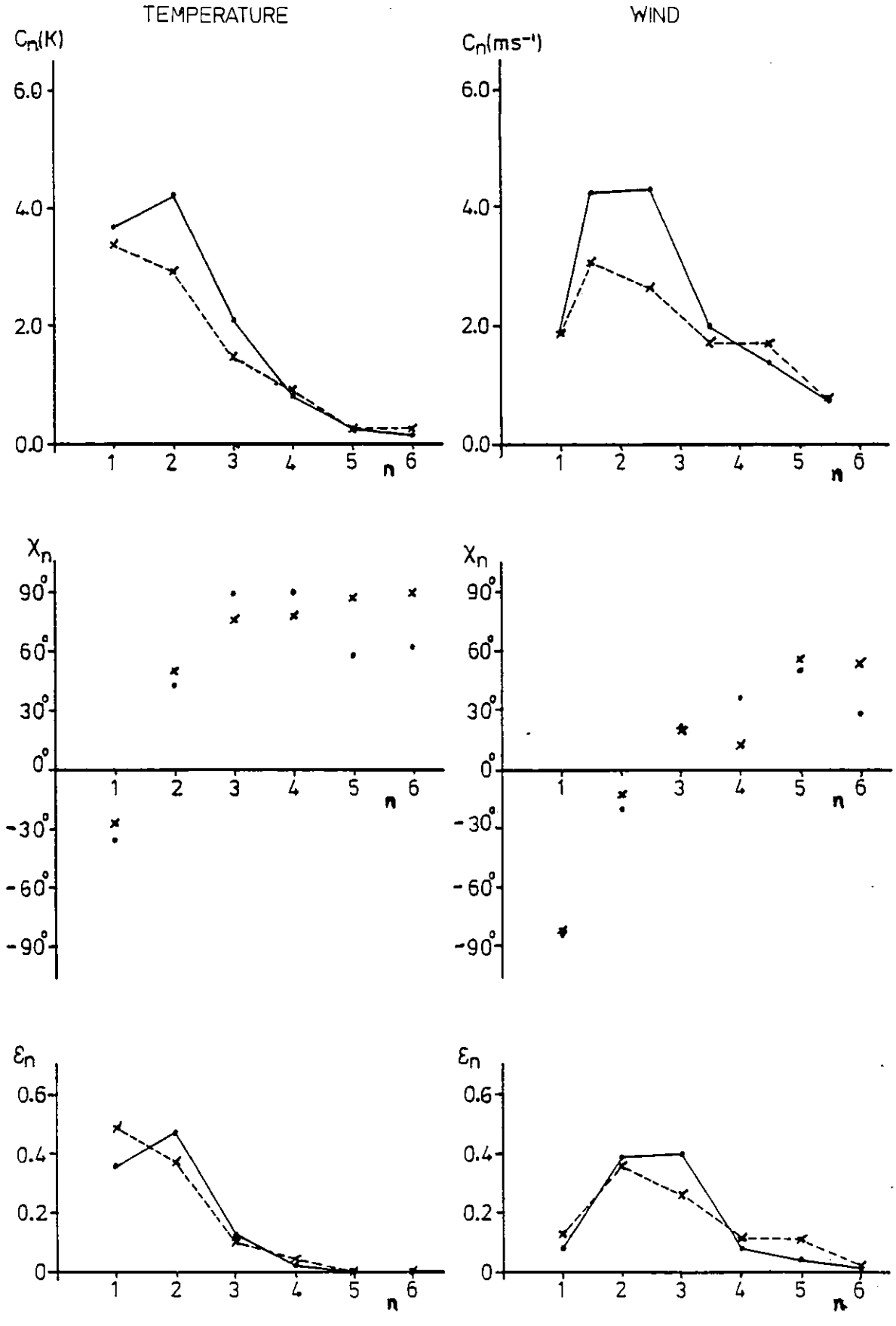

Fig. 3.6b: As Fig. 3.6a, but for January (•———•) and March (×- - -×), from LM data.

contributes less to the variance in the first place. Wavenumbers 1-4 contribute over 99.5% of the variance in the temperature field in all three months.

Wavenumber 3 in the wind field differs a little between DW and LM. In LM it is just stronger than wavenumber 2 in January, and drops considerably to March; in DW wavenumber 2 is strongest in February, and has the largest drop to March, while wavenumber 3 becomes the most important then. Wavenumber 3 being smaller than wavenumber 2 in DW (February) but larger in LM (January) seems to be because there is almost no contribution from wavenumber 3 in 1972; the discrepancy for March has no obvious cause.

The cut-off in significance for the wind field is at a higher wavenumber than for the temperature field: this is easily explained by the fact that $v^* \propto \partial\psi/\partial x$, which in the Fourier expansion of v^* means that $c_m \propto m$ (where, as before, $c_m^2 = a_m^2 + b_m^2$).

Thus both temperature and wind fields are significantly modified in March by the large fall in the amplitude of wavenumber 2 from January and February; the wind field is also affected by the change in wavenumber 3. At 55°N, these wavenumbers are equivalent to wavelengths of around 11 000km and 7 500km respectively. This means that the monthly-mean height and temperature waves are generated by longitudinal variations on the scale of continent - ocean contrasts; hence the cause of the change in eddy heat transport from February to March is likely to be on this scale also. We shall return to this idea in Chapters 4 and 5.

Table 3.9. 'ESHF' is Stationary Eddy Sensible Heat Transport.

FOURIER ANALYSIS OF FEB (DW) ESHF FIELD

N	C	PHASE	N	C	PHASE
0	6.62	0	3	9.82	-70
1	7.66	64	4	7.87	17
2	2.82	64			

SPATIAL VARIANCE OF ESHF FIELD = 112.48

FOURIER ANALYSIS OF FEB (DW) ESHF FIELD

N	C	PHASE	N	C	PHASE
0	8.78	0	4	2.00	95
1	2.13	135	5	10.65	-86
2	7.00	-73	6	3.13	164
3	9.82	-73			

SPATIAL VARIANCE OF ESHF FIELD = 138.66

FOURIER ANALYSIS OF FEB (DW) ESHF FIELD

N	C	PHASE	N	C	PHASE
0	8.96	0	5	6.80	-107
1	.59	-179	6	9.05	-157
2	5.38	-106	7	3.76	115
3	13.05	-83	8	1.23	70
4	2.00	-83			

SPATIAL VARIANCE OF ESHF FIELD = 173.62

FOURIER ANALYSIS OF FEB (DW) ESHF FIELD

N	C	PHASE	N	C	PHASE
0	9.07	0	6	6.74	-143
1	1.07	179	7	7.34	99
2	5.13	-119	8	2.25	9
3	12.78	-70	9	1.20	-64
4	4.74	103	10	.27	156
5	6.80	103			

SPATIAL VARIANCE OF ESHF FIELD = 182.72

FOURIER ANALYSIS OF FEB (DW) ESHF FIELD

N	C	PHASE	N	C	PHASE
0	9.07	0	7	7.69	104
1	1.14	169	8	2.06	-6
2	5.14	-115	9	.93	-61
3	13.41	-70	10	.27	148
4	5.04	117	11	.07	-145
5	7.54	-103	12	.04	14
6	6.74	-103			

SPATIAL VARIANCE OF ESHF FIELD = 199.75

FOURIER ANALYSIS OF MAR (DW) ESHF FIELD

N	C	PHASE	N	C	PHASE
0	4.15	0	3	6.44	-51
1	4.69	61	4	3.62	31
2	2.54	61			

SPATIAL VARIANCE OF ESHF FIELD = 41.49

FOURIER ANALYSIS OF MAR (DW) ESHF FIELD

N	C	PHASE	N	C	PHASE
0	5.71	0	4	4.11	135
1	2.89	122	5	6.29	-105
2	6.93	-102	6	2.52	117
3	6.44	-102			

SPATIAL VARIANCE OF ESHF FIELD = 80.32

FOURIER ANALYSIS OF MAR (DW) ESHF FIELD

N	C	PHASE	N	C	PHASE
0	5.88	0	5	6.07	-133
1	1.85	109	6	2.95	-178
2	7.16	-117	7	2.22	97
3	7.65	-68	8	.48	80
4	4.11	-68			

SPATIAL VARIANCE OF ESHF FIELD = 90.42

FOURIER ANALYSIS OF MAR (DW) ESHF FIELD

N	C	PHASE	N	C	PHASE
0	5.88	0	6	3.03	152
1	1.74	116	7	2.95	121
2	7.82	-118	8	1.21	48
3	6.64	-63	9	.32	20
4	5.37	143	10	.03	-28
5	6.07	143			

SPATIAL VARIANCE OF ESHF FIELD = 96.72

FOURIER ANALYSIS OF MAR (DW) ESHF FIELD

N	C	PHASE	N	C	PHASE
0	5.91	0	7	3.64	118
1	1.75	113	8	.85	81
2	7.91	-117	9	.85	33
3	7.17	-64	10	.24	10
4	6.06	143	11	.09	-69
5	6.76	-135	12	.04	-36
6	3.03	-135			

SPATIAL VARIANCE OF ESHF FIELD = 111.68

Table 3.10. As Table 3.9,but for LM data.

FOURIER ANALYSIS OF FEB (LM) ESHF

N	C	PHASE	N	C	PHASE
0	5.42	0	3	10.80	-47
1	6.44	47	4	6.95	27
2	3.88	47			

SPATIAL VARIANCE OF ESHF FIELD = 110.69

FOURIER ANALYSIS OF FEB (LM) ESHF

N	C	PHASE	N	C	PHASE
0	6.68	0	4	4.80	113
1	4.05	95	5	9.59	-111
2	9.55	-111	6	3.03	110
3	10.80	-111			

SPATIAL VARIANCE OF ESHF FIELD = 174.16

FOURIER ANALYSIS OF FEB (LM) ESHF

N	C	PHASE	N	C	PHASE
0	7.04	0	5	11.29	-128
1	4.33	76	6	2.61	-150
2	11.28	-120	7	2.75	112
3	12.70	-56	8	.63	116
4	4.80	-56			

SPATIAL VARIANCE OF ESHF FIELD = 256.28

FOURIER ANALYSIS OF FEB (LM) ESHF

N	C	PHASE	N	C	PHASE
0	7.09	0	6	.06	116
1	4.31	83	7	5.50	111
2	11.64	-124	8	1.05	-8
3	13.22	-47	9	.70	-28
4	7.11	109	10	.13	-165
5	11.29	109			

SPATIAL VARIANCE OF ESHF FIELD = 269.34

FOURIER ANALYSIS OF FEB (LM) ESHF

N	C	PHASE	N	C	PHASE
0	7.03	0	7	5.39	123
1	4.46	82	8	1.87	-32
2	11.72	-123	9	.38	-56
3	14.00	-47	10	.30	177
4	7.65	119	11	.08	132
5	12.37	-124	12	.07	-17
6	.06	-124			

SPATIAL VARIANCE OF ESHF FIELD = 298.83

FOURIER ANALYSIS OF MAR (LM) ESHF

N	C	PHASE	N	C	PHASE
0	3.80	0	3	7.78	-37
1	4.48	46	4	4.39	37
2	3.16	46			

SPATIAL VARIANCE OF ESHF FIELD = 54.95

FOURIER ANALYSIS OF MAR (LM) ESHF

N	C	PHASE	N	C	PHASE
0	4.82	0	4	4.00	121
1	2.94	92	5	5.90	-112
2	7.09	-112	6	1.87	95
3	7.78	-112			

SPATIAL VARIANCE OF ESHF FIELD = 86.89

FOURIER ANALYSIS OF MAR (LM) ESHF

N	C	PHASE	N	C	PHASE
0	5.13	0	5	7.41	-140
1	3.05	70	6	2.33	-141
2	7.93	-124	7	2.33	92
3	8.35	-53	8	.73	90
4	4.00	-53			

SPATIAL VARIANCE OF ESHF FIELD = 112.15

FOURIER ANALYSIS OF MAR (LM) ESHF

N	C	PHASE	N	C	PHASE
0	5.06	0	6	1.34	129
1	2.79	78	7	4.25	121
2	8.61	-127	8	1.51	27
3	8.33	-41	9	.85	-1
4	6.30	121	10	.19	-67
5	7.41	121			

SPATIAL VARIANCE OF ESHF FIELD = 134.44

FOURIER ANALYSIS OF MAR (LM) ESHF

N	C	PHASE	N	C	PHASE
0	4.99	0	7	4.11	133
1	2.90	73	8	1.85	7
2	8.68	-125	9	.59	-3
3	8.87	-41	10	.23	-119
4	6.98	127	11	.21	158
5	8.26	-135	12	.08	-23
6	1.34	-135			

SPATIAL VARIANCE OF ESHF FIELD = 150.92

3.6.3 Spectral Composition of Eddy Heat Transport.

In this section, the zonal-mean and zonally-asymmetric components of the 55°N, 500mb stationary eddy sensible heat transport are analysed in terms of contributions from different wavenumbers in the meridional wind and temperature fields. As before, let the wavenumbers in these fields be m, n respectively; the component due to a single pair of wavenumbers will be written $v_m^* T_n^*$, and referred to as (m,n).

Tables 3.9 and 3.10 present the build-up of wavenumbers in the heat transport by addition of successive wavenumbers in the wind and temperature fields, starting with m = n = 1 and 2, for DW and LM data respectively. The same cut-off has been used in both constituent fields despite the fact that (as shown above) the higher wavenumbers (4, 5, 6) are more important to v^* than to T^*. The cut-off in each case is half the maximum wavenumber given for the heat transport. From this, the relative importance of particular wavenumbers in the wind and temperature fields can be assessed, although further analysis is required to show precisely which combinations of (m,n) dominate the heat transport. Most of the following discussion is based on these tables.

3.6.3.1 Zonal-Mean Heat Transport.

The contribution of each component (m,n) to the zonal-mean heat transport is shown in Table 3.11. In February, wavenumber 2 dominates the zonal-mean, accounting for nearly half the heat transport, with wavenumbers 1-3 together producing 96% of the zonal-mean. In March, the (2,2) contribution is still largest, but is considerably smaller

than in February, dropping by almost half. This fall accounts for 60% of the total fall in zonal-mean heat transport; (1,1) and (3,3) share the remainder equally. Results for LM are very similar.

Table 3.11

Contribution of wavenumber components to zonal-mean heat transports at 55 N, 500mb in February and March, from DW. Last column is total for all wavenumbers; figures in parentheses refer to percentages of this total.

	(1,1)	(2,2)	(3,3)	(4,4)	TOTAL
February	2.44 (27)	4.19 (46)	2.16 (24)	.18 (2)	9.07
March	1.85 (31)	2.30 (39)	1.56 (26)	.17 (3)	5.91
March/February	.76	.55	.72	.94	.65
Change in E	.59 (19)	1.89 (60)	.60 (19)	.01 (0)	3.16

Wavenumbers 1-3 together account for nearly 70% of the zonal-mean spatial variance in the eddy heat transport in both February and March at 55°N, 500mb (Table 3.9 - DW.): thus these three wavenumbers represent the zonal-mean heat transport almost completely and the zonally-asymmetric component reasonably well. From graphs of heat transport against longitude it can be seen that the main effect of adding in higher wavenumbers is to concentrate the heat transport into narrower and higher peaks, but the general shape is similar.

3.6.3.2 Zonally-Asymmetric Heat Transport.

On account of the strength in the zonal-mean heat transport of the (1,1), (2,2) and (3,3) components, one might expect the even wavenumbers in the heat transport field to be strongest, especially

l = 4 (from (2,2)), in February at least. Tables 3.9 and 3.10 show that this is not the case: for DW, wavenumber 3 is strongest, with 7 and 5 next strongest; 4 is smaller than 6. In March, the strongest are 2, 3 and 5. LM gives slightly different results: for January the strongest is 5, then 3, 2 and 4; however it is still the odd wavenumbers that dominate, and l = 4 accounts for less than 10% of the zonal-mean variance.

This can be explained from a closer study of the contribution by individual combinations of wavenumbers (m,n). In general, one wavenumber l in heat transport is composed of contributions from several (m,n): for example, l = 4 is composed of contributions from (2,2), (1,3), (3,1), (1,5), (5,1), (2,6) and (6,2). Table 3.12 shows these individual contributions for February and March. By looking at the cosine and sine coefficients separately, problems of phase are eliminated, and we can see which (m,n) contributions increase or decrease the coefficients a and b for a particular l.

The strong l = 4 contribution from (2,2) is reduced considerably by the (3,1) contribution, which affects mainly the cosine coefficient. The (3,1) contribution also reduces (2,2). The strong l = 3 component of the heat transport seen in Table 3.9 is due mainly to (2,1), with some contribution from (1,2), these two accounting for some 73% of the amplitude of l = 3; there are also contributions from (4,1) and (5,2). The relative weakness of the l = 2 component results from (3,1) and (4,2) working in opposition.

The difference between Tables 3.9 and 3.10 (ie between DW and LM) can mostly be accounted for by the fact that wavenumber 3 in the meridional wind is much stronger in LM: the stronger l = 5 component

Table 3.12

'ESHF' is Stationary Eddy Sensible Heat Transport.

CONTRIBUTION OF EACH WAVENUMBER-PAIR TO FEB (DW) ESHF FIELD

M	N	/M-N/	A	B	M+N	A	B
1	1	0	2.44	0	2	-2.40	-1.47
1	2	1	-1.96	2.59	3	2.02	-2.54
1	3	2	1.34	.36	4	-1.33	-.39
1	4	3	.76	-.20	5	-.77	.18
1	5	4	-.25	-.10	6	.25	.10
1	6	5	-.08	-.10	7	.08	.10

M	N	/M-N/	A	B	M+N	A	B
2	1	1	5.31	4.30	3	1.27	-6.71
2	2	0	4.19	0	4	7.50	2.38
2	3	1	1.96	-2.73	5	-.26	-3.35
2	4	2	.20	-1.91	6	-1.08	-1.58
2	5	3	-.44	.49	7	-.02	.66
2	6	4	-.30	.09	8	-.17	.27

M	N	/M-N/	A	B	M+N	A	B
3	1	2	3.02	-5.61	4	-6.37	-.00
3	2	1	-6.83	-2.68	5	.88	-7.28
3	3	0	2.16	0	6	-3.02	.82
3	4	1	1.71	.51	7	-1.26	1.26
3	5	2	-.37	-.49	8	.61	-.10
3	6	3	-.03	-.29	9	.27	.11

M	N	/M-N/	A	B	M+N	A	B
4	1	3	-2.61	-3.51	5	-1.86	3.96
4	2	2	-3.66	3.47	6	-4.27	-2.67
4	3	1	-.78	-2.00	7	-.37	2.12
4	4	0	.18	0	8	.42	1.15
4	5	1	.19	-.37	9	.12	-.41
4	6	2	.17	-.11	10	.15	-.14

M	N	/M-N/	A	B	M+N	A	B
5	1	4	-.68	2.71	6	2.71	-.68
5	2	3	3.19	.40	7	.41	3.19
5	3	2	-.67	1.20	8	1.20	-.68
5	4	1	-.67	.40	9	.40	-.67
5	5	0	.11	0	10	-.25	.11
5	6	1	-.02	.13	11	-.13	-.02

M	N	/M-N/	A	B	M+N	A	B
6	1	5	.27	-.72	7	-.77	.10
6	2	4	-.86	-.21	8	-.01	-.89
6	3	3	.22	-.31	9	-.35	.15
6	4	2	.20	-.09	10	-.13	.17
6	5	1	-.04	.06	11	.07	-.02
6	6	0	.00	0	12	.03	.01

Table 3.12 - Continued.

CONTRIBUTION OF EACH WAVENUMBER-PAIR TO MAR (DW) ESHF FIELD

M	N	/M-N/	A	B	M+N	A	B
1	1	0	1.85	0	2	-1.67	-1.91
1	2	1	-1.31	1.68	3	1.47	-1.54
1	3	2	1.32	-.19	4	-1.33	.06
1	4	3	.46	-.15	5	-.47	.10
1	5	4	.02	-.04	6	-.03	.04
1	6	5	-.06	-.14	7	.04	.15

M	N	/M-N/	A	B	M+N	A	B
2	1	1	3.57	2.43	3	2.56	-3.48
2	2	0	2.30	0	4	3.10	1.88
2	3	1	.16	-2.26	5	-.60	-2.18
2	4	2	-.07	-.82	6	-.34	-.75
2	5	3	-.06	-.05	7	-.08	-.03
2	6	4	-.26	.04	8	-.23	.13

M	N	/M-N/	A	B	M+N	A	B
3	1	2	-1.11	-4.67	4	-4.71	.94
3	2	1	-3.99	.57	5	-1.14	-3.87
3	3	0	1.56	0	6	-1.15	2.24
3	4	1	.68	.62	7	-.28	.87
3	5	2	.09	-.01	8	.04	.08
3	6	3	.18	-.23	9	.28	.07

M	N	/M-N/	A	B	M+N	A	B
4	1	3	-1.64	-1.93	5	-1.99	1.57
4	2	2	-1.74	1.23	6	-1.46	-1.55
4	3	1	.26	-1.30	7	-.00	1.33
4	4	0	.17	0	8	.08	.48
4	5	1	.04	.02	9	.04	.03
4	6	2	.14	-.06	10	.15	-.04

M	N	/M-N/	A	B	M+N	A	B
5	1	4	-1.41	.34	6	.29	1.42
5	2	3	.18	1.21	7	-1.17	.35
5	3	2	-.60	-.47	8	.68	.34
5	4	1	-.19	-.20	9	.26	.08
5	5	0	.00	0	10	.02	-.01
5	6	1	.07	.05	11	.02	-.09

M	N	/M-N/	A	B	M+N	A	B
6	1	5	-.52	-.26	7	-.28	.51
6	2	4	-.25	.42	8	-.45	-.19
6	3	3	-.07	-.30	9	.12	.28
6	4	2	-.01	-.11	10	.06	.09
6	5	1	.01	-.01	11	.01	.00
6	6	0	.04	0	12	.03	-.02

of the heat transport comes from the (3,2) contribution, while wavenumber 2 comes mainly from (3,1).

Table 3.9 shows that the main change from February to March is a much-reduced 1 = 3 component: this is a consequence of the decrease in the wavenumber 2 component of the wind and temperature fields, leading in particular to a fall in the (2,1) contribution.

Thus the dominance or weakness of any zonal wavenumber 1 in the eddy heat transport field can be accounted for by the interaction of all pairs of wavenumbers (m,n) in the wind and temperature fields comprising that wavenumber 1. It is difficult to deduce from the Fourier analysis of wind and temperature alone why the eddy heat transport varies with longitude as it does, or even the contribution of each wavenumber to the zonal mean; however the kind of analysis presented above makes it plain.

3.6.4 Summary and Implications of Fourier Analysis.

It has been shown above that the chief cause of the change in the stationary eddy sensible heat transport from February to March is the large fall in the amplitude of wavenumber 2 in the temperature and meridional wind fields: this is the case for both the zonal-mean heat transport and its longitudinal variation.

The longitudinal variation of eddy heat transport can be described by Fourier coefficients which can in turn be derived from the Fourier coefficients of the constituent fields: this is not a simple process, but shows clearly the relative importance of the interactions between different wavenumbers in the temperature and wind fields, and how these different combinations reinforce or oppose one

another. In general, the strongest contributions to the zonally-asymmetric part of the heat transport occur for m n, as we should expect from the Fourier analyses of v and T (see Section 3.6.2).

The results above have several implications for spectral climate models, and in general for the description of eddy heat transport in terms of Fourier coefficients.

Firstly, zonal wavenumbers 1-3 in the constituent fields describe the zonal-mean heat transport very well and its spatial variance reasonably well for monthly means; therefore a spectral climate model needs to carry these three wavenumbers.

Secondly, the stationary eddy heat transport field is completely defined by the spectral components of the meridional wind (or even geopotential height) and temperature fields.

Thirdly, zonal-mean eddy heat transport statistics depend only on the interaction of the same wavenumber in temperature and wind fields, of which wavenumber 2 is dominant.

Finally, calculation of the heat transport as a function of longitude needs to take into account all possible combinations of wavenumbers in the constituent fields.

Spectral and gridpoint analyses of heat transport are complementary: each tells us something about the physical processes involved, but neither presents a complete picture. Gridpoint analysis enables us to relate spatially observed (or physical) quantities to one another and to the underlying topography. Fourier analysis is (in general) a way of describing and modelling a physical situation, but

does not show how, physically, the situation occurs (it is a descriptive approach not a mechanistic one). The atmosphere operates by response to forcing which can be described numerically by Fourier series but not explained by them: a poleward-moving parcel of air only 'knows about' the ambient temperature and wind fields, not their Fourier components. Fourier analysis is best used as a tool for comparing numerical fields derived from models embodying a hypothesis concerning some mechanism with real atmospheric data; it can also furnish information on space- and/or time-scales.

3.7 Interannual Variations.

The interannual variation of eddy heat transports and their constituent fields has been the subject of a number of studies, including van Loon, Jenne and Labitzke (1973), Hsiao (1979) and Hsiao and Reiter (1981). It is here briefly discussed principally in the light of data analysed in the present study, and insofar as it affects the sharp fall in stationary eddy sensible heat transport from February to March (the April - November difference is less obviously important in a particular year, in that the physical relationship between heat transports in the two months is not clear and may indeed be insignificant).

3.7.1 Variation of Heat Transport and Constituent Fields.

The stationary eddy sensible heat transports in key months are given in Table 3.6. It can be seen from this that a sharp fall (by at least one-third) in heat transport from February to March occurs in six of the nine years studied; in the remaining three years (1970, 1971 and 1976) the heat transport is almost the same for the two

months. In 1968 the heat transport fell by two-thirds; in the remaining five years with a marked fall it decreased by between a third and a half. Of the three years when the heat transport didn't change, in 1970 and 1976 it was close to the 9-year February mean for both months (it did not decrease to March); in 1971 the February heat transport was abnormally low (2 standard deviations).

This raises two questions: what in general causes the interannual variation of the heat transport, and why in some years are the heat transports in February and March the same? Both questions are difficult to answer in terms of physical mechanism without a deeper understanding of the stationary wave forcing and a knowledge of both the magnitude and the cause of variation of that forcing for each year; however they can perhaps be answered at a simple level by looking at the wind and temperature fields and their correlation. There is also a problem in that the sample is small (9 years). Table 3.13 shows the spatial variances and correlations of the constituent fields for February, March and March/February.

Taking the months separately, this shows that there is rather more variability in $[\bar{v}^{*2}]$ and $r_2(v,T)$ than in $[\bar{T}^{*2}]$ for both months. There is also very little relation between any of these three quantities; there is apparently no relation between the heat transport and the spatial variances, though in February the correlation between $r_2(v,T)$ and the heat transport is statistically significant at the 95% level. This means that interannual variability in the heat transport is not associated particularly with any of the spatial variances or correlation (except for the February $r_2(v,T)$ - E_{ST} correlation), neither is it necessarily the result of all of these varying in the same sense.

Table 3.13

Values of $[\bar{v}^{*z}]$, $[\bar{T}^{*z}]$ and $r_2(v,T)$ for February, March and March/February in individual years, from OR.

	FEBRUARY			MARCH			MARCH/FEBRUARY		
	$[\bar{v}^{*z}]$	$[\bar{T}^{*z}]$	$r_2(v,T)$	$[\bar{v}^{*z}]$	$[\bar{T}^{*z}]$	$r_2(v,T)$	$[\bar{v}^{*z}]$	$[\bar{T}^{*z}]$	$r_2(v,T)$
1967	34.5	16.7	.53	37.9	11.5	.38	1.10	.69	.72
1968	30.8	11.7	.44	19.0	5.3	.30	.62	.45	.68
1969	26.9	23.3	.44	24.1	12.3	.42	.90	.53	.95
1970	63.1	17.1	.32	40.3	15.2	.41	.64	.89	1.28
1971	27.1	19.5	.30	16.5	9.8	.54	.61	.50	1.80
1972	36.5	19.7	.33	15.5	10.9	.41	.42	.55	1.24
1975	47.7	16.5	.40	12.8	7.6	.55	.27	.46	1.38
1976	39.9	17.3	.40	31.0	14.6	.48	.78	.84	1.20
1977	34.2	16.3	.46	11.3	10.8	.46	.33	.66	1.00
MEAN	37.9	17.6	.40	23.2	10.9	.44	.63	.62	1.14

Looking at the changes in heat transport and associated quantities from February to March, there is again no discernible or statistically significant relation between any of $[\bar{v}^{*2}]$, $[\bar{T}^{*2}]$, $[\bar{v}^{*}\bar{T}^{*}]$ or r (v,T). This means that the magnitude of the fall in heat transport (where the fall occurs) is unrelated to any particular variation or combination of variations in the constituent quantities. However, for the three 'odd' years, when no fall occurs, certain common features are noticeable. In all these years, the spatial correlation increases (although this is not unique to those years). In 1970 and 1976 the temperature variance (which is close to the 9-year mean in February) does not fall much, these being the years in which the heat transport in March is close to the February 9-year mean. In 1971 the temperature variance is halved in March, the wind variance falls by 40%, but the correlation nearly doubles, hence the heat transport does not change. Hence when $[\bar{T}^{*2}]$ hardly falls, the heat transport remains similar in March, though the converse is evidently not true.

Reasons for the heat transport not falling to March in those three years can also be seen in the appropriate monthly-mean (DW) charts, by comparison with a year in which it does fall (eg 1969). In 1970, the Pacific trough remains quite strong in March, so the large heat transport to the west of this does not fall much, and a ridge to the south of Greenland intensifies, leading to increased heat transport off the East coast of North America. In 1971 and 1976 the Pacific trough again remains strong in March, keeping the heat transport to its west high. Thus the years when the heat transport is similar in February and March are those in which the 500mb trough over the North Pacific and eastern Asia does not weaken in March. The heat

transport in February 1971 is relatively low because that trough is weak then compared with other Februaries.

It was seen in Section 3.5 that the intensity of this Pacific trough dominates the variation of the zonal-mean midlatitude stationary eddy sensible heat transport from February to March in a climatic average taken over several years; the varying intensity from year to year of this same trough governs to a large extent the interannual variation of the heat transport and its change (or lack of change) from February to March.

3.7.2 Variation of Fourier Coefficients.

As in Section 3.6, an alternative approach to the problem of eddy heat transport variation is to look at the Fourier components of the wind and temperature fields. From the close correspondence noted above between the primary causes of intra-annual and inter-annual variations, one might well expect similar correspondence for the Fourier analyses, ie a strong dependence on the amplitude and phase of zonal wavenumber 2 in the wind and temperature fields.

No strong tie is seen (in the Fourier analysis of DW data) between the behaviour of wavenumber 2 and the variances for the individual months, however there are stronger links for the change from February to March. This is especially noticeable for 1971 when the amplitude of wavenumber 2 (and of most other wavenumbers) in both temperature and wind fell by about 40% but the phase difference between the two decreases from 75° to 32°, thus increasing by 20% the contribution from wavenumber 2 (though the main contribution to the heat transport is from wavenumber 1). This is consistent with the

Table 3.14

Contributions by first four wavenumbers in temperature and wind to zonal-mean heat transport in February and March, for 9 years; from DW.

	1967		1968		1969		1970		1971		1972		1975		1976		1977		MEAN	
	Feb	Mar	Feb	Mar	Feb	Mar	Feb	Mar	Feb	Mar	Feb	Mar	Feb	Mar	Feb	Mar	Feb	Mar	Feb	Mar
(1,1)	2.0	.5	1.5	.5	6.4	2.1	2.0	3.1	2.7	2.9	1.4	1.3	2.5	2.0	2.5	3.0	2.7	2.4	2.4	1.9
(2,2)	7.2	4.9	2.8	1.0	3.6	2.0	4.5	3.0	1.5	1.8	5.7	1.5	7.0	2.6	3.9	5.3	7.2	1.7	4.2	2.3
(3,3)	3.0	2.5	2.7	.9	.2	3.1	3.9	2.5	1.9	1.4	.2	1.8	4.6	1.6	3.1	1.5	1.8	.8	3.2	2.6
(4,4)	.3	.1	1.9	.4	0	-.2	-.2	1.6	.6	.8	.2	.3	.6	.5	.7	.4	-.3	-.1	.2	.2

data for that year in Table 3.13, which shows marked falls in $[\bar{v}^{*2}]$ and $[\bar{T}^{*2}]$ but a large increase in their correlation $r_2(v,T)$.

A summary of the contribution analysis, similar to Table 3.12, for the zonal-mean heat transport for each February and March is given in Table 3.14.

The Fourier analysis, spatial variances, correlation and zonal-mean heat transport for February 1976 are a close analogue to the 9-year mean; similarly for March 1969. Comparing March 1976 with March 1969 (ie an 'odd' and 'normal' March respectively), the effect of wavenumber 2 is very pronounced: whereas the (2,2) contribution to the zonal-mean heat transport drops by about 50% in March 1969, it increases by about 35% in March 1976, as can be seen in Table 3.14, even though the amplitudes of wavenumber 2 in temperature and wind fields each fall by about 15%: the increase in the (2,2) contribution is due to the decrease in phase difference between the two from 70° to 54°.

In 1970 however the situation is a little different. It is not clear from the Fourier analysis of the wind and temperature fields why the heat transport should be maintained in March, but the contribution analysis shows that while the (2,2) and (3,3) contributions both fall, the (1,1) and (4,4) contributions rise by a similar amount to maintain the heat transport. The (2,2) and (3,3) contributions fall because the amplitudes of those waves in the connstituent fields fall (the phase difference changing little); (1,1) increases because the amplitudes rise to March, and (4,4) increases because of the change in phase difference between the two components. It appears from Table 3.13 that on a year-to-year basis the behaviour of the (2,2)

contribution to the zonal-mean stationary eddy sensible heat transport in February and March generally (though not infallibly) gives an indication at least of whether the heat transport will fall significantly to March, though there is no relation between the size of the fall in the (2,2) contribution and the fall in heat transport. However, the small sample size prohibits one from drawing firm conclusions.

3.8 Summary of Conclusions.

It has been shown that the marked fall in stationary eddy sensible heat transport from February to March is statisticaly significant. It results mainly from decreases in the temperature and meridional wind spatial variances rather than in their correlation. At 500mb this in turn is due principally to the weakening in March of a trough which in January and February lies over the North Pacific and Eastern Asia. In Fourier space, the variation of heat transport is largely controlled by the amplitude of wavenumber 2 in the temperature and meridional wind fields. The fall occurs in averages taken over several years and in different groups of years; it occurs in a majority of years but not in every year.

CHAPTER 4

POSSIBLE CAUSES OF VARIATIONS IN EDDY HEAT TRANSPORT AND MERIDIONAL TEMPERATURE GRADIENT

Introduction.

Several hypotheses to account for the observed variation of eddy heat transport with respect to meridional entropy gradient are presented and discussed. This leads to consideration of the nature of the stationary wave forcing and its implications for describing the variation of the heat transport and the entropy gradient, and their relation. The aim is to understand the physical mechanism or mechanisms underlying the variation of these two quantities, in order to relate them, if possible, in a physically meaningful and numerically correct way.

4.1 Some Hypotheses.

4.1.1 Time-lag in Response to Variations in Forcing.

Perhaps the most obvious hypothesis to account for the observed two-valued behaviour of eddy heat transport with respect to meridional entropy gradient is that, if variations in one force changes in the other, there is a time-lag in the response of the forced quantity to those variations in the forcing quantity. Lorenz (1979) suggests that, on the time- and space-scales under consideration here, variations in the entropy gradient force variations in the heat transport (see Chapter 1, Section 1.2); this also implies a causal (or physical) relationship between the two. Note that Green (1970) says nothing about the possibility of a time-lag.

It is clear from Fig. 1.1 that variations in eddy heat transport lead rather than lag variations in entropy gradient, contrary to our expectations. Fig. 4.1 shows that the lead is about 3-4 weeks in winter and about 1 week in summer. This does not automatically imply

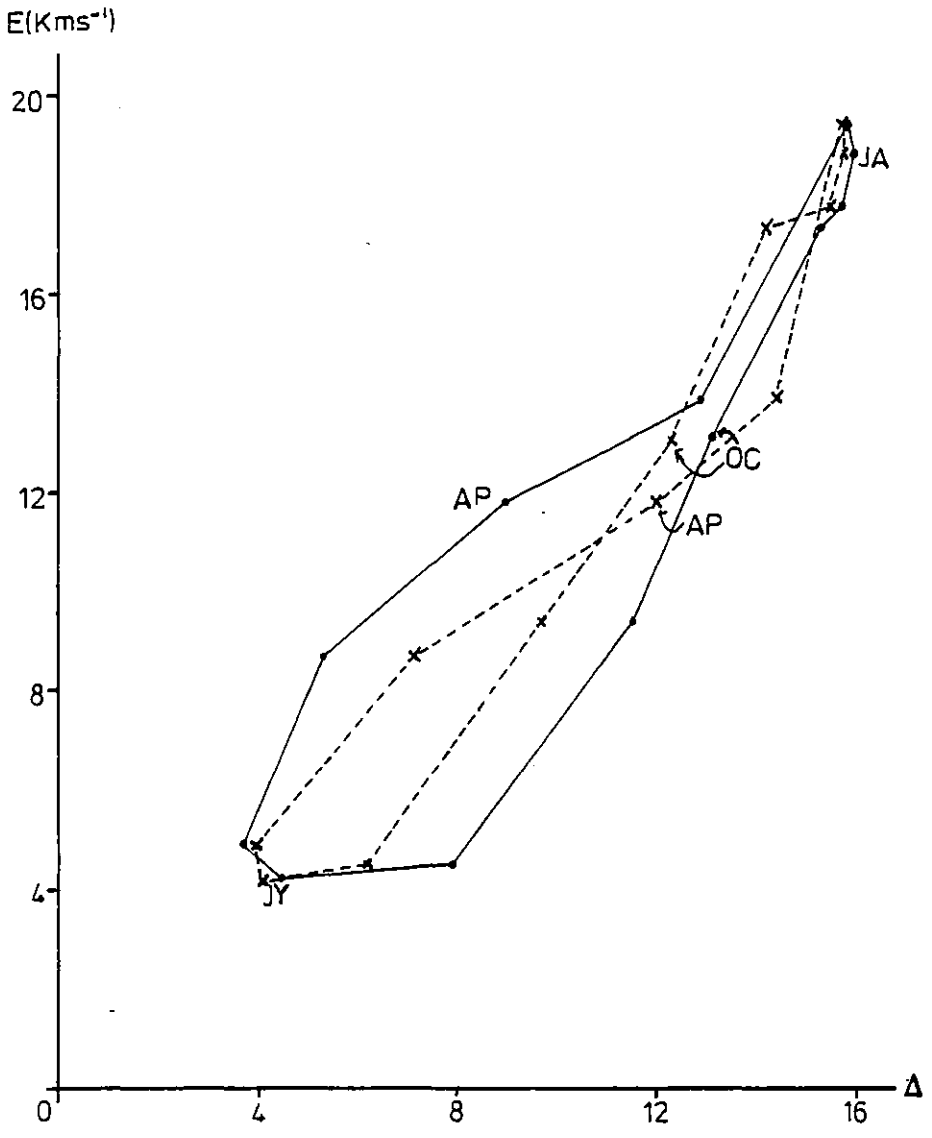

Fig. 4.1: Total eddy sensible heat transport against entropy gradient advanced by ½ month (×----×) and 1 month (•——→), defined as in Fig. 1.1. Months refer to eddy transport; both quantities are tropospheric averages.

that variations in eddy heat transport directly cause changes in the entropy gradient, merely that the forcing cannot be the other way round (there is no known way in which variations in the heat transport could anticipate changes in the entropy gradient by such a long time as in winter). It is also curious that the lead is much longer in winter than in summer, since changes in the circulation (on the synoptic scale at least) in general take place much faster in winter (the circulation being stronger then), so that a change in forcing would be propagated more rapidly then and the time-lag in the response would be shorter. This tends to suggest that although some kind of time-lag exists, it is not a lag in the response of the entropy gradient to direct forcing by variations in the eddy heat transport.

Given that a time-lag describes the observed variations but does not tell us anything about the physical mechanism or mechanisms underlying them, is the physical link between eddy heat transport and meridional entropy gradient direct or indirect? A direct link means that changes in one force changes in the other; an indirect link would result from changes in each being individual responses to variations in the external forcing.

Note that a relation such as Eq. (1.2) does not necessarily imply a direct physical link, or postulate a mechanism for such; it may only provide a way of defining numerically one quantity in terms of the other.

If there is a direct physical link between eddy heat transport and meridional entropy gradient, then one might hypothesize that the variations in heat transport depend on whether the entropy gradient is increasing or decreasing with time, via the constant α in Eq. (1.2).

This seems implausible, as the transit time of an air-mass moving from tropical to polar regions is around one week, during which time the change in entropy gradient is negligible.

The apparent time-lag is reduced to two possible causes: either some other predictor besides meridional entropy gradient is required to define uniquely the eddy heat transport (that predictor ought to have some physical link with eddy heat transports) -- in which case the time-lag need not bother us -- or else the two quantities both change in response to variations in their external forcing, in which case we need to derive separate predictors for them from their forcing mechanism(s) and then to relate the two via these predictors. The former possibility is discussed in the next two subsections; both are discussed further in Section 4.2.

The latter case still admits of the possibility of a kind of time-lag, in one of two ways: either the meridional entropy gradient responds more slowly to changes in external forcing than does the eddy heat transport, or the forcing itself is different for the two quantities (in a time-dependent way); such a time-lag is different from that postulated at the start of this section, which implied a direct physical link.

4.1.2 Changes in the Zonal-Mean Temperature Structure.

It is clear from the meridional cross-section shown in Fig. 4.2 that this is very similar in February and March throughout most of the troposphere; it therefore seems unlikely that such could account for the observed variations in eddy heat transport at that time.

The only seasonally-varying quantity involved in α, the constant

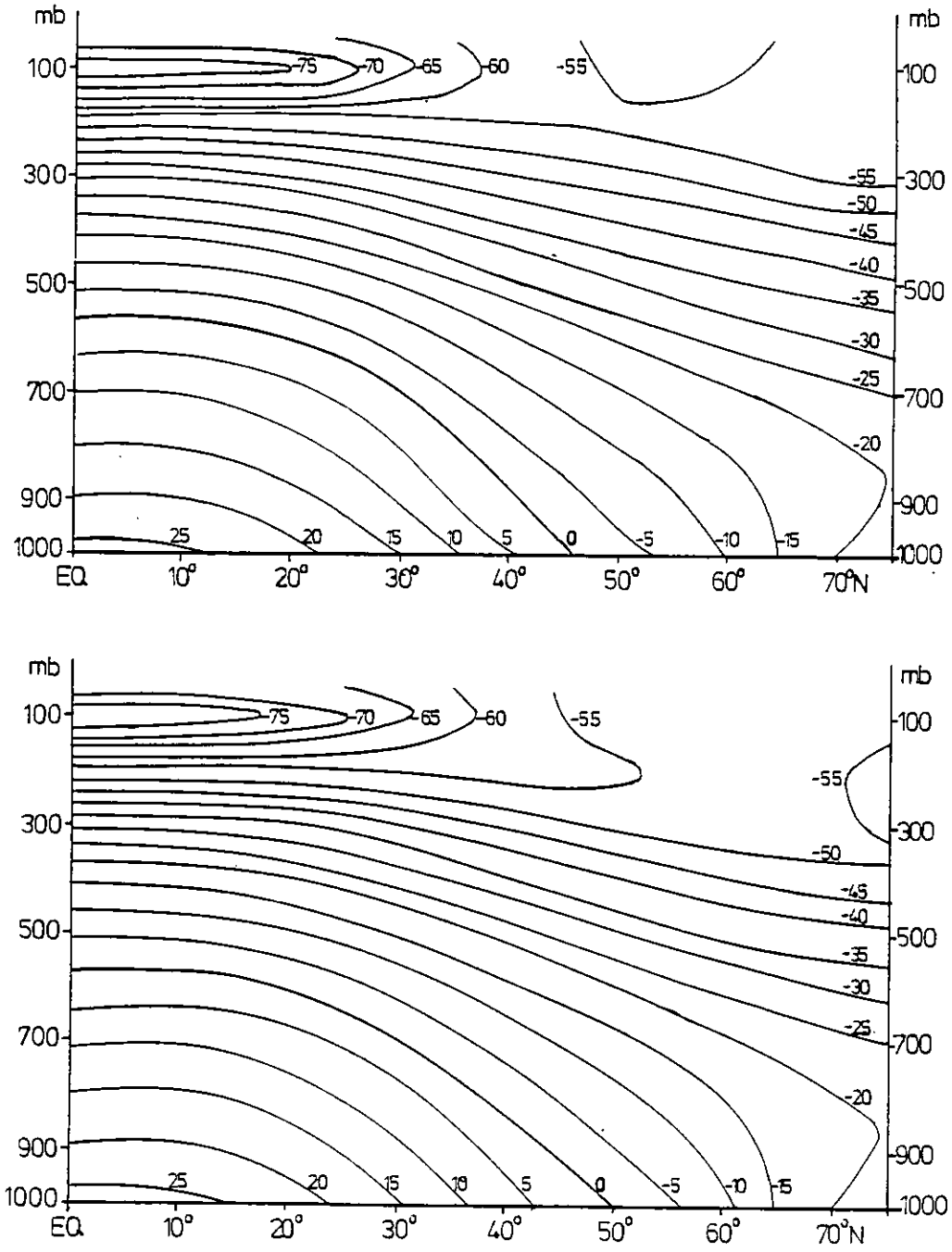

Fig. 4.2: Meridional cross-section of zonal-mean atmospheric temperature in February and March. Units: °C.

in Eq. (1.2), is the static stability; this is also invoved in Stone's (1972) and Held's (1978) theories, as discussed in Chapter 1, Section 1.1. Green pointed out that the annual variation of midlatitude tropospheric static stability is only 4%, compared with a factor of 4 in the entropy gradient, so it seems unlikely that this could be the cause of the eddy heat transport being two-valued with respect to entropy gradient. Table 4.1 gives the relevant values of static stability at different levels in the troposphere.

Table 4.1

Values of Static Stability, $\partial\Phi/\partial z$, at 55°N in the troposphere, for four key months, calculated from OR data. Units: $10^{-5}m^{-1}$.

	Feb.	Mar.	Apr.	Nov.
300 - 400mb	1.9	1.9	1.7	1.8
400 - 500mb	1.2	1.2	1.2	1.2
500 - 700mb	1.5	1.5	1.5	1.5
700 - 850mb	2.1	2.0	1.7	2.0
850 - 900mb	2.6	2.2	1.7	2.0
900 - 950mb	2.3	2.0	1.8	1.7
950 - 1000mb	1.6	2.0	2.1	1.5
MEAN	1.79	1.74	1.75	1.68

For the tropospheric averages above 700mb, differences over these months are negligible. Below this, the changes look possibly significant, but they are in opposite directions above and below 900mb; the dependence in both Green (1970) and Stone (1972) is in any case on the square root of B, so the effect will be small compared with the variations in heat transport whether the dependence is on $B^{+1/2}$ (as in Stone (1972)) or on $B^{-1/2}$ (as in Green (1970)). Thus while

changes in static stability may have some influence on the eddy heat transport, this is insignificant in the current problem.

4.1.3 Changes in the Stratospheric Circulation.

The effect of the stratospheric zonal wind in controlling upward and hence poleward energy propagation was referred to in Chapter 2, Section 2.3.2 in connexion with the vertical extent of two-valued behaviour in the eddy heat transport. Here, we consider the hypothesis that the variations in sign and magnitude of the zonal wind cause the observed two-valued behaviour.

This could occur in two possible ways: either by reversal of this wind leading to complete trapping of the waves in the troposphere, or by increasing its speed which progressively traps the waves. Examination of 30mb zonal wind data (Labitzke (1972)) shows that neither alternative is valid. The change from westerly to easterly flow occurs between April and May, far too late to account for the sharp February - March fall (the zonal windspeed decreasing throughout this period). The transition back to westerlies occurs simultaneously with the stationary eddy heat transport becoming positive (around the end of August). In autumn the speed is faster than in spring, so it cannot account for the heat transport being larger then also. In general it appears that while the zonal wind has some effect on the poleward eddy heat transport, as we expect, it cannot account for the two-valued behaviour of its variation with respect to meridional entropy gradient.

4.1.4 Changes in Correlation and Phase.

Another possible cause of change in the eddy heat transport is variations in either the relative phase of the temperature and meridional wind fields or else in their absolute phase (ie with respect to topography or heat sources and sinks). It was shown in Chapter 3, sections 3.1 and 3.6.2 that the correlation or phase difference between these fields changes little from February to March, and that changes in the heat transport were due to changes in their amplitudes. However these changes might in turn force shifts in their absolute phases, so that the forcing effect of orography or heat sources/sinks would be different. While Fig. 3.6 shows phase changes from February to March in the various Fourier modes, the direction and size of these varies between the modes such that there is no net shift of the stationary wave pattern, as shown by Figs. 3.3 - 3.5 (as we might well expect, since the sources/sinks do not move). We may therefore conclude that the change in stationary eddy heat transport from February to March cannot be explained by any changes of phase in the constituent fields.

4.1.5 The Effects of Latent Heat.

It was noted in Chapter 2, Section 2.1 that midlatitude eddy latent heat transports were also higher in autumn than in spring; we discuss here other possible effects of the oceans on eddy heat transport.

Near the tropics, energy is transferred from the oceans to the atmosphere in the form of latent and sensible heat (besides long-wave radiation). The latent heat may then either be transported to

midlatitudes (ie as $[\overline{v}^{*}\overline{q}^{*}]$ and $[\overline{v'q'}]$), or may be released through condensation and precipitation. It is quite possible that this process will enhance the eddy sensible heat transport, since it will modify the temperature field (and hence, presumably, the wind field also). The hypothesis is that for the same reason as the eddy latent heat transport is higher in autumn (see Chapter 2, Section 2.1), the eddy sensible heat transport is also enhanced at this time compared with spring, by this process of evaporation and latent heat release; hence for the same meridional entropy gradient the heat transport will be larger; alternatively, as for March and October, the same heat transport is achieved with a smaller entropy gradient.

From the data available on ocean temperatures -- Monthly Meteorological Charts of the Oceans (Meteorological Office: 1947, 1949, 1950) -- it is difficult to tell whether this is possible, since although temperatures are higher in autumn than in spring the temperature difference between ocean and atmosphere generally appears smaller; however with the non-linearity of vapour pressure as a function of temperature and the possible error in the temperature difference being large, it is impossible to draw firm conclusions. In Section 4.3 below this is further discussed, and in Chapter 5 shown (by implication) to be possibly important.

This could explain the spring/autumn difference in eddy heat transport, but as at first glance the ocean temperature doesn't change much from February to March it doesn't look as though it could explain the sharp fall in stationary eddy sensible heat transport at this time. However, the principal regions of heating are over the Gulf Stream and the Kuroshio current (see Fig. 5.1 and Lau (1979)): if the air passing over them is warmer in March (but still colder than those

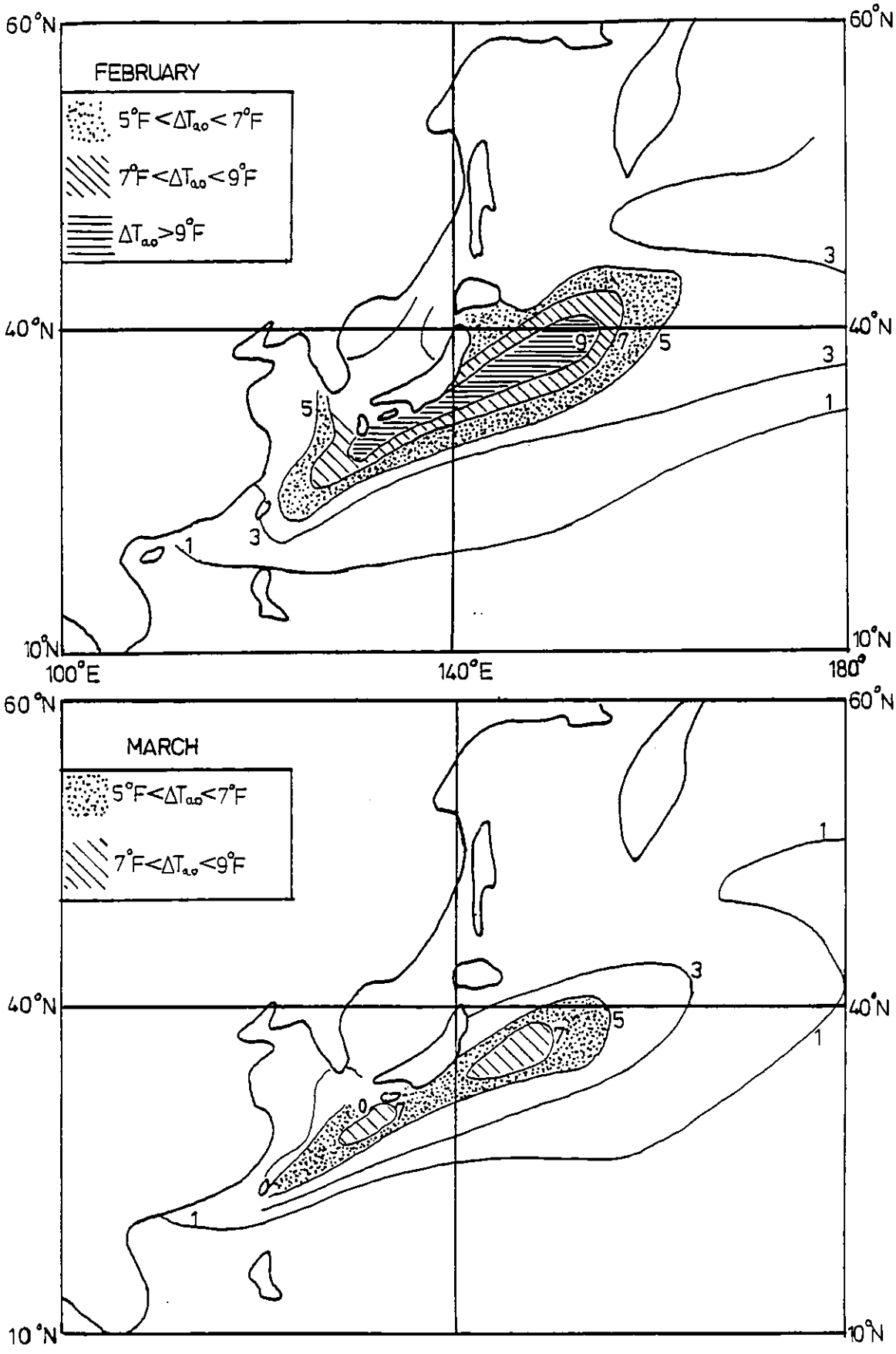

Fig. 4.3: Temperature difference between ocean and atmosphere, ΔT_{ao}, in region of Kuroshio current, during February and March.

currents), then the energy transfer will be smaller and hence the stationary wave thermal forcing also less (see below, section 4.3.3). Fig. 4.3 shows the temperature difference between the Pacific Ocean and the atmosphere above it in the vicinity of the Kuroshio current: there is a small but definite decrease in the temperature difference in March, which may well contribute at least to the fall in heat transport.

4.2 The Stationary/Transient Eddy Problem.

One aspect of the problem of the annual variation of eddy heat transports which has so far only been partially treated is the partitioning of the eddies into stationary and transient components. We now examine further this distinction to see if it is valid.

In Chapter 1, Section 1.4 the question was raised of whether the observed stationary eddy heat transport could really be due to essentially transient baroclinic eddies developing in preferred locations on a stationary wave pattern which itself produces little heat transport.

The question to be answered here is: are the regions of large heat transport due apparently to stationary eddies also regions where we might expect large transports due to baroclinic eddies maintained in stationary positions? In this case, the heat transport defined numerically as being due to stationary eddies should really be included with the transient component; it might well then be that the transient eddy heat transport would be proportional to throughout the year, and parameterizations of the form of Eq. (1.2) vindicated.

Frederiksen (1979) suggests from model experiments that the maximun transient eddy heat transport should be downstream and poleward of the jet maxima. An observational study of the Northern Hemisphere wintertime circulation by Blackmon et. al. (1977) confirms that this is where transient eddy heat transport is largest. They applied temporal filters to the data: a band-pass filter picked out variations on the 2.5 - 6-day time-scale, variations on longer time-scales were identified with a low-pass filter. The latter might be expected to identify regions where eddy heat transport could appear in unfiltered data to be due to stationary eddies but would in fact be 'transient' in that it is due to baroclinic eddies: such regions, for both the band-pass and low-pass filtered data, are indeed where Frederiksen's model would predict them to be. This is also shown in a volume of Northern Hemisphere circulation statistics compiled by Lau, White and Jenne (1981).

Looking at Figs. 3.2 and 3.5 together, it can be seen that whereas the heat transport maximum over the Western Atlantic is in such a region, that over eastern Asia is upstream of the jet maximum, completely the wrong place for it to be explained as being due to transient baroclinic eddies. It is this latter maximum which dominates the wintertime heat transport and which is primarily responsible for the large fall in eddy heat transport from February to March (see Chapter 3, Section 3.5). It therefore seems unlikely that the large wintertime heat transport apparently due to stationary eddies should really be ascribed to transient eddies, although perhaps that over the Western Atlantic can be; even if this is done, it would still leave a substantial wintertime stationary eddy heat transport which falls sharply to March.

4.3 The Type of Solution Required.

A reasonable explanation to account for the form of the observed variations of stationary eddy sensible heat transport and of entropy gradient can now be formulated. After discussion of the possible forcing mechanisms operating to produce both the zonal-mean meridional entropy gradient and the stationary eddy heat transport, the requirements for such an explanation are established; this is then stated, and observational evidence presented in support of it.

4.3.1 Forcing Mechanisms.

In Section 4.1 it became apparent that it is most realistic to regard the meridional entropy gradient and eddy sensible heat transport as, in the first instance, individual responses to separate (though possibly linked) forcing mechanisms.

$[\Delta \phi]$ must result from latitudinally-varying zonal-mean temperature forcing (by definition: it is a measure of this).

E_{ST} must result from longitudinally-varying forcing: it was shown in Chapter 3, Section 3.1 that variations in the stationary eddy sensible heat transport are due to varying degrees of zonal asymmetry in the constituent fields, which must in turn result from zonally-asymmetric forcing.

The prima facie cause of latitudinal variation in forcing is the latitudinal variation in insolation. Longitudinal variations on the other hand are the result of zonal asymmetry at the bottom of the atmosphere: the existence of continents and oceans. This produces two kinds of forcing: orographic and thermal. Various studies have

suggested that one or other of these is dominant; at the present time there seems to be no concensus of opinion on the matter, but it seems that both could be important.

Of course, the processes at the bottom of the atmosphere affect the zonal-mean entropy gradient also; but whereas this involves averaging out the effects of land and oceans, the zonally-asymmetric forcing precisely requires a knowledge of the consequent longitudinal contrasts in topography and/or heating.

Cloudiness is one factor not so far considered: this varies longitudinally and temporally. It affects the radiation balance in the atmosphere, and hence forcing of both meridonal entropy gradient and stationary eddies. However, this is not an external forcing agent, whereas the processes mentioned above may be considered to be so (though thermal forcing would be internal to a combined ocean-atmosphere model).

Note that Green (1970) is treating a zonal-mean case entirely defined by processes internal to the atmosphere; it appears that consideration of external forcing is crucial to the problem.

Thus I contend that variations in entropy gradient and in heat transport result from variations in their separate forcing mechanisms, which are fundamentally different in operation though having their origins in the same physical processes (insolation, surface heating/orography, long-wave radiation to space).

4.3.2 Requirements for a Reasonable Explanation.

(i) It must account for the sharp fall in stationary eddy sensible heat transport from February to March and for the meridional entropy gradient remaining the same during this time.

(ii) It must account for the time-lag postulated in Section 4.1.1.

(iii) It must demonstrate the forcing mechanisms operating according to Section 4.3.1 above.

(iv) It must take account of longitudinal as well as latitudinal variations.

(v) It must show that changes in forcing are of the right magnitudes to account for the observed changes in entropy gradient and eddy heat transport.

4.3.3 The Hypothesis - to account for the observed variations of meridional entropy gradient and stationary eddy meridional heat transport.

The original question which prompted the present study was: why is eddy meridional heat transport two-valued with respect to global meridional entropy gradient? Green (1970) suggests that the total eddy sensible heat transport should be single-valued: since the

transient component is so, the problem was reduced to explaining why the stationary eddy transport is not. Since this is approximately proportional to the spatial variance of the temperature field, the question becomes one of the relationship between the zonal-mean and zonally-asymmetric components of that field.

Definition of a zonal-mean quantity (eg [T]) does not uniquely define the zonal asymmetry (or spatial variance) of that quantity. Take for example a simple sine-wave:-

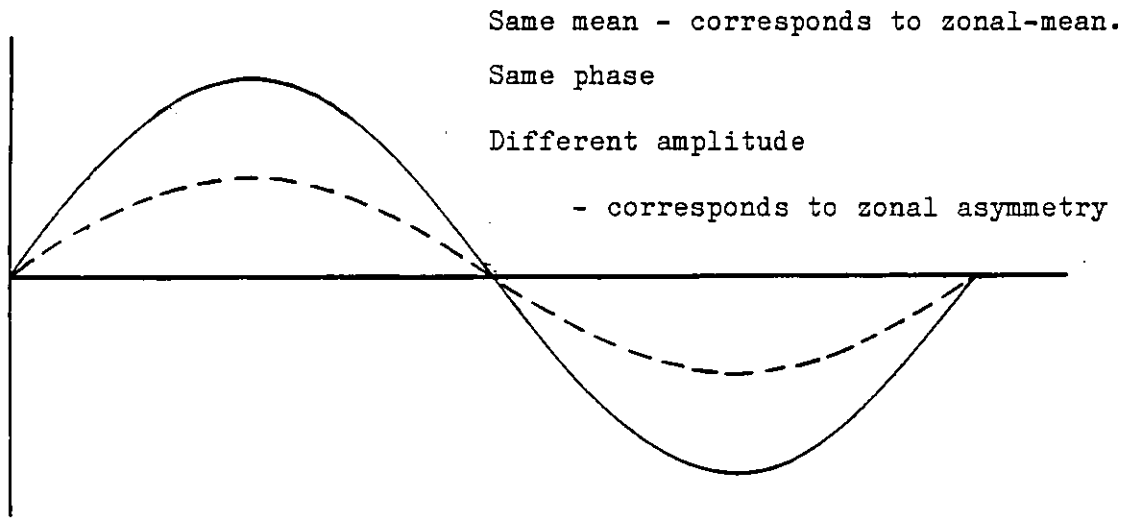

There is no a priori reason to expect a unique spatial variance for a given zonal mean, hence there is no reason why a given zonal-mean temperature gradient should lead to a unique value of $[\bar{T}^{*2}]$ and hence of E_{ST} associated with it. It is therefore possible for the spatial variance in the temperature field to change while the zonal-mean temperature remains constant, so the stationary eddy heat transport could vary considerably between two months while the zonal-mean temperature gradient is the same.

The stationary eddies are a consequence of zonal asymmetry and of atmosphere-Earth interaction -- the latter by way of land-ocean

thermal contrasts which lead to thermal forcing of stationary waves. The degree of contrast is all-important to this; it is however irrelevant to the zonal-mean temperature forcing.

The fact that the stationary eddy sensible heat transport appears related to the temperature gradient is a consequence of their both following similar annual cycles of variation. These cycles are not in phase because the forcing or response to forcing of the meridional entropy gradient lags the forcing or response to forcing of the stationary eddies.

The heat transports are larger in autumn than in spring for the same entropy gradient because the thermal forcing is stronger then -- the contrast between cooling over the land and warming over the oceans is greater; the meridional contrast in heating is similar for months when the entropy gradient is similar. This also applies to the sharp decrease in eddy heat transport from February to March.

Note that the 'latent heat effect' suggested in Section 4.1.5 could play a major role in this: wintertime thermal forcing of stationary waves is due to the difference between heating over the oceans and cooling over land, heating over the oceans being by means of upward transfer of energy from ocean to atmosphere predominantly in the form of sensible and latent heat; thus a larger latent heat flux (vertically) could well modify the thermal forcing such as to increase the eddy heat transport.

4.3.4 Evidence in Support of the Hypothesis.

If the above hypothesis is correct, then it should be possible to demonstrate that the stationary eddy sensible heat transport is a

function of some suitable measure of longitudinal temperature contrast, such as either a temperature difference between air over land and ocean, or the temperature spatial variance (as a measure of average thermal contrast around a complete latitude circle).

A measure of thermal contrast should be typical of the troposphere as a whole. One such measure is the temperature difference between the coldest point over Asia and the warmest over the Pacific (in winter); another is the zonal-mean spatial variance; both being taken on one latitude circle. Figs. 4.4a and b illustrate both possibilities for 55°N. They show that, omitting the months when the stationary eddy sensible heat transport is negative (June, July and August) and the circulation is rather different, the stationary eddy heat transport is very well correlated with both temperature difference and variance. The best-fit straight line does not give a zero intercept in either case: for the temperature difference the intercept is negative (one can imagine that a certain minimum temperature contrast is required to produce any eddy heat transport at all); for the variance it is positive, but a zero intercept fits almost as well. More revealing is Table 4.2 (over), which shows a correlation between eddy heat transport and temperature variance of higher than 99% significance for all latitudes from 35° to 65°N, and an almost constant slope of around .44 between 40° and 60°N.

Alternatively, since heating is mostly at the surface, it is reasonable to look at surface air temperature contrasts between Central Asia (near the centre of the Siberian Anticyclone in winter) and the Gulf of Alaska. Specifically, we look at the temperature difference between Irkutsk (52°N 104°E), averaged over 1921-50 (Clayton (1934, 1947); US Weather Bureau (1959)), and 50°N 156°W

Table 4.2

Slopes, Intercepts and Correlations for Stationary Eddy Sensible Heat Transport against Temperature Variance at 500mb, from months September-May. Data from LM.

LATITUDE	SLOPE	INTERCEPT	CORRELATION
70° N	.075	.30	.479
65° N	.277	.16	.909
60° N	.426	-.15	.988
55° N	.468	-.11	.997
50° N	.444	.18	.995
45° N	.401	.06	.989
40° N	.437	-.44	.992
35° N	.474	-.80	.752

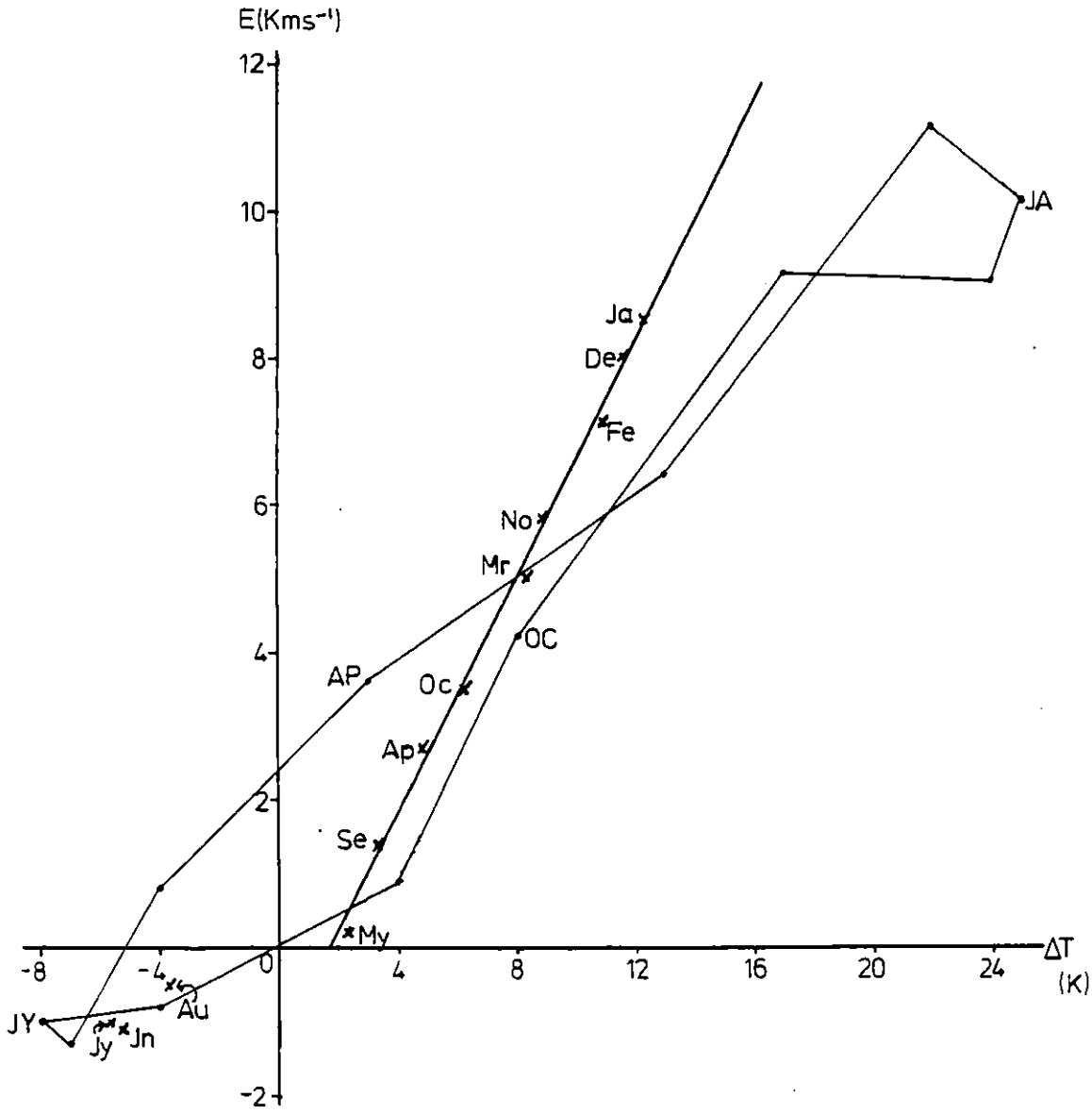

Fig. 4.4a: Stationary eddy sensible heat transport at 55 N against Gulf of Alaska - Central Asia temperature difference: at 500mb (×) and for tropospheric average transport against surface temperature difference (⟵⟶).

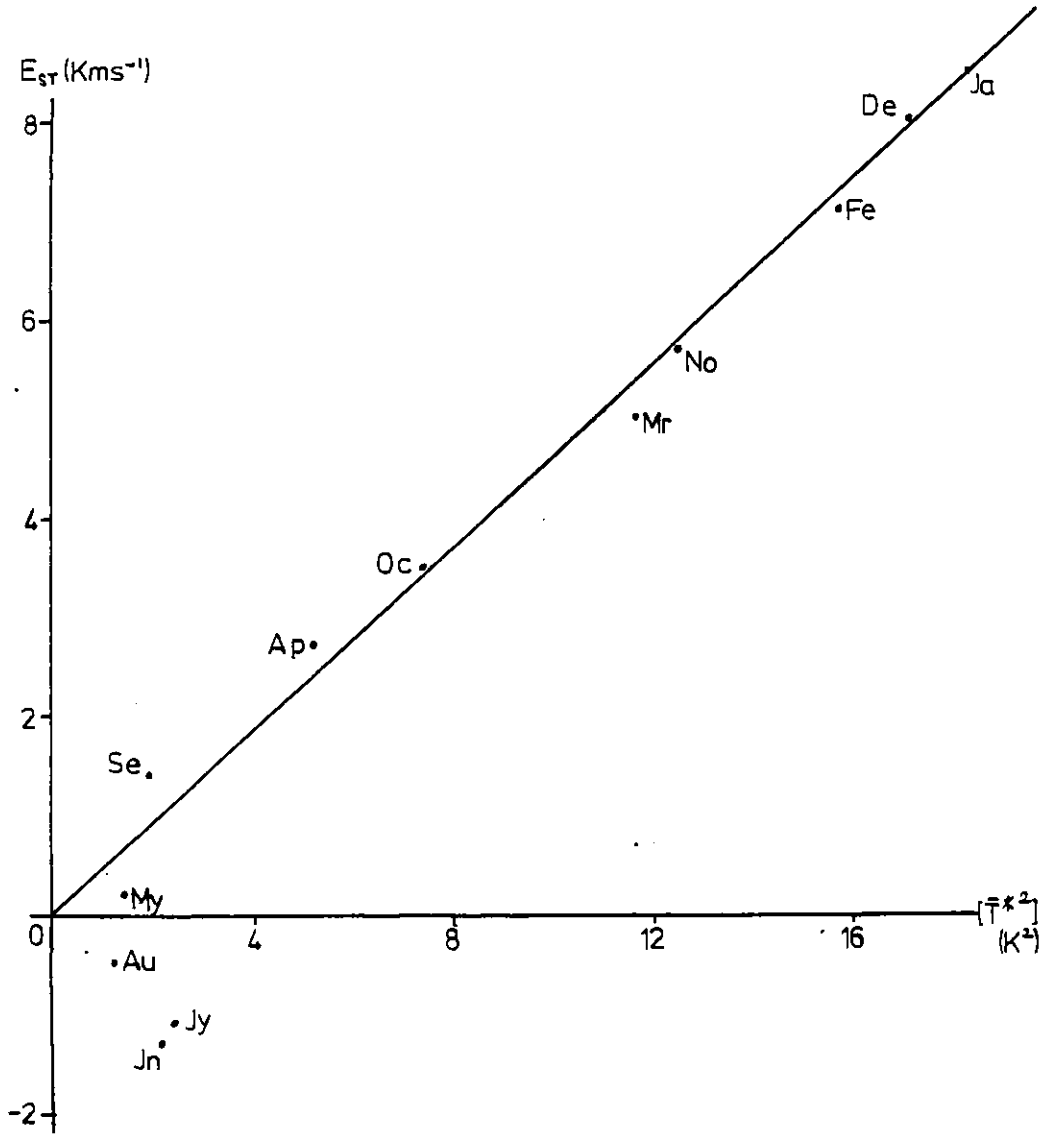

Fig. 4.4b: Stationary eddy sensible heat transport against $[\bar{T}^{*2}]$ at 55°N, 500mb. Data from OR.

(a convenient point to read data off the Monthly Meteorological Charts of the Oceans): this is shown in Fig. 4.4a. Again, there is very strong correlation (.993) between the heat transport and this temperature difference, indicating that the two are strongly linked, though there is a positive non-zero intercept (but as this particular temperature difference is chosen for convenience of obtaining numerical data, this is not necessarily important). It is clear, for example, that the marked decrease in eddy heat transport from February to March coincides with a marked decrease in temperature contrast.

It therefore seems that the stationary eddy sensible heat transport in midlatitudes is closely related to longitudinal thermal contrasts, much more so than to meridional contrast (entropy gradient); this in turn suggests that variations in thermal forcing of stationary waves are responsible for the observed variations in eddy heat transport. This will be shown more conclusively in Chapter 5.

Note that this does not in itself give a useful means of parameterizing eddy heat fluxes, since it is the transient eddy flux, if any, that requires parameterization. In climate models, the stationary waves (planetary waves, ultra-long waves) are carried explicitly, so the heat flux due to them can be calculated exactly.

However, it was stated in Chapter 1 that stationary and transient eddies are not independent of one another: therefore the transient eddy heat flux is probably controlled by the stationary wave pattern, in turn modifying the stationary eddy heat transport by some kind of feedback or diffusion process. This possibility is examined in Chapter 6.

CHAPTER 5

AN ENERGY BUDGET FOR THE ATMOSPHERE

Introduction.

One forcing mechanism for stationary (planetary) waves is the longitudinal asymmetry in diabatic heating of the atmosphere caused by the presence of land and oceans. It was suggested in the previous chapter (Section 4.3.3) that a large change in this thermal forcing would cause the sharp fall in stationary eddy heat transport observed to occur from February to March, and the difference between spring and autumn transports. There are two ways of calculating diabatic heating in the atmosphere. In a column the depth of the atmosphere it is defined by:-

(I) Diabatic Heating = (Net radiation at top of atmosphere) - (Net energy flux at bottom of atmosphere)

or (II) Diabatic heating = (Rate of heat storage in atmosphere) - (Vertically-integrated horizontal heat flux divergence)

The first may be described as the 'Heat Balance' or 'Energy Budget' Method, which forms the basis of this chapter. II is the 'Thermodynamic Equation Method'. The 'Net energy flux at the bottom of the atmosphere' in I consists of all forms of energy transfer: net radiation, sensible heat transfer and the balance between precipitation and evaporation. The heat flux divergence is that due to all forms of energy transport by both mean meridional circulation and eddies: sensible and latent heat, potential and kinetic energy.

Both methods have been used by various authors to calculate diabatic heating of the atmosphere, mainly for the winter season. The first approach has been tried by Smagorinsky (1953) and subsequently Clapp (1961), who compares results for the two methods. II has also

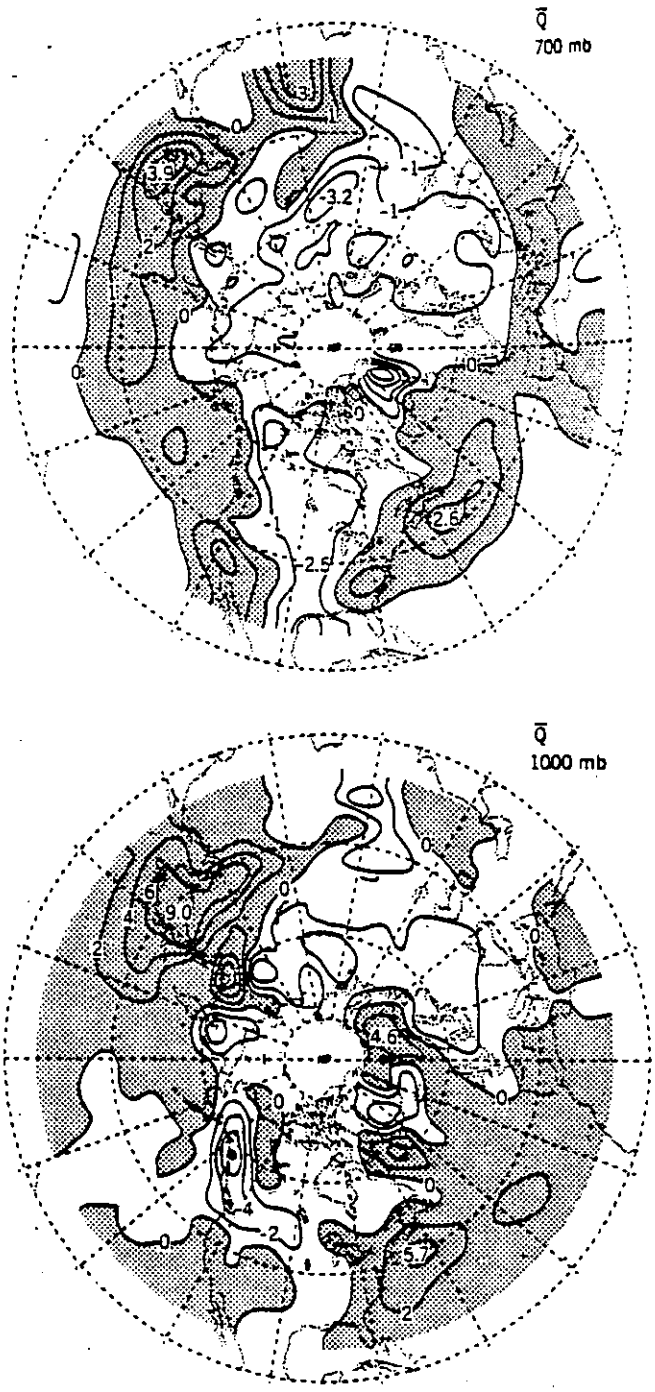

Fig. 5.1: Distribution of diabatic heating rate Q at 700 and 1000mb. Contour interval 1° and 2°C day respectively. From Lau (1979).

been used by Brown (1964), Geller and Avery (1978) and Lau (1979): this method has yielded more reliable results as the availability and quality of data have increased, becoming the standard method. Fig. 5.1 presents Lau's results for 1000mb and 700mb in winter: it shows that the maxima of heating are over the Kuroshio current and Gulf Stream, with minima over North America and Eastern Asia, as we should expect.

However, none of these studies shows the month-to-month variation in diabatic heating: it is this we require in order to see if the ideas of Chapter 4, Section 4.3.3 are valid. Since we are concerned with the degree of zonal asymmetry, it will be sufficient to calculate diabatic heating over land and oceans, averaged across each, which can be calculated from net flux data by Method I, as will be described below.

5.1 Data-Set Used.

5.1.1 Data Presented.

The data used have been taken entirely from Oort and Vonder Haar (1976 - hereafter designated OVH), who calculated from a number of sources all the zonal-mean energy budget terms for both the atmosphere and land/ocean underlying it. The energy budget equations for a column in the atmosphere and ocean, neglecting some very small terms, are

$$\text{ATMOSPHERE:}\quad F_{TA} - F_{BA} - S_A - \mathrm{div}(H_A) = 0 \qquad (5.1)$$

$$\text{OCEAN:}\quad F_{TO} - S_O - \mathrm{div}(H_O) = 0 \qquad (5.2)$$

where

F refers to net vertical flux

S refers to heat storage: $S = (c_p \Delta p/g)\partial T/\partial t$

H refers to horizontal heat transport by eddies and mean circulation.

Subscripts T, B refer to Top, Bottom; A, O to Atmosphere, Ocean

All terms are given in Wm^{-2}.

Diabatic Heating, $\dot{Q}$, of the atmosphere can be written

$$\dot{Q} = F_{TA} - F_{BA} = S_A + \mathrm{div}(H_A) \qquad (5.3)$$

Storage of heat by land is negligible compared with that by the oceans, so we can write $F_{TO} \approx F_{BA}$. How numerical values of these quantities are found is described in Section 5.1.2 below.

The numerical values presented are means for each of the twelve months of the year; they are for zonal belts throughout the Northern Hemisphere. The storage and flux divergence terms are vertical integrals.

Note that the vertically-integrated meridional heat transport at a latitude can be obtained by areal integration of the flux divergences for all the zonal belts from that latitude northwards (as the meridional flux at the Pole is zero by definition).

5.1.2 Origin and Sources of Data.

The net radiation flux at the top of the atmosphere is calculated from measurements taken over a period of eight years by a total of six

different satellites: most months of the year are represented by 2 or 3 different years' data. The satellites measured reflected solar and emitted infra-red radiation, the incoming solar radiation being known independently. Further information on these data are presented in Ellis and Vonder Haar (1976).

The storage and divergence terms are in principle derived from OR, although there are certain inconsistencies between the two data-sets which will be discussed in the next section. They are based on the analysis of daily aerological records for five years from May 1958, as described in Chapter 1, Section 1.3.1.

The net energy flux at the bottom of the atmosphere is due to four separate components: long-wave radiation, sensible heat transfer, evaporation and precipitation. In principle, it can be derived from separate estimates of each of these components, as was done by Clapp (1961), Budyko (1963) and more recently by Esbensen and Kushnir (1981). Alternatively, it may be calculated from Eq. (5.1) as a residual term, assuming an accurate knowledge of the other three quantities: it is this indirect method which OVH use, which they consider more reliable than measurements of the components for calculation of the zonal-mean.

For the oceans, the only quantity for which data both reliable and extensive enough are available is the temperature, whence the heat storage can be calculated. F_{BQ} has already been calculated indirectly, so making use of these two quantities and Eq. (5.2) the horizontal flux divergence can be calculated.

Thus for the atmosphere all quantities but one are known from direct measurements; for the ocean, only one is known directly.

5.1.3 Errors in the Data.

These fall into four categories, viz:-

(i) Errors in original measurements.

(ii) Cumulative errors from (i) in calculation of 'indirect' quantities such as F_{BA}.

(iii) Errors in data presentation.

(iv) Errors found through comparison with equivalent data-sets, or by inspection.

The first two of these are assessed in Appendix B of OVH and, for the satellite data, in Ellis and Vonder Haar (1976). They state that the largest source of uncertainty in the data is year-to-year variability: it is this which is assessed explicitly in that appendix. From October to March the standard error in F_{TA} is less than 10%; that in F_{BA} (calculated from the law of propagation of independent errors) is generally no more than 20% in the same period. As the quantities we are interested in (see below, Section 5.2) are generally at least as large as either F_{TA} or F_{BA}, these errors are acceptable, as the points to be made in Section 5.3 will not be critically dependent on such errors.

There are also at least two internal inconsistencies in OVH's tabulated data (found by application of Eqs. (5.1) and (5.2)). The atmospheric flux divergence for December in the 70°-80°N belt should read -159 not 159 (as is obvious from their Fig. 4.4); the oceanic flux divergence in February should probably be -7 not 7Wm^{-2} for Eq. (5.2) to balance, though it is not absolutely clear from OVH's figures that it is this component which is wrong. All other quantities appear to balance.

The remaining errors are more difficult to correct: these became apparent whenn the energy budget was calculated (see below, Section 5.3), and appear suspect in OVH, but their origin cannot be ascertained. One of these is F_{BA} in March, 60°-70°N, which looks suspect and gives odd budget results. Inspection of tables and figures suggests that F_{TA} may be wrong: a figure of -90 to -95Wm^{-2} would appear from their Fig. 2 to be more reasonable, which would reduce F_{BA} to around 20Wm^{-2}. Inspection of Ellis and Vonder Haar (1976) suggests that the calculation of solar radiation absorbed in an Earth-atmosphere column may be a little high at 83.1Wm^{-2}, which derives from a low satellite measurement of the reflected solar radiation. The correct values cannot be further ascertained without recourse to the original satellite data.

The other errors of this nature appearing in OVH concern the total meridional heat transport at 50°N. There are three published versions of this from the same original data source: OR, OVH and Oort (1971). There is good agreement between all three sets for all months except February and November. Of these, OR and OVH agree for February, but Oort (1971) is at least consistent with LM in showing a more gradual fall in the stationary eddy heat transport from January to March rather than a sudden fall from February; hence OR and OVH may both be wrong. Even so, the required correction is probably to the flux divergences for February and March in the 60°-70°N belt, which will not greatly alter our results.

A more irreconcilable discrepancy appears in November, for which all three data-sets are mutually inconsistent. Of these, OR gives the highest total flux and a larger stationary eddy component than Oort (1971): we recall from Chapter 2 that November transports seemed

unusually large in places. The November divergence in the 50°-60°N belt is given as $31 Wm^{-2}$ which is rather higher than the values around, consistent with too large a flux at 60°N in OR: if this were changed to around $-20 Wm^{-2}$, say, F_{BA} would then also be more reasonable (say $-100 Wm^{-2}$ instead of $-154 Wm^{-2}$), and the whole budget would look more plausible -- this should be borne in mind when considering the results presented in Section 5.3. It would also be more consistent with the behaviour observed in LM, where November showed no abnormally large heat transport.

Apart from these discrepancies, all three of OR, OVH and Oort (1971) appear to be mutually consistent in their heat transports, so atmospheric flux divergences and hence F_{BA} are more likely to be right. Having found these problems, it should now be possible to calculate acceptable energy budgets to test the ideas of Chapter 4, Section 4.3.3.

5.2 The Energy Budget.

The fundamental equations are Eqs. (5.1) - (5.3). The simplest form of the budget is to determine the heating or cooling over the land and the ocean, the zonal-mean part of this and the zonal asymmetry. This will suffice to show the degree of zonal asymmetry in the diabatic heating, but will give no idea of the variation in that heating across the oceans or land: essentially we are using a step-function which might look like this:-

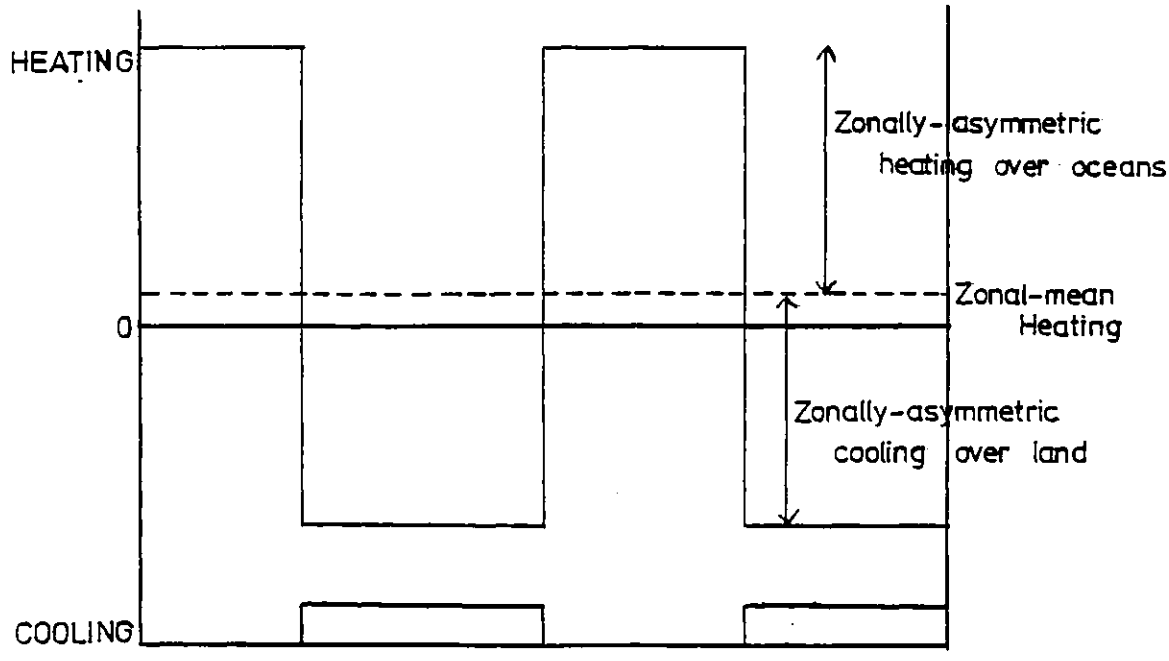

Note that the zonally-asymmetric components of heating over land and ocean are not necessarily identical: the reason for this will become apparent.

In order to determine the various components of the heating, we require to know the fraction ε of each zonal belt covered by ocean. We assume $F_{BA} = 0$ over land (this is a good approximation outside ice-capped regions at least). Hence, since F_{BA} as given is a zonal-mean (ie it is assumed to be the same all the way round the zonal belt), the real value of F_{BA} over the oceans is F_{BA}/ε.

We can therefore write down

$$\dot{Q}_{LAND} = F_{TA} \tag{5.4a}$$

$$\dot{Q}_{OCEAN} = F_{TA} - F_{BA}/\varepsilon \tag{5.4b}$$

The zonal-mean component of this is given by

$$\overline{\dot{Q}}^{*} = F_{TA} - F_{BA}$$

as before (Eq. (5.3)).

Hence the asymmetric parts of the heating, which will be written as $\dot{Q}^{*}$, are given by

$$\dot{Q}^{*}_{LAND} = F_{BA} \qquad (5.5a)$$

$$\dot{Q}^{*}_{OCEAN} = -F_{BA}(1 - 1/\varepsilon) \qquad (5.5b)$$

This formulation is capable of refinement in several ways. One of these is to calculate explicitly the various surface fluxes, to assess the effect of each (in particular, of the latent heat transfer). Given gridpoint surface flux data and satellite radiation data it would of course be possible to calculate the diabatic heating in an atmospheric column directly as a function of longitude. However, the formulation above will suffice to show the variations in thermal forcing through the year.

5.3 Results.

Table 5.1 shows the various terms in Eqs. (5.3) - (5.5) for 10° zonal belts from 20° to 70° N. The last three columns are the most important: they show $\overline{\dot{Q}}^{*}$, $\dot{Q}^{*}_{LAND}$ and $\dot{Q}^{*}_{OCEAN}$. Bearing in mind the possible errors and corrections suggested in Section 5.1.3, we can see from this how both zonal-mean forcing (of meridional entropy gradient) and zonally-asymmetric forcing (of stationary waves) vary through the year.

Table 5.1

Energy budget terms for each month

ENERGY BUDGET TERMS FOR MONTH OF JAN — UNITS OF W/M**2

LAT.	FTA	FBA	LAND HEATING	OCEAN HEATING	MEAN	HEATING ASYM. LAND	HEATING ASYM. OCEAN
60-70	-156	-32	-156	-34	-124	-32	90
50-60	-144	-138	-144	185	-6	-138	191
40-50	-114	-130	-114	149	16	-130	133
30-40	-82	-64	-82	28	-18	-64	46
20-30	-50	-109	-50	123	59	-109	64

ENERGY BUDGET TERMS FOR MONTH OF FEB — UNITS OF W/M**2

LAT.	FTA	FBA	LAND HEATING	OCEAN HEATING	MEAN	HEATING ASYM. LAND	HEATING ASYM. OCEAN
60-70	-130	2	-130	-138	-132	2	-6
50-60	-102	-123	-102	192	21	-123	171
40-50	-76	-110	-76	146	34	-110	112
30-40	-46	-21	-46	-10	-25	-21	15
20-30	-13	-61	-13	84	48	-61	36

ENERGY BUDGET TERMS FOR MONTH OF MAR — UNITS OF W/M**2

LAT.	FTA	FBA	LAND HEATING	OCEAN HEATING	MEAN	HEATING ASYM. LAND	HEATING ASYM. OCEAN
60-70	-78	36	-78	-215	-114	36	-101
50-60	-56	-67	-56	104	11	-67	93
40-50	-23	-40	-23	58	17	-40	41
30-40	7	16	7	-20	-9	16	-11
20-30	35	-35	35	91	70	-35	21

ENERGY BUDGET TERMS FOR MONTH OF APR — UNITS OF W/M**2

LAT.	FTA	FBA	LAND HEATING	OCEAN HEATING	MEAN	HEATING ASYM. LAND	HEATING ASYM. OCEAN
60-70	-72	0	-72	-72	-72	0	0
50-60	-12	-14	-12	21	2	-14	19
40-50	20	8	20	4	12	8	-8
30-40	34	-3	34	39	37	-3	2
20-30	42	-12	42	61	54	-12	7

ENERGY BUDGET TERMS FOR MONTH OF MAY — UNITS OF W/M**2

LAT.	FTA	FBA	LAND HEATING	OCEAN HEATING	MEAN	HEATING ASYM. LAND	HEATING ASYM. OCEAN
60-70	-12	4	-12	-27	-16	4	-11
50-60	30	32	30	-46	-2	32	-44
40-50	57	29	57	-2	28	29	-30
30-40	68	34	68	10	34	34	-24
20-30	66	24	66	28	42	24	-14

ENERGY BUDGET TERMS FOR MONTH OF JUN — UNITS OF W/M**2

LAT.	FTA	FBA	LAND HEATING	OCEAN HEATING	MEAN	HEATING ASYM. LAND	HEATING ASYM. OCEAN
60-70	42	43	42	-121	-1	43	-120
50-60	52	33	52	-27	19	33	-46
40-50	68	53	68	-39	15	53	-54
30-40	78	37	78	14	41	37	-27
20-30	68	32	68	17	36	32	-19

ENERGY BUDGET TERMS FOR MONTH OF JLY — UNITS OF W/M**2

LAT.	FTA	FBA	LAND HEATING	OCEAN HEATING	MEAN	HEATING ASYM. LAND	HEATING ASYM. OCEAN
60-70	48	72	48	-226	-24	72	-202
50-60	55	46	55	-55	9	46	-64
40-50	65	66	65	-68	-1	66	-67
30-40	79	43	79	5	36	43	-31
20-30	76	62	76	-22	14	62	-36

ENERGY BUDGET TERMS FOR MONTH OF AUG — UNITS OF W/M**2

LAT.	FTA	FBA	LAND HEATING	OCEAN HEATING	MEAN	HEATING ASYM. LAND	HEATING ASYM. OCEAN
60-70	-11	28	-11	-117	-39	28	-78
50-60	15	21	15	-35	-6	21	-29
40-50	37	56	37	-76	-19	56	-57
30-40	57	28	57	9	29	28	-20
20-30	61	48	61	-15	13	48	-28

ENERGY BUDGET TERMS FOR MONTH OF SEP — UNITS OF W/M**2

LAT.	FTA	FBA	LAND HEATING	OCEAN HEATING	MEAN	HEATING ASYM. LAND	HEATING ASYM. OCEAN
60-70	-50	28	-50	-156	-78	28	-78
50-60	-18	14	-18	-51	-32	14	-19
40-50	-5	18	-5	-41	-23	18	-18
30-40	11	4	11	4	7	4	-3
20-30	37	5	37	29	32	5	-3

ENERGY BUDGET TERMS FOR MONTH OF OCT — UNITS OF W/M**2

LAT.	FTA	FBA	LAND HEATING	OCEAN HEATING	MEAN	HEATING ASYM. LAND	HEATING ASYM. OCEAN
60-70	-135	-26	-135	-36	-109	-26	73
50-60	-104	-80	-104	87	-24	-80	111
40-50	-65	-46	-65	28	-19	-46	47
30-40	-37	-21	-37	-1	-16	-21	15
20-30	-6	-52	-6	77	46	-52	31

ENERGY BUDGET TERMS FOR MONTH OF NOV — UNITS OF W/M**2

LAT.	FTA	FBA	LAND HEATING	OCEAN HEATING	MEAN	HEATING ASYM. LAND	HEATING ASYM. OCEAN
60-70	-158	-56	-158	55	-102	-56	157
50-60	-138	-154	-138	230	16	-154	214
40-50	-106	-87	-106	70	-19	-87	89
30-40	-76	-46	-76	3	-30	-46	33
20-30	-42	-81	-42	87	39	-81	48

ENERGY BUDGET TERMS FOR MONTH OF DEC — UNITS OF W/M**2

LAT.	FTA	FBA	LAND HEATING	OCEAN HEATING	MEAN	HEATING ASYM. LAND	HEATING ASYM. OCEAN
60-70	-160	-48	-160	23	-112	-48	135
50-60	-150	-112	-150	117	-38	-112	155
40-50	-122	-140	-122	161	18	-140	143
30-40	-91	-63	-91	17	-28	-63	45
20-30	-60	-106	-60	108	46	-106	62

5.3.1 Zonally-Asymmetric Heating.

While not all the features of the annual variation in this differential heating can be closely related to variations in stationary eddy sensible heat transport, the main features of the latter can. The justification for doing this is that $[\overline{T}^{*2}]$ should be closely related to differential heating, and the stationary eddy sensible heat transport was shown (Chapter 4, Section 4.3.4) to be strongly correlated with $[\overline{T}^{*2}]$. In particular, the variation in heat transport during the first four months of the year is closely linked to the variation in heating -- if anything, the heat transport is 'too high' in March and April (indicating a lag in response to changes in forcing, which it is reasonable to expect: this is about 10 days). Similarly, using modified November values it is clear that the heat transport then should be much larger than in April, as it is. Using a modified December F_{BA} (Fig. 5 of OVH suggests that $-120 Wm^{-2}$ is closer than $-112 Wm^{-2}$), the October - January variations can be closely correlated also. Thus we can relate very well the variations in forcing and response for October-April, with possibly a lag of ten days or so when the forcing changes sharply, as in October and March.

Note that the February-March fall in heating contrast is a result of both F_{TA} and F_{BA} being halved. The former is due principally to the change in the Earth's inclination towards the Sun (from orbital geometry); the latter must be due mainly to changes in the surface latent and sensible heat fluxes.

The stationary eddy heat transport at 30°N falls steeply from January to February (Fig. 2.2), as does the heating contrast in the 20°-40°N zonal belt: so the stationary eddy heat transports at these

latitudes are also closely linked to the heating contrast between land and oceans.

For the remaining months of the year, it is rather more difficult to relate differential heating and eddy heat transport: the contrast between land and sea is reversed in May but the zonal-mean stationary eddy heat transport does not become equatorward until June, similarly in September there is still more heating over land but the heat transport reverts to being poleward then. However, meridional heat transport also depends on the sign of the stratospheric zonal wind: this is easterly in May, so the poleward heat transport then still seems mysterious, but it is so small it can probably be ignored. In general, the summer circulation is rather different from that in winter, and reversal of heat sources and sinks need not reverse the eddy heat transport.

Considering now the effect of clouds on F_{TA} in the 50°-60°N belt, the likelihood is that in winter there will be high cloud over the oceans, low cloud over land, which will in turn accentuate heating over the ocean/cooling over land by reducing/increasing the infra-red radiation to space over ocean/land below/above the zonal mean, so that $F_{TA} > \overline{F}^{x}_{TA}$ over land, $F_{TA} < \overline{F}^{x}_{TA}$ over the ocean. With the surface flux F_{BA} producing heating over the ocean/cooling over land, the heating asymmetry in winter will tend to be increased. Thus even if errors in F_{BA} arising from its calculation as a residual term might tend to reduce the asymmetry, the longitudinal variation of F_{TA} will maintain it. The mean cloud field changes little from February to March.

It seems reasonable to relate the stationary eddy sensible heat transport directly to the degree of longitudinal asymmetry in the

diabatic heating field rather than to the meridional entropy gradient, at least for October through to April.

5.3.2 Zonal-Mean Heating.

From Table 5.1 it is immediately apparent that the difference between zonal-mean heating in the 20°-30°N and 60°-70°N zonal belts, which maintains the meridional entropy gradient between about 25° and 65°N, is roughly constant from January to March, as is Δ; it then drops steeply to April, as does Δ. Thus it seems that the variations in both the stationary eddy sensible heat transport and the meridional entropy gradient are consistent with the thermal forcing mechanisms acting to produce them.

Fig. 5.2 shows the annual variation of Δ with respect to meridional difference in diabatic heating. Except for November and December, it shows good correspondence between them, but a distinct lag in the response of Δ, of about 1 month. This can be explained by the annual cycle of $\mathrm{div}(H_A)$, in particular the eddy sensible heat component which dominates in midlatitudes, in the zonal belt 60°-70°N (treating 20°-30°N as roughly isothermal: Fig. 2.7 shows that the annual variation here is small compared with that at 60°-70°N). The reduction in $-\mathrm{div}(H_A)$ from March to June will tend to hold the zonal-mean temperature at around 65°N lower than if that temperature depended only on F_{TA} and F_{BA}, ie with the divergence remaining constant. The entropy gradient depends on this temperature, so it does not rise as fast as changes in F_{TA} and F_{BA} would suggest. Similarly, Δ is held low in September and October by $-\mathrm{div}(H_A)$ increasing, maintaining $\overline{T}^{\times}_{65}$ higher than it would otherwise be, and hence Δ lower.

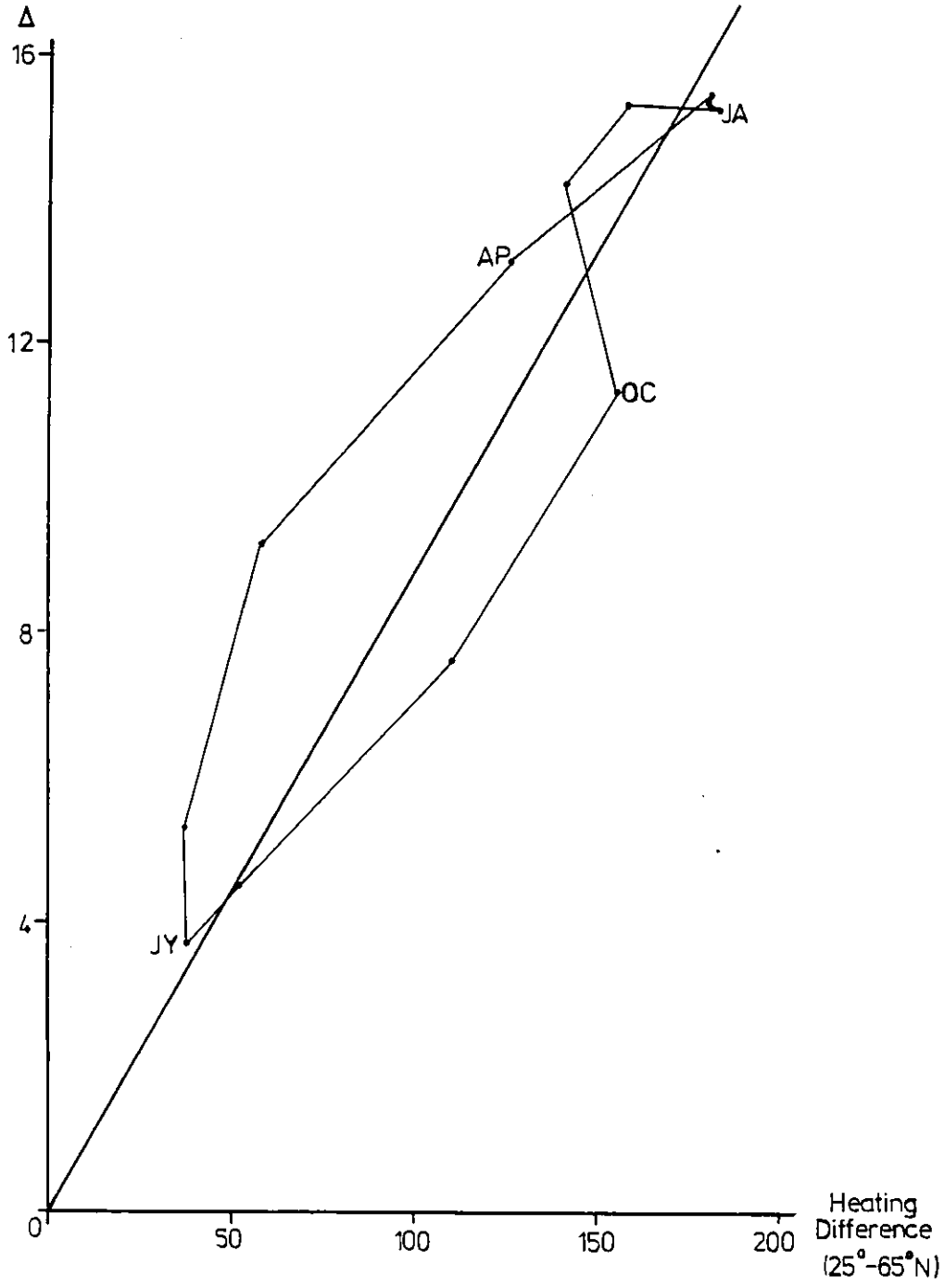

Fig. 5.2: Zonal-mean entropy gradient at 500mb against meridional difference in zonal-mean diabatic heating (Units: Wm^{-2}).

5.4 Discussion.

The annual variation of the stationary eddy sensible heat transport can be explained successfully in terms of variations in the land-ocean heating contrast. That of the entropy gradient can similarly be explained by variations in the latitudinal heating contrast, modified by eddy heat transports producing a lag in response to changes in that contrast. Thus, the response-time to variations in forcing seems to be about 10 days for the eddy heat transport (strictly, in $[\overline{T}^{*2}]$), 30 days for the entropy gradient, consistent with the lag between these two quantities being around 3 weeks in winter, 1 week in summer (Chapter 4, Section 4.1.1).

In winter, the large deficit in radiation heating at middle and high latitudes is compensated principally by the horizontal heat flux divergence. The change in $\overline{T}^{x}_{65°}$ during spring is less than would be expected from changes in the vertical flux difference ($F_{TA} - F_{BA}$), since the horizontal flux divergence is smaller. This in turn results from the reductions in meridional heat flux -- in particular, that in the stationary eddy contribution to the flux, which arises from a reduction in the heating contrast between land and oceans. It is therefore possible to produce a scheme for variations in stationary eddy heat flux and meridional entropy gradient:-

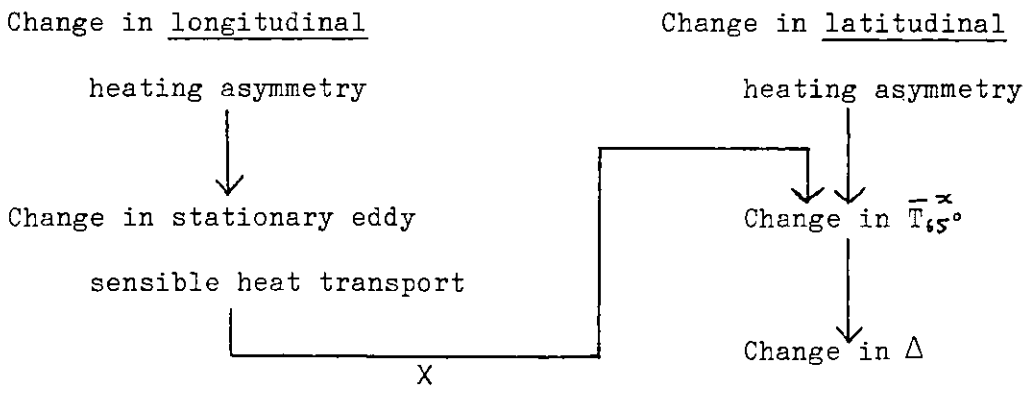

Of course, there will be other feedback loops besides that denoted X, but this scheme plus the data presented above now explain much of the annual cycles of variation in both the stationary eddy sensible heat transport and meridional entropy gradient, and the lag of entropy gradient behind heat transport. Thus several of the features to be explained in Fig. 1.1 have been accounted for; the cause of the 'loop' in those figures is now understood, empirically at least.

CHAPTER 6

AN ANALYTIC MODEL FOR HEAT TRANSPORT BY STATIONARY WAVES

Introduction.

One aspect of the problem of the annual variation of eddy heat fluxes which has so far not been investigated in this study is the problem of why the transient eddy flux is for most of the year apparently independent of meridional temperature gradient, and how the transient and stationary eddies interact. It was suggested in Chapter 1, Section 1.4 that the transient eddies acted upon the stationary eddies in winter to modify their meridional heat transport: in this chapter we examine how they might do this. In winter, the stationary waves give rise to temperature gradients with a large zonal component in places: transient eddies will transport heat down local gradients, so in such places they will produce a strong transport of heat in the zonal direction as well as a meridional flux. This could modify significantly the amplitudes and relative phase of the temperature and geopotential height waves, and hence the stationary eddy heat transport. Furthermore, as the stationary waves increase in intensity, the longitudinal component of the temperature gradient will also become greater, and the transient eddy flux vector will point increasingly in the zonal direction.

We investigate in this chapter whether the (longitudinal) diffusion of heat (or rather, potential vorticity) caused by the process described above will enhance or damp the stationary eddy heat transport. If it enhances this transport, it will show that this kind of interaction between stationary and transient eddies can account for the stationary eddy heat transport increasing in autumn and winter while the transient eddy heat transport hardly varies, as seen in Fig. 1.1.

It is immediately apparent that the stationary wave pattern, which is 'externally' forced (as described in Chapters 4 and 5), will in this process control the transient eddy heat transport and thus in some way the effect of transient eddies on itself. Here we look only at how the stationary waves are modified by the diffusive action of transient eddies; a full treatment of the interaction between stationary and transient eddies is beyond the scope of this study. White and Green (1982) investigated the steady-state response to steady thermal forcing in a model incorporating parameterized transient eddies, and hinted at the need to formulate a time-dependent numerical model to study the growth of transient eddies on a long-wave field and the dynamical self-interaction in such a system.

Here, a simple analytic model is used to investigate the effect of transient eddies, represented by a diffusion term, on the meridional sensible heat transport due to planetary waves of zonal wavenumber m = 2.

6.1 The Model.

The linearised quasi-geostrophic potential vorticity equation may be written

$$U\frac{\partial}{\partial x}\left[\nabla_H^2 \psi + \frac{f_o^2}{gB}\frac{\partial^2 \psi}{\partial z^2}\right] + \beta\frac{\partial \psi}{\partial z} = K_H \nabla_H^2\left[\nabla_H^2 \psi + \frac{f_o^2}{gB}\frac{\partial^2 \psi}{\partial z^2}\right] + \frac{f_o}{B}\frac{\partial S}{\partial z} \qquad (6.1)$$

where

U is zonal wind - taken to be constant with height and latitude

K_H is a diffusion coefficient

Other symbols have their usual meanings

The first term on the right hand side of Eq. (6.1) is the diffusion of potential vorticity by the transient eddies, the effect of which we wish to investigate; the second is the entropy source term (so that the waves are thermally forced).

The linearised thermodynamic equation is

$$U\frac{\partial \Phi'}{\partial x} + wB = K_H \nabla_H^2 \Phi' + S \qquad (6.2)$$

We can write $\Phi = \frac{f_0}{g}\frac{\partial \psi}{\partial z}$

Note that primes now refer to departures from zonal mean.

Given an entropy source function

$$S = S_0 e^{ikx} e^{-bz} \cos ly$$

We seek solutions to Eq. (6.1) of the form

$$= Ae^{ikx}e^{i\nu z}\cos ly + A'e^{ikx}e^{-i\nu z}\cos ly + Ce^{ikx}e^{-bz}\cos ly \qquad (6.3)$$

We choose the upward-propagating mode (trough-lines tilting westward with height), with no lid, by taking A' = 0.

We write A, C and ν in the following forms:-

$$A = |A| e^{i(\pi + \chi - \phi/2)}$$

$$C = |C| e^{i\xi}$$

$$= |\nu| e^{i\phi/2} = \nu_R + i\nu_I$$

Utilising the lower boundary condition w = 0 at z = 0 (ie no orographic forcing) yields the solutions (see Appendix for method)

$$|A| = \frac{G}{|\nu|\sqrt{F}}\{1 + D^2[FD^2X + 2(1 + EW)]\}^{1/2} \tag{6.4a}$$

$$\chi = \tan^{-1}\left\{\frac{\left[\frac{E}{F} + D^2 W\right]}{\left[\frac{1}{F} + D^2\right]}\right\} \tag{6.4b}$$

$$|C| = \frac{GD^2\sqrt{X}}{b} \tag{6.5a}$$

$$\xi = \tan^{-1}\left(\frac{-P}{E\lambda_*^2}\right) \tag{6.5b}$$

$$|\nu| = \left(\frac{\beta}{Q^2 U}\right)\left\{\frac{F + T^2F - 2F}{F}\right\}^{1/4} \tag{6.6a}$$

$$\phi = \tan^{-1}\left(\frac{E}{1 - FT}\right) \tag{6.6b}$$

where

$$\lambda_*^2 = \lambda^2 - Q^2 b^2 \qquad D^2 = \frac{Q^2 b^2}{XP}$$

$$E = \frac{K_H \lambda^2}{k U} \qquad F = 1 + E^2$$

$$G = \frac{g S_0}{f_0 U k} \qquad P = \lambda_*^2 - \beta/U$$

$$Q^2 = \frac{f_o^2}{gB} \qquad T = \upsilon\lambda^2/\beta$$

$$W = \frac{E\lambda_*^2}{P} \qquad X = 1 + W^2$$

For algebraic purposes, $\lambda^2 = (k^2 + l^2)$, however numerically we substitute its value from spherical geometry, given by

$$\lambda^2 = \frac{(n-1)(n+2)}{R_e}$$

where

R_e is the radius of the Earth

n is as in the associated Legendre polynomial P_n^m

K_H, the diffusion coefficient, can be defined such that

$$(K_H\lambda^2)^{-1} = \tau_D \qquad (6.7)$$

where τ_D is the time in which planetary waves would be completely damped by the action of transient eddies in the absence of forcing. Lau (1979) calculates from mean temperatures and transient eddy heat flux divergences that τ_D is about 7 days for m = 2 at 50 N, though earlier estimates were about 4 days.

By setting $K_H = 0$ we can calculate the heat transport due to waves forced solely by diabatic heating, unmodified by transient eddies.

The surface pressure and temperature waves may be expressed as

$$p_s' = \rho_s f_o \psi_s = \rho_s f_o |p| e^{i\theta_1}$$

$$T_s' = \frac{\xi_o}{g}\left(\frac{\partial \psi}{\partial z}\right)_s = \frac{\xi_o}{g}|T|e^{i\theta_2}$$

where the subscript "s" indicates the value at the surface.

Writing

$$\pi + \chi - \phi/2 = F_1$$
$$\pi/2 + \phi/2 + F_1 = \chi_2$$
$$F_1 - \xi = F_2$$

yields

$$|p| = \{|A|^2 + |C|^2 + 2|A||C|\cos F_2\}^{1/2} \tag{6.8a}$$

$$|T| = \{|A|^2|\nu|^2 + b^2|C|^2 - 2b|\nu||A||C|\cos(\chi_2 - \xi)\}^{1/2} \tag{6.9a}$$

$$\theta_1 = \tan^{-1}\left\{\frac{|A|\sin F_1 + |C|\sin\xi}{|A|\cos F_1 + |C|\cos\xi}\right\} \tag{6.8b}$$

$$\theta_2 = \tan^{-1}\left\{\frac{|A||\nu|\sin\chi_2 - b|C|\sin\xi}{|A||\nu|\cos\chi_2 - b|C|\cos\xi}\right\} \tag{6.9b}$$

The entropy transport may be written as

$$[v'\Phi'] = \frac{1}{2}\frac{\xi_o}{g}Re\left\{\left(\frac{\partial\psi}{\partial x}\right)\left(\frac{\partial\psi}{\partial z}\right)^*\right\} \tag{6.10}$$

Substitution of ψ from Eq. (6.3) yields

$$[v'\Phi'] = \frac{1}{2}\frac{\xi_o}{g}\{\nu_R k|A|^2 e^{-2z} + [K|A||C|e^{-(b+\nu_I)z}] \times [(b-\nu_I)\sin(F_2 + \nu_R z) + \nu_R\cos(F_2 + \nu_R z)]\}\cos^2 ly \tag{6.11}$$

6.2 Results.

Although we are working in Cartesian geometry, we shall define the meridional modes according to the equivalent spherical harmonics: thus, for example, n = 3 represents a mode with one peak between equator and pole (since the number of peaks for a given associated Legendre polynomial is (n - m)). We shall use odd harmonics only, and look at zonal wavenumber m = 2. We shall also set cos ly = 1, to maximise the flux in midlatitudes.

There are thus five parameters we can vary in the expressions for A, C and ν, namely U, the zonal windspeed; S_o, the heating amplitude; K_H, the diffusion coefficient; B, the static stability; and n. In general, we take $S_o = 6.7 \times 10^{-8} s^{-1}$, corresponding to heating of 1.5 K day^{-1}, and $B = 1.5 \times 10^{-5} m^{-1}$; the effect of varying these is investigated in Section 6.2.1 below. We take b to be $(4km)^{-1}$. U must be chosen so that it is large enough to simulate the effect of the stronger zonal wind from the tropopause upwards, yet not so large that it damps out all eddy motion near the surface. The stratospheric zonal wind is important in this case as its strength controls the upward propagation of planetary waves, and hence their poleward heat transport. Locally, fluxes near the surface (in this type of model it is the surface fluxes which are generally largest) are controlled by the zonal wind near the surface (as for example in the Siberian Anticyclone), but we are here interested in global-scale waves extending at least throughout the troposphere. A value of 5 ms^{-1} or 7.5 ms^{-1} is realistic.

The value of K_H to be used depends on λ (see Eq. (6.7)), and also on the estimated damping time. The values to be used for

different n are given in Table 6.1.

There exists for $K_H = 0$ a critical zonal windspeed U_c for which the waves become evanescent (with no diffusion) and hence trapped at the tropopause - ν is pure imaginary in this case. This is given by

$$U_c = \frac{\beta}{\lambda^2} \tag{6.12}$$

as can be seen from Eq. (A7): E = 0 and hence F = 1. Values of U_c for different n are given in Table 6.1.

Table 6.1

n	U_c (ms^{-1})	K_H (m^2s^{-1})	Damping Time (Days)
3	58.94	10^7	4.7
5	21.01	3.35×10^6	5
7	10.90	1.74×10^6	5
9	6.69	1.07×10^6	5
11	4.53	7.23×10^6	5

In the ensuing sections, heat transport profiles are given up to 15 km: we do not expect this model to simulate well the stratospheric profile, as the zonal wind and static stability are much stronger there.

6.2.1 n = 3 Mode.

A number of experiments were run with this mode, to test the effects of varying K_H, S_o, U and B. In all cases, $U < U_c$, so the waves are not trapped.

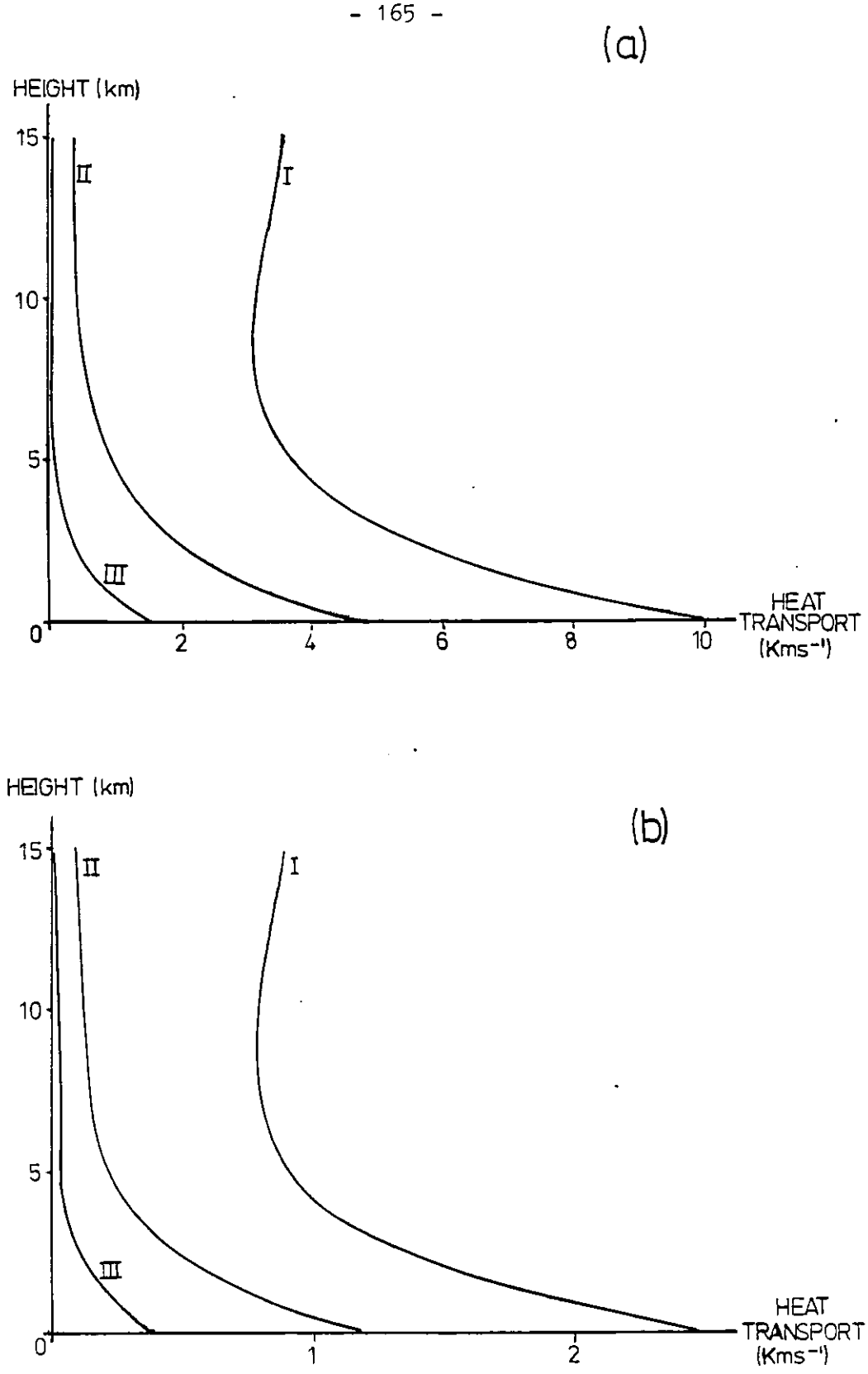

Fig. 6.1: Vertical profile of heat transport for n = 3 mode, with (a) $S_o = 6.7\times10^{-8}s^{-1}$; (b) $S = 3.35\times10^{-8}s^{-1}$.
I: $K_H = 0$; II: $K_H = 0.5\times10^{7}\ m^2s^{-1}$; III: $K_H = 10^{7}m^2s^{-1}$.
$U = 5ms^{-1}$; $B = 1.5\times10^{-5}\ m^{-1}$.

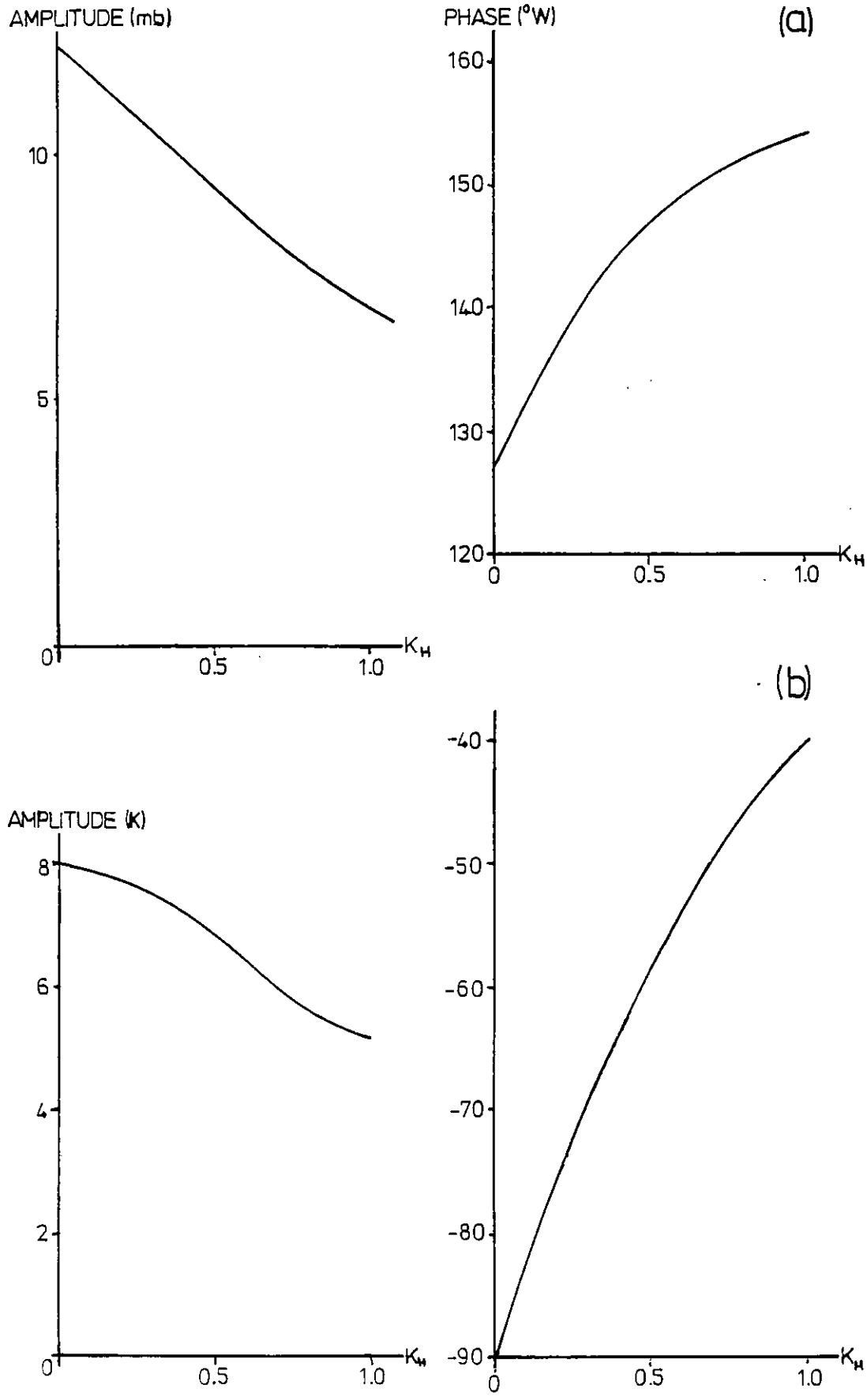

Fig. 6.2: Surface amplitudes and phases of (a) pressure and (b) temperature for n = 3 mode. K_H in units of $10^7 m^2 s^{-1}$.

6.2.1a Varying K_H.

The vertical profiles of heat transport for two different heating rates are shown in Fig. 6.1; the surface pressure and temperature perturbation amplitudes and phases in Fig. 6.2.

When $K_H = 0$, the transport decreases with height to a minimum value at about 8 km, then rises again to a roughly constant value which is less than the surface value. Except in the bottom 2 km or so, the profile is similar to that in the real troposphere (Oort and Rasmusson (1971)). Near the surface, model transports are much larger than observed transports due to the absence of friction in the model - this could be rectified by putting in an Ekman boundary layer. When $K_H > 0$, the flux continues to decay exponentially with height in the stratosphere.

The presence of diffusion by transient eddies exerts a strong dissipative effect on the stationary waves. Even with K_H only a quarter of its value in Table 6.1 (corresponding to a damping time of nearly 20 days), the mid-tropospheric heat transport is not much more than half its value for $K_H = 0$; with $K_H = 10^7 m^2 s^{-1}$ (as in Table 6.1), the stationary waves are strongly damped so that their heat transport is negligible except near the surface. This is due to the change in relative phase between temperature and wind fields as well as the reduction in their amplitudes, as can be seen in Fig. 6.2. Hence for this mode the transient eddies act to reduce greatly the stationary wave heat transport rather than to enhance it.

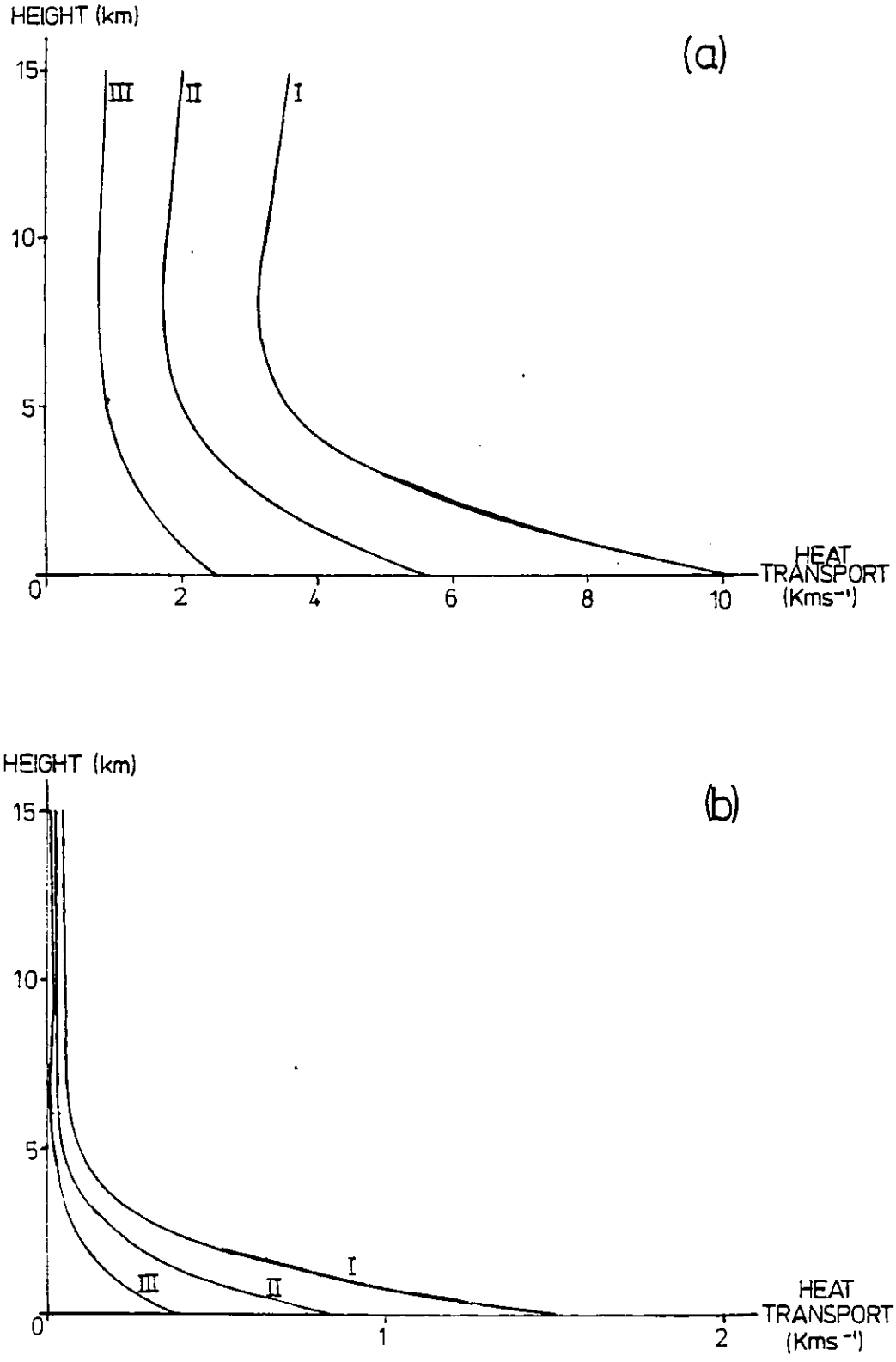

Fig. 6.3: Vertical profile of heat transport for n = 3 mode, with (a) $K_H = 0$; (b) $K_H = 10^{7} m^2 s^{-1}$. I: $S_o = 6.7 \times 10^{-8} s^{-1}$; II: $S_o = 5.0 \times 10^{-8} s^{-1}$; III: $S_o = 3.35 \times 10^{-8} s^{-1}$. $U = 5 ms^{-1}$; $B = 1.5 \times 10^{-5} m^{-1}$.

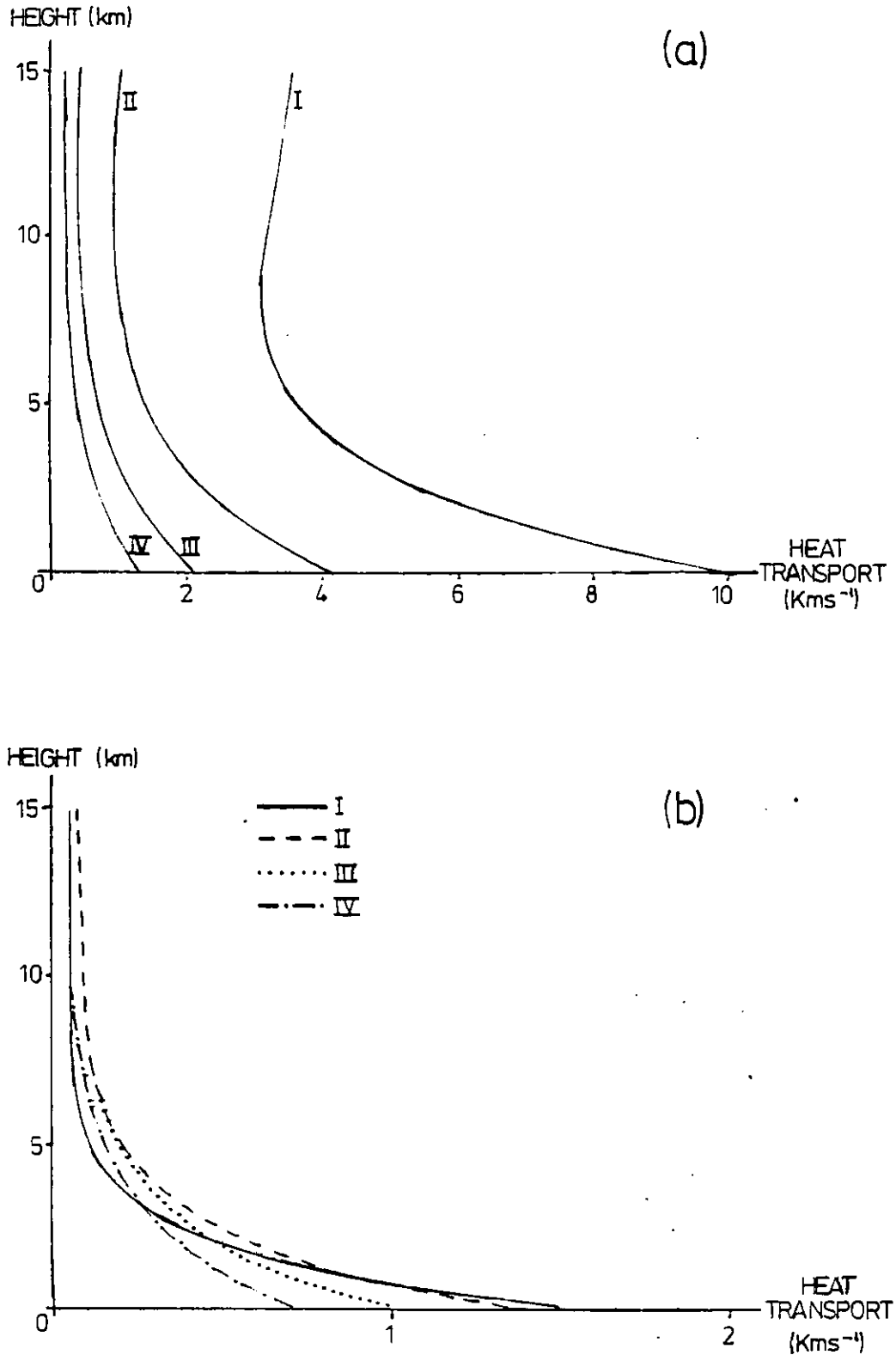

Fig. 6.4: Vertical profile of heat transport for n = 3 mode, with (a) $K_H = 0$; (b) $K_H = 10^7 m^2 s^{-1}$. I: $U = 5ms^{-1}$; II: $U = 7.5ms^{-1}$; III: $U = 10ms^{-1}$; IV: $U = 12.5ms^{-1}$. $S_o = 6.7 \times 10^{-8} s^{-1}$; $B = 1.5 \times 10^{-5} m^{-1}$.

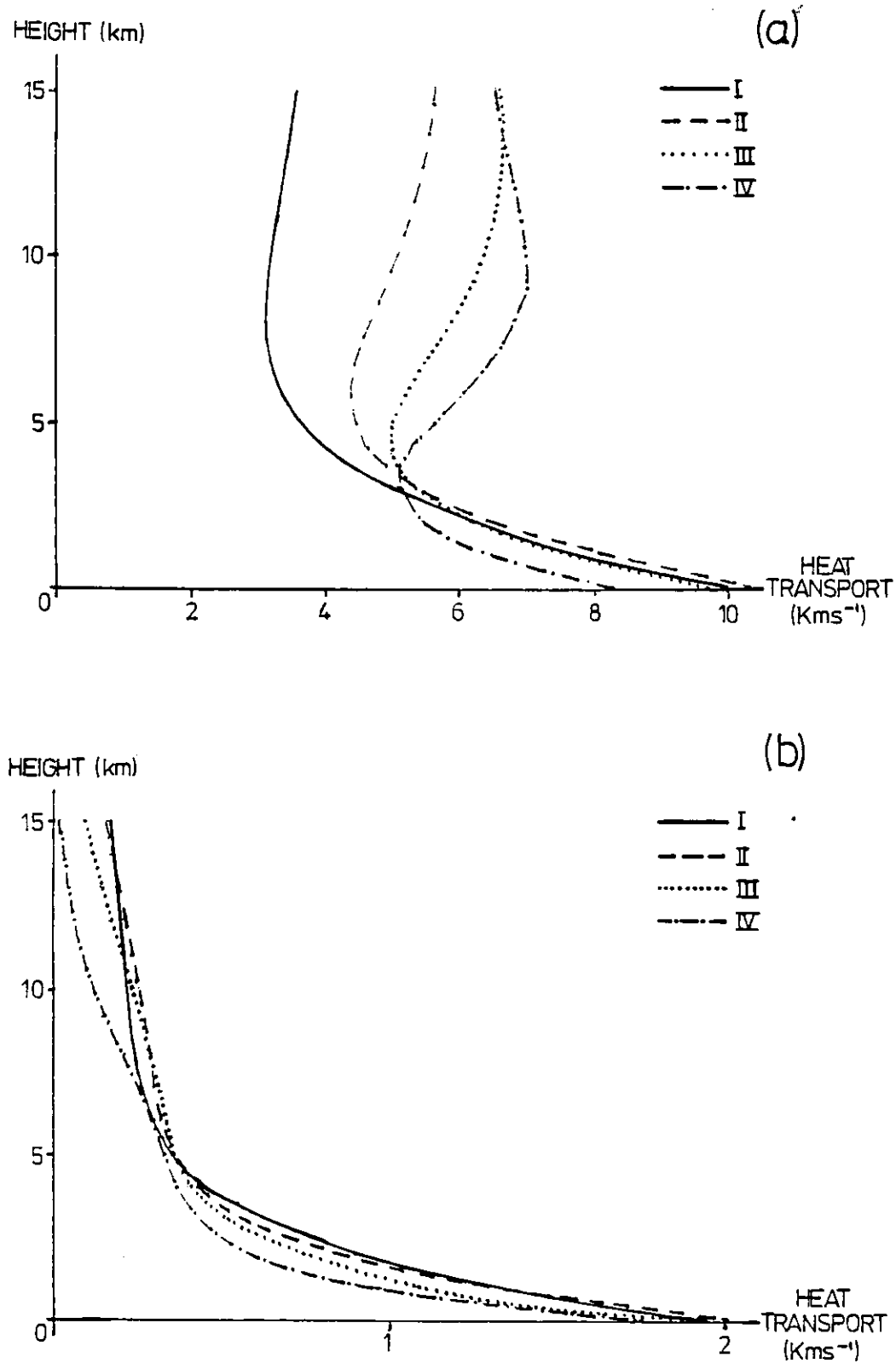

Fig. 6.5: Vertical profile of heat transport for n = 3 mode, with (a) $K_H = 0$; (b) $K_H = 10^7 m^2 s^{-1}$. I: B = $1.5 \times 10^{-5} m^{-1}$; II: B = $3.0 \times 10^{-5} m^{-1}$; III: B = $5.0 \times 10^{-5} m^{-1}$; IV: B = $10.0 \times 10^{-5} m^{-1}$. U = $5 ms^{-1}$; $S_o = 6.7 \times 10^{-8} s^{-1}$.

6.2.1b Varying S_o, U, B.

Since Eq. (6.1) is linear, the heat transport should vary as the square of heating rate (as both temperature and wind fields will vary linearly); Fig. 6.3 shows that this is indeed the case. It was suggested in Chapter 5 that the large change from February to March in stationary eddy sensible heat transport could be caused by the observed change in diabatic heating: qualitatively, these results show that this is easily possible (as we should expect from a linear model). Changing S_o only changes the amplitudes of the surface pressure and temperature fields, not their phases; this is consistent with the change in heat transport from February to March being the result of changes in the amplitudes of the temperature and meridional wind variances rather than in their correlation, as noted in Chapter 3, Section 3.1.

Increasing U has the effect of progressively trapping upward energy propagation and hence poleward heat transport. This is seen in Fig. 6.4: when $K_H = 0$, increasing U substantially reduces the heat transport throughout the troposphere. With $K_H = 10^7 m^2 s^{-1}$, increasing U to $7.5 ms^{-1}$ and $10 ms^{-1}$ actually increases the transport above 2km, and reduces it only slightly below this, although as the transports are so small this is hardly significant; with $U = 12.5 ms^{-1}$ the transport at all levels is smaller, but the reduction is less than with $K_H = 0$.

With $K_H = 0$, it can be seen from Fig. 6.5a that doubling B to $3 \times 10^{-5} m^{-1}$ has the effect of increasing the heat transport at all levels, but especially so above 6km; the level of minimum transport is brought down from 8km to 6km. Increasing B further to $5 \times 10^{-5} m^{-1}$ brings the level of minimum transport down to 4km, increases the

minimum transport by 40%, reduces the transport below 3km, and further increases the transport above 4km. There is a slight maximum in transport at around 13.5km, and a profile up to 32km (not presented) shows a slight minimum at 22km. Increasing B has the effect of decreasing the vertical wavelength (it can be seen from Eq. (6.6a) that $|\nu|$ goes as $B^{-1/2}$), hence the lowering of the level of minimum transport in the troposphere and the exponentially decaying oscillation in the vertical. With $B = 10^{-5} m^{-1}$, some six times larger than the typical tropospheric static stability, the tropospheric minimum in heat transport is at 3km, there is a maximum at 9km, with transports between these levels being further increased. Below 3km, the transports are smaller than for B half as large; above 15km the transport reaches a roughly constant value which is also slightly smaller. Thus the overall effect of increasing B while keeping $K_H = 0$ is to reduce the vertical wavelength, resulting in the tropospheric minimum in transport being at a lower level, transports above this being generally increased, and transports near the surface being decreased.

With $K_H = 0.5 \times 10^{7} m^2 s^{-1}$, Fig 6.5b shows that increasing B to $5 \times 10^{-5} m^{-1}$ increases transports in the upper half of the troposphere, decreases them slightly above this, and has little effect on those in the lower troposphere. With $B = 10^{-5} m^{-1}$, transports are decreased above about 8km and in the lowest 2km, but are roughly the same as for $K_H = 0$ in between. A similar effect can be seen for $K_H = 10^{7} m^2 s^{-1}$ (not shown). As for $K_H = 0$, increaing B decreases the vertical scale of the motion.

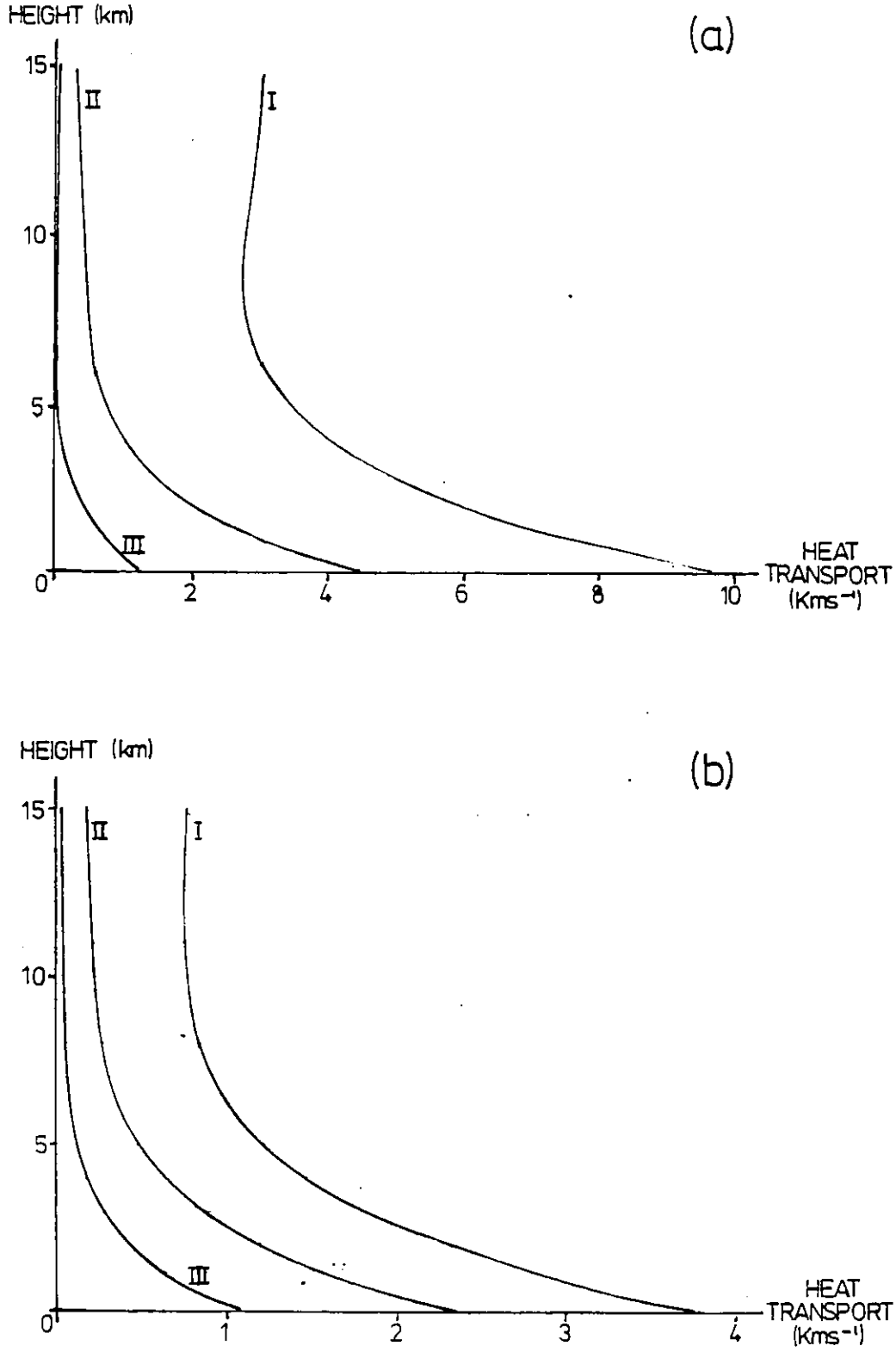

Fig. 6.6: Vertical profile of heat transport for n = 5 mode, with (a) U = $5ms^{-1}$; (b) U = $7.5ms^{-1}$. I: $K_H = 0$; II: $K_H = 0.17\times10^{7} m^2 s^{-1}$; III: $K_H = 0.335\times10^{7} m^2 s^{-1}$. B = $1.5\times10^{-5} m^{-1}$; $S_o = 6.7\times10^{-8} s^{-1}$.

6.2.2 n = 5 mode.

Since the zonal wind required to produce evanescent waves in the case $K_H = 0$ is still much larger than a reasonable tropospheric value, results for this mode should be qualitatively similar to those for the n = 3 mode. Fig. 6.6a shows the vertical profile of heat transport for three different vlues of K_H, with U = 5ms^{-1}. With no diffusion, transports are 90% or more of the n = 3 values; increasing K_H has a progressively more marked effect compared with n = 3. particularly on the transports above the lowest few km. Increasing the zonal wind to 7.5ms^{-1} has a similar effect to the n = 3 case (cp. Figs. 6.6b and 6.4).

6.2.3 n = 7 mode.

With n = 7 it is possible to run the model with a zonal windspeed greater than U_c but not unrealistic for the troposphere. We therefore compare results for U = 7.5ms^{-1} (ie less than U_c) and U = 11ms^{-1} (just larger than U_c); we investigate in more detail the variation of heat transport with K_H for the case of U = 11ms^{-1}.

For U = 7.5ms^{-1} the heat transport is smaller than for n = 3 and n = 5 but similar in vertical profile to these cases for K_H both zero and non-zero (see Fig. 6.7a). With U = 11ms^{-1} and $K_H = 0$ there is no heat transport whatsoever since the relative phase of the temperature and meridional wind field is exactly 90° (see Fig. 6.8). With $K_H = 1.74 \times 10^6 m^2 s^{-1}$, equivalent to a damping time of 5 days (see Table 6.1), the heat transport is roughly half that for U = 7.5ms^{-1}. However, the largest heat transport occurs for $K_H = 0.7 \times 10^6 m^2 s^{-1}$, ie a damping time of around 12.4 days.

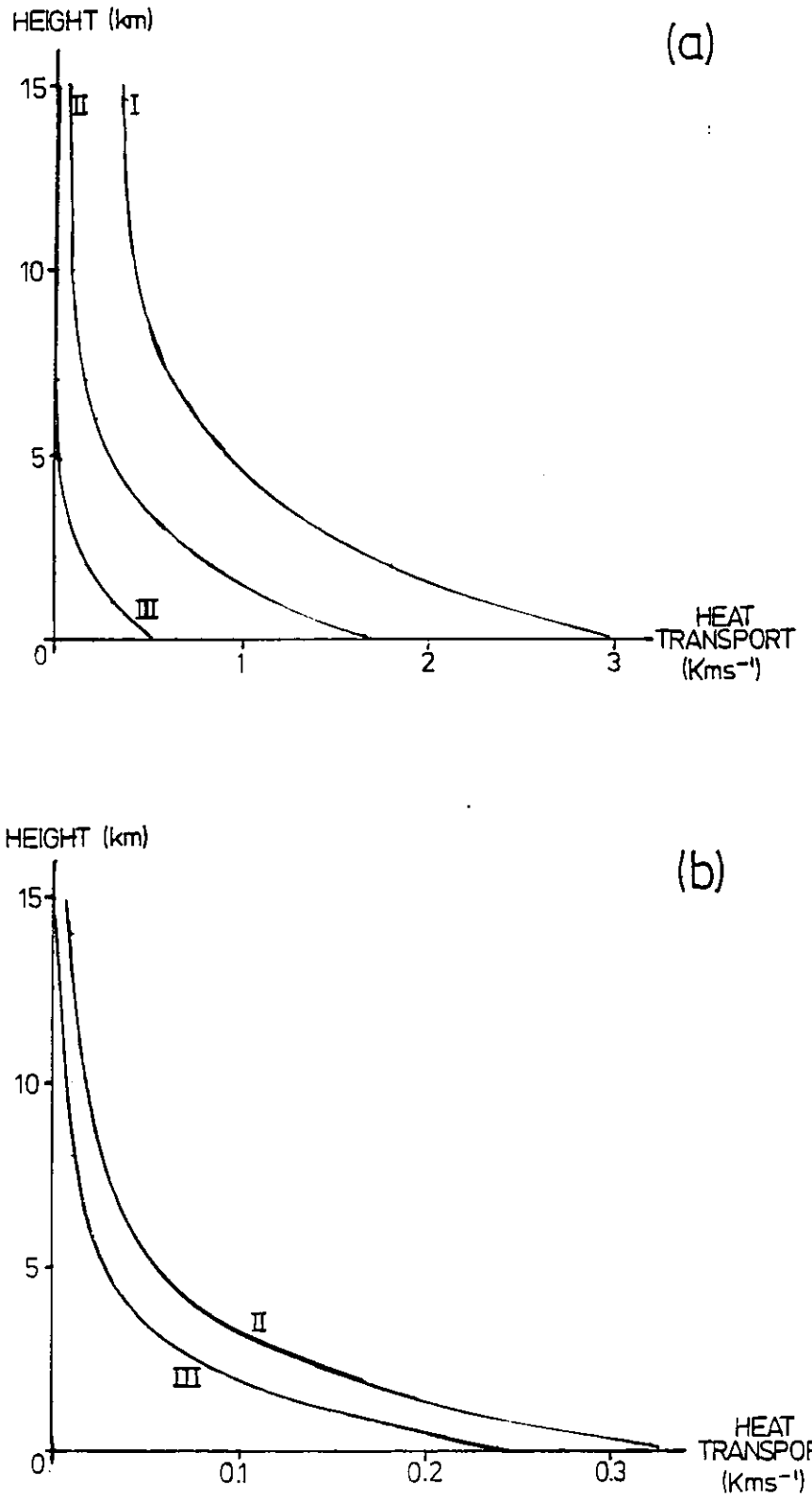

Fig. 6.7: Vertical profile of heat transport for n = 7 mode, with (a) $U = 7.5 ms^{-1}$; (b) $U = 11 ms^{-1}$. I: $K_H = 0$; II: $K_H = 0.67 \times 10^{7} m^2 s^{-1}$; III: $K_H = 0.174 \times 10^{7} m^2 s^{-1}$. $B = 1.5 \times 10^{-5} m^{-1}$; $S_o = 6.7 \times 10^{-8} s^{-1}$.

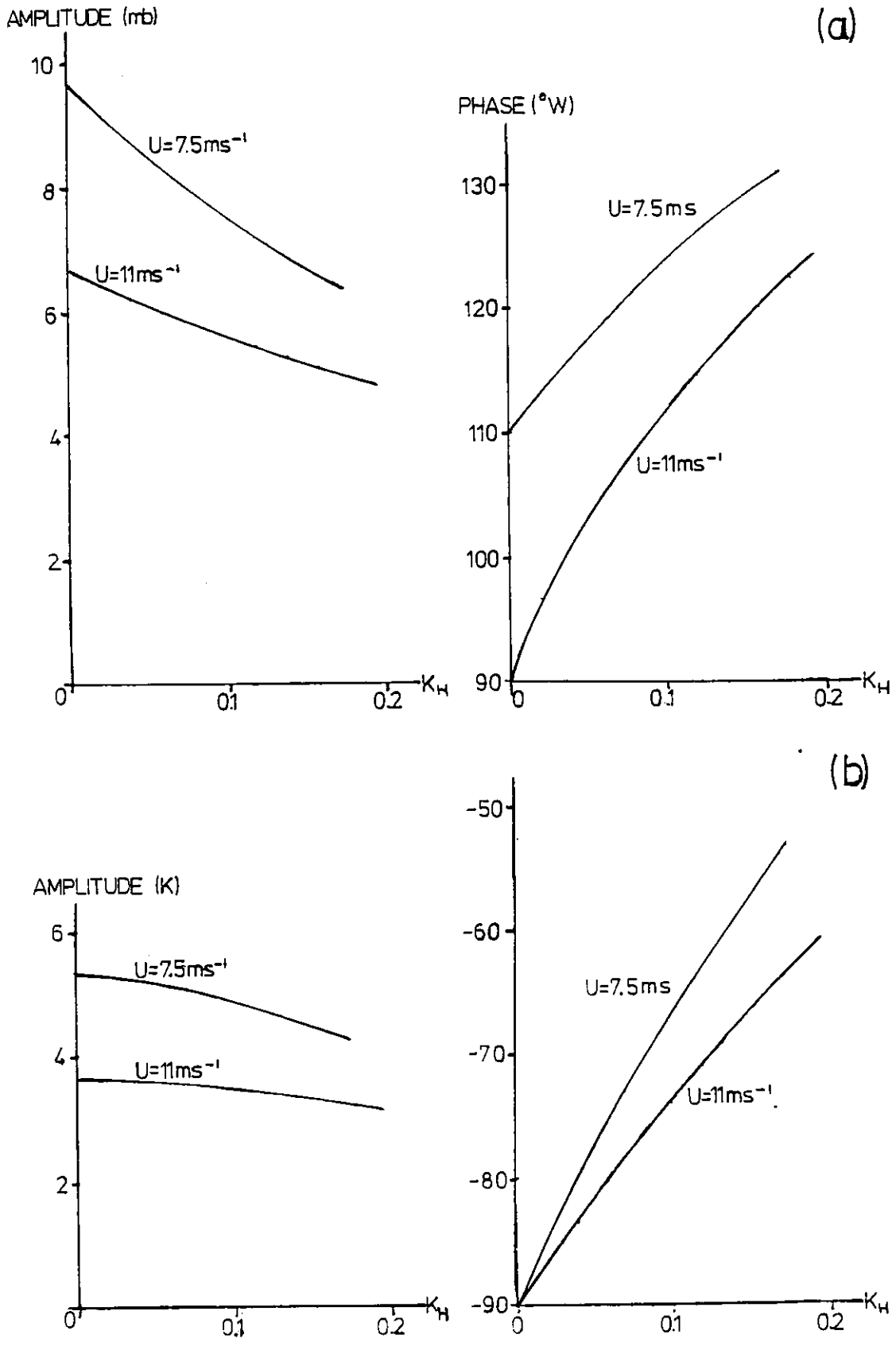

Fig. 6.8: Surface amplitudes and phases of (a) pressure and (b) temperature for n = 7 mode. K_H in units of $10^7 m^2 s^{-1}$.

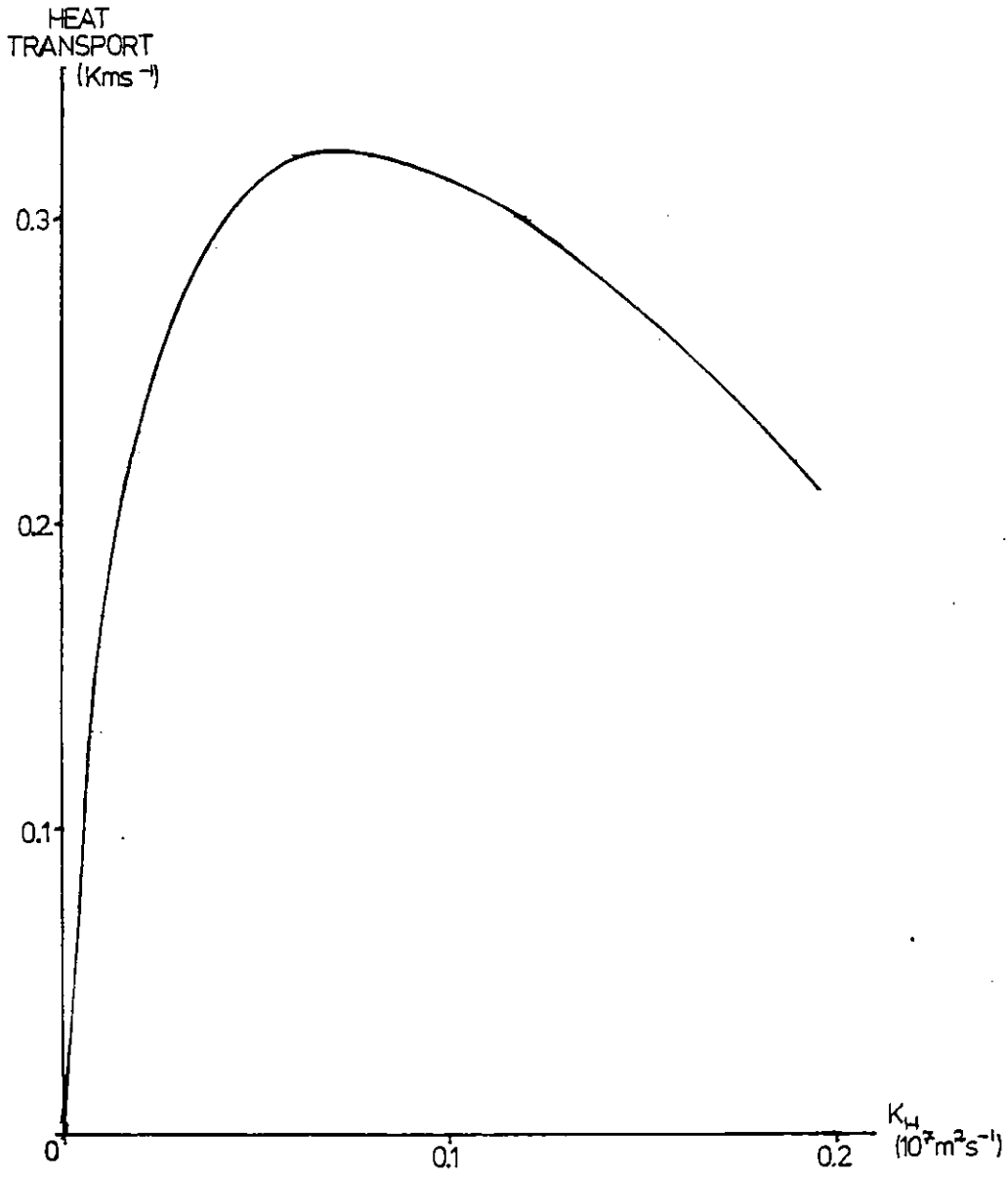

Fig. 6.9: Variation of heat transport with K_H for n = 7 mode, U = 11ms^{-1}. K_H in units of 10^7m^{2}s^{-1}.

Fig. 6.9 shows the variation with K_H of heat transport at the surface for U = 11ms^{-1}. From Fig. 6.8 it can be seen that the effect of increasing K_H is to decrease the amplitudes of both surface pressure and temperature fields, particularly that of the pressure field, and also to shift their phases westwards. For K_H increasing up to $0.7 \times 10^6 m^2 s^{-1}$, the change in their relative phase is rapid, leading to the rapid rise in heat transport seen in Fig. 6.9. As K_H increases further, the phase change is much slower, so that the heat transport falls even though the relative phase decreases (ie the phase difference between maximum temperature and meridional wind drops further below 90°) until $K_H = 1.05 \times 10^6 m^2 s^{-1}$ (damping time of 8.3 days).

Both waves retrogress faster than their relative phase changes, except for K_H near zero. The phase difference between wind and temperature fields at maximum heat transport is only 5° less than for $K_H = 0$, yet this apparently small difference produces a significant change in heat transport. Fig. 6.9 also shows that the choice of K_H is not critical to the heat transport due to this mode provided it takes a reasonable value.

6.2.4 n = 9 mode.

For this mode, a value of U = 7.5ms^{-1} was used, which is greater than U_c, so that for $K_H = 0$ the waves are evanescent and hence trapped. With this value of U, typical of the troposphere, heat transports are nearly twice as large as for n = 7 and U = 11ms^{-1} (due to the smaller zonal windspeed) for the equivalent K_H, reaching a maximum of 0.56 Kms^{-1}: thus the heat transport due to this mode is

about 20% of that by the n = 3 mode with equivalent diffusion coefficient and the same zonal windspeed, which is not negligible. As for n = 7, the heat transport is a maximum for K_H given by a damping time somewhat longer than 5 days, in this case around 15 days. In general, the behaviour of this mode is similar to that of the n = 7 mode.

6.2.5 n = 11 mode.

With U = $5ms^{-1}$, again larger than U_c, the variation with K_H of the heat transport at the surface, shown in Fig. 6.10, produces interesting results. The maximum heat transport of $1.3Kms^{-1}$ is for $K_H = 0.15 \times 10^5 m^2 s^{-1}$, which represents a 25-day damping time. When K_H reaches $0.3 \times 10^5 m^2 s^{-1}$ the transport in the middle troposphere starts to turn negative, this region extending up and down until $K_H = 0.55 \times 10^5 m^2 s^{-1}$, by which time the heat transport at all heights is negative. The heat transport at the surface reaches its largest negative value for $K_H = 1.1 \times 10^5 m^2 s^{-1}$; thereafter the (negative) transport decreases at all heights. This means that with K_H equal to its 5-day (or even 7-day) damping time value, the heat transport is negative (equatorwards); however it is not clear whether the same damping time applies to these higher modes as to the untrapped modes. Typical vertical profiles for different K_H's are shown in Fig. 6.11.

Fig. 6.12 shows how this variation with K_H comes about. As with the n = 7 and n = 9 modes, increasing K_H decreases the amplitudes of the surface pressure and temperature fields, and causes both to retrogress (twice as fast as in the case of n = 7 for equivalent damping times). They retrogress in such a way that for $K_H > 0.53 \times 10^5 m^2 s^{-1}$ the phase difference between temperature and

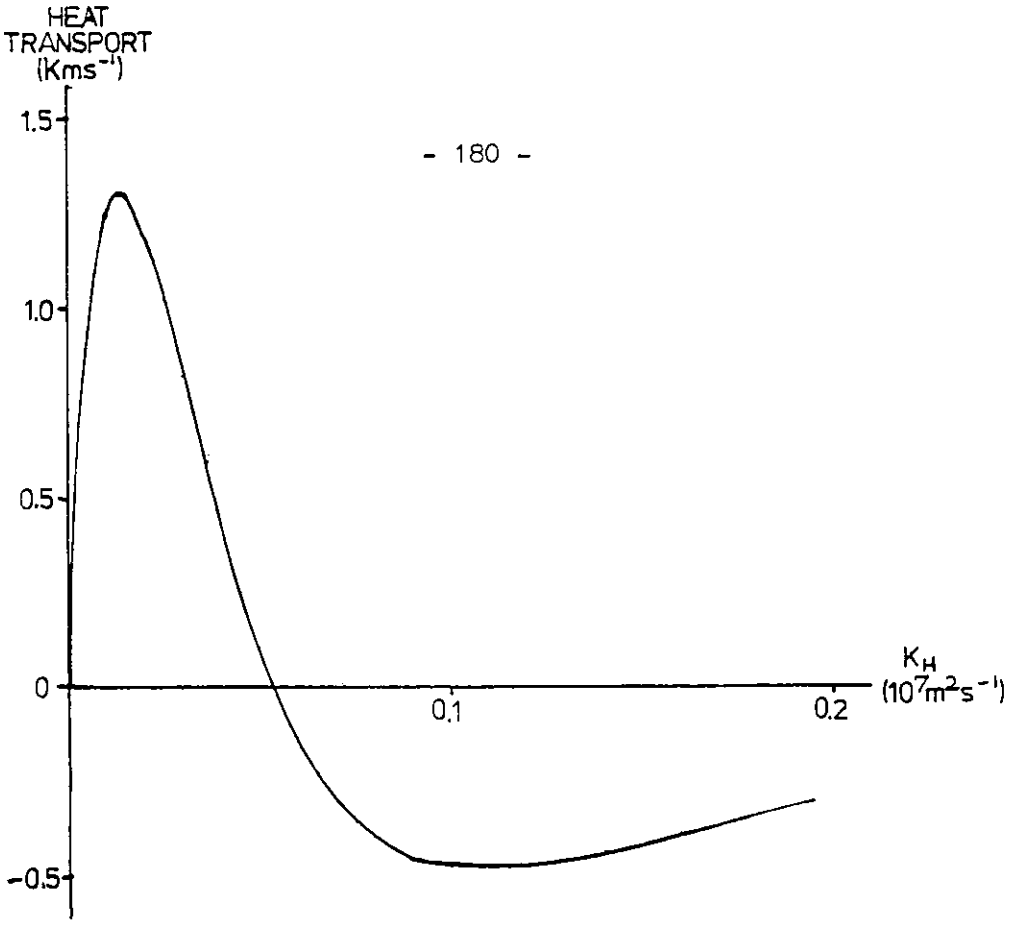

Fig. 6.10: Variation of heat transport with K_H for n = 11 mode, U = $5ms^{-1}$. K_H in units of $10^7 m^2 s^{-1}$

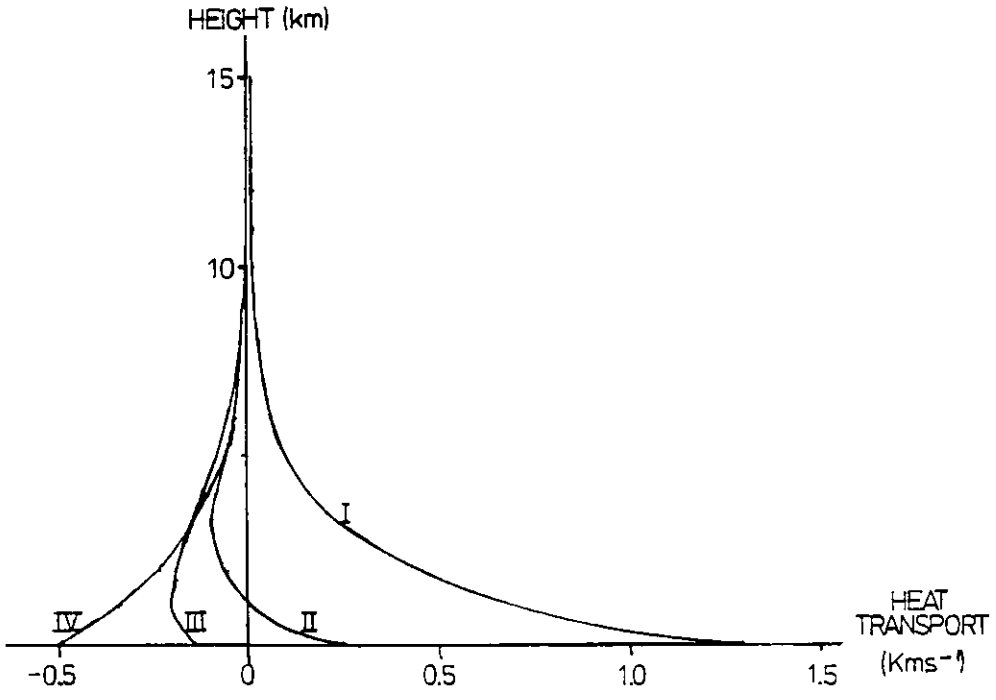

Fig. 6.11: Vertical profile of heat transport for n = 11 mode.
I: $K_H = 0.015 \times 10^7 m^2 s^{-1}$; II: $K_H = 0.04 \times 10^7 m^2 s^{-1}$;
III: $K_H = 0.06 \times 10^7 m^2 s^{-1}$; IV: $K_H = 0.11 \times 10^7 m^2 s^{-1}$.
U = $5ms^{-1}$; B = $1.5 \times 10^{-5} m^{-1}$; $S_o = 6.7 \times 10^{-8} s^{-1}$.

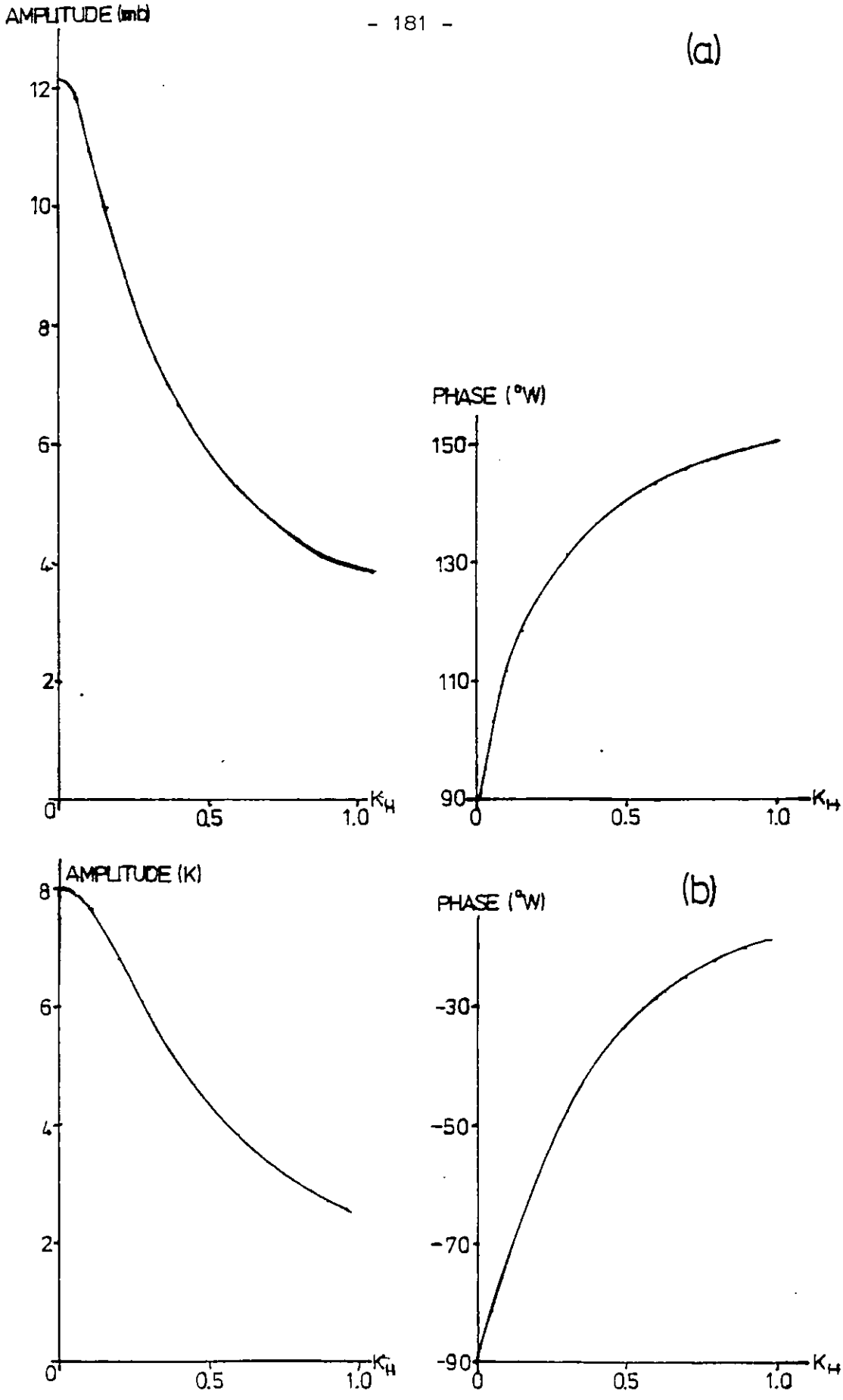

Fig. 6.12: Surface amplitudes and phases of (a) pressure and (b) temperature for n = 11 mode. K_H in units of $10^7 m^2 s^{-1}$.

meridional wind fields becomes larger than 90°, their correlation negative, and hence warmer air is transported equatorwards, colder air polewards. Thus, whereas for n = 7 there is significant poleward heat transport for a wide range of K_H's, for n = 11 this exists only for small K_H.

6.3 Conclusions.

For all modes, the effect of introducing diffusion of potential vorticity into the model is to decrease the amplitude of the surface temperature and meridional wind fields, to shift their phases westwards, and to modify their relative phase; significant heat transport becomes limited to the troposphere. With subcritical zonal windspeeds the heat transport is invariably reduced considerably by diffusion of potential vorticity; only with supercritical zonal windspeeds is the heat transport enhanced by this diffusion. This enhancement is maximised when the diffusion coefficient represents a damping time considerably in excess of that believed to apply in the atmosphere; with a damping time of 5 days only two modes yield positive (poleward) heat transports at supercritical zonal windspeeds, namely n = 7 and n = 9. However, this result must be treated with caution, as the damping time appropriate to the higher modes is not necessarily the same as for lower modes.

The number of untrapped modes is small compared to the number of trapped modes, and the thermal forcing contains significant components due to these higher modes, so that it is reasonable to suggest that the higher modes, when summed together, produce a major part of the poleward heat transport. However, from this simple model it seems

that the region of parameter-space in which transient eddies enhance the stationary wave heat transport is relatively limited, so that the effect is likely to be swamped by other variations.

There is a more fundamental objection to the hypothesis formulated at the beginning of this chapter. The modes whose heat transport is enhanced by transient eddies, and which could therefore produce large wintertime stationary wave heat transports in the troposphere due to this, are invariably trapped below the stratosphere by the zonal wind: hence the transient eddies will have no effect on the stratospheric stationary wave heat transport, and we should not therefore expect this to rise as it does in the troposphere. However, it was shown in Chapter 2, Section 2.3.2, that in winter the stratospheric stationary eddy heat transport is large, indeed the increase from summer to winter is much more marked than in the troposphere. It was stated that this is due to upward propagation of tropospheric stationary waves, which seems likely; therefore the large stationary eddy heat transports observed in the troposphere in winter cannot be produced by the effect of transient eddies acting on the stationary wave field, since it is only the non-vertically propagating waves whose heat transport is thus enhanced. Alternatively, the wintertime stationary wave heat transports are not the result of upward propagation from the troposphere, but this seems unlikely.

We cannot firmly conclude from this that the rise in stationary eddy heat transport in winter while the transient eddy heat transport remains roughly constant is not due to the stationary eddy transport being enhanced by the transient eddies, however from this simple model it seems unlikely. A deeper investigation might look at the effects of taking a heating function more realistic than one Fourier mode, as

well as including orography and surface friction, and also of allowing vertical shear in the zonal wind so that the zonal windspeed is realistic at all heights.

CHAPTER 7. CONCLUSIONS AND SUGGESTIONS FOR FURTHER WORK.

It has been found that a knowledge of the zonal-mean temperature field is not sufficient to define uniquely the eddy meridional heat flux at any time of year. Conventional partitioning of this into stationary and transient components reveals that the transient eddy sensible heat flux is almost independent of meridional entropy gradient (except in summer), which is often used to parameterize that flux in climate models. The total eddy sensible heat flux is more closely related to meridional entropy gradient, but nevertheless displays two-valued behaviour with respect to this, which is accounted for by the annual variation of the stationary eddy component of the flux.

It is inappropriate to use meridional entropy gradient to determine the stationary eddy flux, as this is a result of longitudinal rather than latitudinal variations in temperature structure. For October to April, this flux is closely related to the contrast in diabatic heating between land and oceans. Similarly, the annual variation of meridional entropy gradient is closely related to the difference in zonal-mean diabatic heating between tropical and high latitudes. The annually-varying forcing mechanisms for each are different in nature, though linked; the annual variations in stationary eddy heat transport and in entropy gradient can be regarded as separate responses to these different forcing mechanisms, rather than stationary eddy heat transport being a function of meridional entropy gradient. Both exhibit time-lags with respect to changes in forcing: that in entropy gradient is longer, probably because this is modified by the eddy heat transport.

Use of a time-dependent model would be useful to investigate whether the observed cycles of variation can be reproduced in such a model, and in particular to study the interaction between meridional eddy heat transport and entropy gradient, as well as their response times to changes in forcing.

This still leaves the problem of transient eddy heat fluxes: how can these be parameterized in both zonal-mean models and those calculating explicitly longitudinally-varying fields? In particular, further work is needed to understand the development of transient disturbances on long-wave fields, and how in a time-dependent model the long-wave field acts upon itself, for instance via generation of transient eddies. Such work would make possible revised parameterization schemes for transient baroclinic eddies, as well as revealing the nature of the interaction betwen stationary and transient eddies.

As regards the problem of whether the conventional distinction between stationary and transient eddies represents a distinction in physical mechanisms, the present study suggests that this is for the most part valid, in that observed variations in stationary eddy heat transport can be accounted for without reference to transient eddies, which may depend in the first place on the long-wave field but represent a distint class of physical behaviour (ie baroclinic instability). However, it is possible that a small but not insignificant part of the meridional heat flux apparently due to stationary eddies is in fact a result of transient eddies developing in preferred locations on the long-wave field.

This study has also demonstrated the important role of the oceans

in determining atmospheric eddy heat fluxes, via the transfer of energy from oceans to atmosphere.

With the advent of many years' satellite radiation data, and recent studies presenting surface flux statistics, a much-refined atmospheric energy budget could be carried out to determine the diabatic heating more exactly as a function of longitude and latitude. This might lead to a better understanding of causes of interannual climate variation, if such variations in the atmospheric circulation can be demonstrated to be closely correlated with changes in the top and bottom (vertical) energy fluxes. In the present context, the intra-annual variation of the eddy heat fluxes might be explained, and the reason for the presence or absence of a sharp February-March fall in this established.

APPENDIX -- DERIVATION OF MODEL EXPRESSIONS.

The expressions for A, C and ν given in Eqs. (6.4) - (6.6) are derived as follows.

Substitution of Ψ from Eq. (6.3) into the potential vorticity terms in Eq. (6.1) gives

$$\left[\nabla_H^2\Psi + Q^2\frac{\partial^2\Psi}{\partial z^2}\right] = -(\lambda^2 + Q^2\nu^2)\, Ae^{ikx}e^{i\nu z}\cos ly - (\lambda^2 - Q^2b^2)\, Ce^{ikx}e^{-bz}\cos ly \qquad (A1)$$

where

$$\lambda^2 = (k^2 + l^2)$$

$$Q^2 = f_o^2/gB$$

Sustituting this and the expressions for Ψ and S into Eq. (6.1) yields

$$\{[-ikU(\lambda^2 + Q^2\nu^2)] + ik\beta\}Ae^{i\nu z} + \{[-ikU(\lambda^2 - Q^2b^2)] + ik\beta\}Ce^{-bz} = K_H\lambda^2(\lambda^2 + Q^2\nu^2)\, Ae^{i\nu z} + K_H\lambda^2(\lambda^2 - Q^2b^2)\, Ce^{-bz} - \frac{f_obS_o}{B}e^{-bz} \qquad (A2)$$

The terms in $e^{i\nu z}$ and e^{-bz} are now separately equated:-

$$\{[-ikU(\lambda^2 + Q^2\nu^2)] + ik\beta\} = K_H\lambda^2(\lambda^2 + Q^2\nu^2) \qquad (A3)$$

$$\{[-ikU(\lambda^2 - Q^2b^2)] + ik\beta\}C = [K_H\lambda^2(\lambda^2 - Q^2b^2)]C - \frac{f_obS_o}{B} \qquad (A4)$$

Use (A4) to obtain an expression for C:-

Writing $\left(\frac{K_H\lambda^2}{kU}\right) = E$ and $(\lambda^2 - Q^2b^2) = \lambda_*^2$ leads to

$$\left\{E\lambda_*^2 + i\left(\lambda_*^2 - \frac{\beta}{U}\right)\right\} C = \frac{f_o b S_o}{kUB}$$

Now, writing $\left(\lambda_*^2 - \frac{\beta}{U}\right) = P$; $\left(\frac{E\lambda_*^2}{P}\right) = W$; $(1 + W^2) = X$

we obtain $$(W + i)\, C = \frac{f_o b S_o}{kUBP}$$

Multiplying by $(W - i)$ and rearranging gives

$$C = \frac{f_o b S_o\, (W - i)}{kUBXP} \tag{A5}$$

Writing $C = |C| e^{i\xi}$, we find

$$|C| = \frac{f_o b S_o}{kUB|P|\sqrt{X}} \tag{A6a}$$

$$\xi = \tan^{-1}(-1/W) + n_1 \pi \tag{A6b}$$

where $\begin{cases} n_1 = 0 \text{ if } P > 0 \\ n_1 = 1 \text{ if } P < 0 \end{cases}$

We now solve for ν, using Eq. (A3), which can be rearranged in the form

$$Q^2\nu^2(E + i) = -E\lambda^2 + i\left(\frac{\beta}{U} - \lambda^2\right)$$

whence $$Q^2\nu^2(1 + E^2) = \left\{-E\lambda^2 + i\left(\frac{\beta}{U} - \lambda^2\right)\right\}(E - i)$$

Writing $(1 + E^2) = F$ and $\frac{U\lambda^2}{\beta} = T$ gives

$$Q^2\nu^2 F = \left(\frac{\beta}{U} - F\lambda^2 + iE\frac{\beta}{U}\right) \tag{A7}$$

and hence $\nu^2 = \frac{\beta}{Q^2U}\left\{\frac{[1 - FT + iE]}{F}\right\}$

Expressing this in the form $\nu^2 = |\nu^2|e^{i\phi}$, so that $\nu = |\nu|e^{i\phi/2}$ and $|\nu| = \sqrt{|\nu^2|}$, gives

$$|\nu| = \left(\frac{\beta}{Q^2U}\right)^{1/2}\left\{\frac{[F + T^2F - 2T]}{F}\right\}^{1/4} \qquad \text{(A8a)}$$

$$\phi = \tan^{-1}\left\{\frac{E}{1 - ST}\right\} \qquad \text{(A8b)}$$

To obtain A, we first rewrite Eq. (6.2) in streamfunction form:-

$$U\frac{f_o}{g}\frac{\partial}{\partial x}\left(\frac{\partial \Psi}{\partial z}\right) + wB = K_H\frac{f_o}{g}\nabla_H^2\left(\frac{\partial \Psi}{\partial z}\right) + S \qquad \text{(A9)}$$

Substituting for Ψ in this yields

$$\left\{-Uk\nu + iK_H\lambda^2\nu\right\}Ae^{i\nu z} + wB = \left\{[K_H\lambda^2 b + iUkb]C + \frac{gS_o}{f_o}\right\}e^{-bz}$$

Using the lower boundary condition w = 0 at z = 0 and dividing through by Uk yields

$$-\{(1 - iE)\nu\}A = \left\{(E + i)\ bC + \frac{gS_o}{f_o Uk}\right\}$$

Writing $\frac{gS_o}{f_o Uk} = G$ and multiplying by (E - i) gives

$$-F\nu A = i\{SbC + G(E - i)\}$$

whence $A = -\left\{\frac{G}{\nu S}\right\} - i\left\{\frac{bC}{\nu} + \frac{GE}{\nu S}\right\}$

Extracting the factor $1/\nu$ from this and substituting for C from Eq. (A5) gives

$$A = \frac{-G}{\nu}\left\{\left[\frac{1}{S} + \frac{Q^2 b^2}{XP}\right] + i\left[\frac{Q^2 b^2 W}{XP} + \frac{E}{S}\right]\right\}$$

Writing $\frac{Q^2 b^2}{XP} = D^2$, replacing ν by its complex form and putting A into the form

$$A = |A| e^{i(\Pi + \chi - \phi/2)}$$

gives

$$|A| = \frac{G}{\sqrt{S}\,|\nu|}\left\{1 + D^2\left[SD^2X + 2(1 + EW)\right]\right\}^{1/2} \qquad \text{(A10a)}$$

$$\chi = \tan^{-1}\left\{\frac{\left[\frac{E}{S} + D^2 W\right]}{\left[\frac{1}{S} + D^2\right]}\right\} \qquad \text{(A10b)}$$

The expressions for A, C and ν given in Eqs. (A10), (A6) and (A8) respectively are those used in Chapter 6.

ACKNOWLEDGEMENTS

I wish to thank all members of the Atmospheric Physics Group, Imperial College, for their advice, friendship and support during the course of this research. In particular I should like to thank my supervisor, Dr. J.S.A. Green, for his guidance and criticism of this work, and Drs. K.J. Bignell and G.J. Shutts for valuable assistance.

I wish to thank also many other friends who have encouraged me in my work.

The work was financed by a NERC Studentship. This thesis was prepared and typed using the Imperial College Computer Centre's word processing software "Draft/Format".

I thank God who through Christ, by His Holy Spirit, has inspired and upheld me in this work.

REFERENCES

BATES, J.R., 1977: Dynamics of stationary ultra-long waves in middle latitudes. Quart. J. R. Met. Soc., 103, 397-430.

BLACKMON, M.L., WALLACE, J.M., LAU, N.-C., and MULLEN, S.L., 1977: An observational study of the Northern Hemisphere wintertime circulation. J. Atm. Sci., 34, 1040-1053.

BROWN, J.A., 1964: A diagnostic study of tropospheric diabatic heating and the generation of available potential energy. Tellus 16, 371-388.

BUDYKO, M.I., 1963 (1955): Atlas of the heat balance of the Earth. USSR, 69pp.

BUDYKO, M.I., 1969: The effect of solar radiation variations on the climate of the Earth. Tellus, 21, 611-619.

CHARNEY, J.G., and DRAZIN, P.G., 1961: Propagation of planetary-scale disturbances from the lower into the upper atmosphere. J. Geophys. Res., 66, 83-109.

CLAPP, P.F., 1961: Normal heat sources and sinks in the lower troposphere in winter. Mo. Wea. Rev., 89, 147-162.

CLAPP, P.F., 1970: Parameterization of macroscale transient heat transport for use in a mean-motion model of the general circulation. J. Appl. Met., 9, 554-563.

CLAYTON, H.H., 1934: World weather records 1921-1930. Smithsonian Institution, 616pp.

CLAYTON, H.H., and CLAYTON, F.L., 1947: World weather records 1931-1940. Smithsonian Institution, 646pp.

DEFANT, A., 1921: Die Zirculation der Atmosphäre in den gemässigten Breiten der Erde. Geograf. Ann., 3, 209-266.

EADY, E.T., 1949: Long waves and cyclone waves. Tellus, 1(3), 33-52.

ELIASEN, E., 1958: A study of the long atmospheric waves on the basis of zonal harmonic analysis. Tellus, 10, 206-215.

ELLIS, J.S., and VONDER HAAR, T.H., 1976: Zonal average Earth radiation budget measurements from satellites for climate studies. Atmospheric Science Paper No. 240, Colorado State University.

ESBENSEN, S.K., and KUSHNIR, Y., 1981: The heat budget of the global ocean: an atlas based on estimates from surface marine observations. Climatic Research Institute Report No. 29, Oregon State University.

FREDERIKSEN, J.S., 1979: Baroclinic instability of zonal flows and planetary waves in multi-level models on a sphere. J. Atm. Sci., 36, 2320-2335.

GELLER, M.A., and AVERY, S.K., 1978: Northern Hemisphere distributions of diabatic heating in the troposphere derived from general circulation data. Mo. Wea. Rev., 106, 629-636.

GERMAN WEATHER SERVICE, 1967-1977: Die Grosswetterlagen Europas (various months).

GREEN, J.S.A., 1970: Transfer properties of the large-scale eddies and the general circulation of the atmosphere. Quart. J. R. Met. Soc., 96, 157-185.

GREEN, J.S.A., LUDLAM, F.H., and McILVEEN, J.F.R., 1966: Isentropic relative-flow analysis and the parcel theory. Quart. J. R. Met. Soc., 92, 210-219.

HELD, I.M., 1978: The vertical scale of an unstable baroclinic wave and its importance for eddy heat flux parameterizations. J. Atm. Sci., 35, 572-576.

HOLOPAINEN, E.O., 1970: An observational study of the energy balance of the stationary disturbances in the atmosphere. Quart. J. R. Met. Soc., 96, 626-644.

HSIAO, C.-N., 1979: Interannual variation of atmospheric meridional eddy transports. Environmental Research Paper No. 17, Colorado State University.

HSIAO, C.-N., and REITER, E.R., 1981: Numerical studies of the interannual variations in meridional eddy transports. Environmental Research Paper No. 30, Colorado State University.

LABITZKE, K., 1972: Climatology of the stratosphere in the Northern Hemisphere, 1, Heights, temperatures and geostrophic resultant wind speeds. Meteor. Abh., 100(4-5).

LAU, N.-C., 1979: The observed structure of tropospheric stationary waves and the local balances of vorticity and heat. J. Atm. Sci., 36, 996-1016.

LAU, N.-C., WHITE, G.H., and JENNE, R.L., 1981: Circulation statistics for the extratropical Northern Hemisphere based on NMC analyses. NCAR Technical Note NCAR/TN-171+STR.

LEJENÄS, H., and MADDEN, R.A., 1982: The annual variation of the large scale 500mb and sea level pressure fields. University of Stockholm Report DM-35.

LORENZ, E.N., 1979: Forced and free variations of weather and climate. J. Atm. Sci., 36, 1367-1376.

MANABE, S., and TERPSTRA, T.B., 1974: The effects of mountains on the general circulation of the atmosphere as identified by numerical experiments. J. Atm. Sci., 31, 3-42.

METEOROLOGICAL OFFICE, 1947: Monthly meteorological charts of the Western Pacific Ocean. M.O. 484, H.M.S.O., 120pp.

METEOROLOGICAL OFFICE, 1949: Monthly meteorological charts of the Atlantic Ocean. M.O. 483, H.M.S.O., 122pp.

METEOROLOGICAL OFFICE, 1950: Monthly meteorological charts of the Eastern Pacific Ocean. M.O. 518, H.M.S.O., 122pp.

NORTH, G.R., 1975: Theory of energy-balance climate models. J. Atm. Sci., 32, 2033-2043.

OORT, A.H., 1971: The observed annual cycle in the meridional transport of atmospheric energy. J. Atm. Sci., 28, 325-339.

OORT, A.H., 1977: The interannual variability of atmospheric circulation statistics. NOAA Prof. Paper 8, US Dept. of Commerce, 76pp.

OORT, A.H., and PEIXOTO, J.P., 1974: The annual cycle of the energetics of the atmosphere on a planetary scale. J. Geophys. Res., 79, 2705-2719.

OORT, A.H., and RASMUSSON, E.M., 1971: Atmospheric circulation statistics. NOAA Prof. Paper 5, US Dept. of Commerce, 323pp.

OORT, A.H., and VONDER HAAR, T.H., 1976: On the observed annual cycle in the ocean-atmosphere heat balance over the Northern Hemisphere. J. Phys. Oceanogr., 6, 781-800.

SALTZMANN, B., 1968: Steady state solutions for axially-symmetric climatic variables. Pure and Appl. Geophys., 69, 237-259.

SHUTTS, G.J., 1978: Quasi-geostrophic planetary wave forcing. Quart. J. R. Met. Soc., 104, 331-350.

SMAGORINSKY, J., 1953: The dynamical influence of large-scale heat sources and sinks on the quasi-stationary mean motions of the atmosphere. Quart. J. R. Met. Soc., 79, 342-366.

SRIVATSANGAM, S., 1978: Parametric study of large-scale atmospheric properies. Part I: Eddy fluxes. J. Atm. Sci., 35, 1212-1219.

STONE, P.H., 1972: A simplified radiative-dynamical model for the static stability of rotating atmospheres. J. Atm. Sci., 29, 405-418.

STONE, P.H., 1974: The meridional variation of the eddy fluxes by baroclinic waves and their parameterization. J. Atm. Sci., 31, 444-456.

STONE, P.H., 1978: Baroclinic adjustment. J. Atm. Sci., 35, 561-571.

STONE, P.H., and MILLER, D.A., 1980: Empirical relations between seasonal changes in meridional temperature gradients and fluxes of heat. J. Atm. Sci., 37, 1708-1721.

U.S. WEATHER BUREAU, 1959: World weather records 1941-1950. US Dept. of Commerce, 1361pp.

VAN LOON, H., 1979: The association between latitudinal temperature gradient and eddy transport. Part I: Transport of sensible heat in winter. Mo. Wea. Rev., 107, 525-534.

VAN LOON, H., JENNE, R.L., and LABITZKE, K., 1973: Zonal harmonic standing waves. J. Geophys. Res., 78, 4463-4471.

WHITE, A.A., and GREEN, J.S.A., 1982: A non-linear atmospheric long wave model incorporating parameterization of transient baroclinic eddies. Quart. J. R. Met. Soc., 108, 55-85.

WIIN-NIELSEN, A., BROWN, J.A., and DRAKE, M., 1963: On atmospheric energy conversions between the zonal flow and the eddies. Tellus, 15, 261-279.

WIIN-NIELSEN, A., BROWN, J.A., and DRAKE, M., 1964: Further studies of energy exchange between the zonal flow and the eddies. Tellus, 16, 168-180.

YAO, M.-S., 1980: Maintenance of quasi-stationary waves in a two-level quasi-geostrophic spectral model with topography. J. Atm. Sci., 37, 29-43.